An integrated analysis of the protein-protein interaction network of the conserved mitotic kinase, Polo

Submitted by Katarzyna Sierzputowska, to the University of Exeter as a thesis for the degree of Masters by Research in Biological Sciences, 30th October, 2020.

I certify that all material in this thesis which is not my own work has been identified and that any material that has previously been submitted and approved for the award of a degree by this or any other University has been acknowledged.

(Signature)

Acknowledgments

“A person’s most useful asset is not a head full of knowledge, but a heart full of love, an ear ready to listen, and a hand willing to help others.”—Unknown

Thankfully, my supervisors had all of the above and the knowledge expertise to boot. My sincere and deepest gratitude goes to Prof James Wakefield and Prof Benjamin Housden, whose assistance proved monumental towards the success of this project. Thank you for your endless support in all of my endeavours, be it conferences, outreach events, lab retreats, and even a career change into teaching science.

I would like to recognise the current and former members of both the Wakefield and Housden labs for their contributions to my academic career and sanity during the past 3 years: Dr Karolina Jaworek, Dr Lori Borgal, Dr Novia Wang, Ammarah Tariq, James Marks, James Pearce, Constantino Salomao, Chris Baxter and JY Lee. Thank you for all the help with protocols and softwares, navigating British culture (and bureaucracy), late night LSI film and pizza parties, being amazing conference/travel buddies and for the invaluable input on the theme and taste level of the annual lab Christmas Dash costumes.

Heartfelt thanks:

To Dr Selena Gell and Dr Leila Rieder for being my first mentors in my research journey. A big trans-Atlantic hug goes to Dr Rieder for encouraging me to pursue grants to explore gene editing technologies in *Drosophila* as an undergrad and providing immeasurable science and life advice that led me to my research career.

To Dr Norbert Perrimon, Dr Stephanie Mohr, Dr Jonathan Zirin, and Dr Claire (Yanhui) Hu at the Harvard Medical School DRSC/TRiP Functional Genomics Resources facility for all help and support with reagents necessary for getting this project started.

To LSI S02.01 office inhabitants, current and former, especially those not already named (Khulood, Mathilde, Rob, Salil, Seema, Sophie, Sumita, Vasilis) for the amazing memories, discussions, and congenial spirit in and out of the lab. Charades will never be the same.

To Ana Jesus Correia Da Silva for endless patience and always helping me troubleshoot spinning disk or the SP8 scopes.

To Dr Jeremy Metz for his assistance with all things related to automated image analysis.

To Dr Chris Sampson for his unparalleled insight into most matters related to academia, teaching, coding and nerdom, and especially for all the discussion and assistance in preparing to enter the British secondary school setting.

To Agnieszka Kaczmar for working tirelessly to provide excellent technical support and controlling her homicidal urges when receiving requests for last minute 8-sleeve apple juice plate orders.

To Amy, Alice, Ben, and Sadie, for being my second family when I first moved to Exeter and always making me feel welcome.

To Karolina for going literally above and beyond to help on multitude of occasions. For being the best personal cheerleader anyone could ask for. And for the unrestricted bathtub use for Lush bath bomb purposes, even if it does get occasionally spoiled by Java and his colon.

To my science super woman, Melanie Ort, for her unwavering enthusiasm, exquisite taste in tea and porridge, late night existential crisis emotional support and for reminding me why the long hours in the lab are worth it.

To Nec and Emrah, for feeding my stomach, heart and soul. For everything you have taught me.

To Gosia and Sławek, za wszelką pomoc gdy przyjechałam do Anglii, za traktowanie mnie jak swoją córkę i za słowa otuchy.

To Karolina, Kuba, Michael, and Christine, for their unconditional love, daily cat and pupper updates, and amazing care packages. Miss you, you goofy goobers.

To my parents, dziękuję Wam za niezachwiane wsparcie i wiarę w moją zdolność do ukończenia studiów w Wielkiej Brytanii. Mam nadzieję, że sprawiłam, że jesteście ze mnie dumni. Kocham Was.

And finally, to my life partner, Ahmet Furkan, hayatımın önemli bir parçası olduğun için ve bana hep ağladığım zaman omzunda bir yer verdiğin için teşekkür ederim. İlk adımı atamayacak kadar korktuğumda ve tembellik yaptığımda beni motive ettiğin için teşekkür ederim. Beni laboratuvardan ve sıkıntılı hayatımdan çıkarıp birçok yeni deneyimle tanıştırdığın içinde teşekkür ederim. Umarım akademik yolculuğuna devam ederken bana destek olduğun gibi ben de sana aynı desteği verebilirim. Hayatımın geri kalanını seninle geçirmeyi dört gözle bekliyorum. Kimseyi görmedim ben senden daha güzel, kimseyi tanımadım ben senden daha özel…

سبحان الله انتهيت من درجتي. شكرا لك على كل نعمك.

Abstract

Polo kinase, first identified in *Drosophila* over 30 years ago, is a highly conserved enzyme that functions pleiotropically during multiple stages of cell division. Members of this protein family have crucial roles in cell cycle progression, centriole duplication, mitosis, cytokinesis and the DNA damage response. Although some Polo substrates and regulatory mechanisms have been identified, we still lack complete understanding of the cellular and molecular roles of this kinase. Previous work in the Wakefield lab identified 40 proteins that physically interact with Polo in *Drosophila* embryos, but the functional significance of these components remains unknown. As genetic interaction screening can identify functional relationships between genes, I performed a highly sensitive assay called Variable Dose Analysis (VDA) in *Drosophila* S2R+ cells to determine which of the physical interactors also have genetic interactions with Polo. Inhibiting Polo using the selective small-molecule inhibitor BI-2536 and transfecting shRNA against the genes of interest allowed to easily screen cells based on their viability phenotype. Known Polo genetic interactors, Map205 and mtrm, were identified by the VDA screen, validating its robustness and utility in identifying genetic interactors. Fourteen genes were selected as hits, with components of the ubiquitination system enriched among them, particularly all member proteins of the Skp, Cullin, F-box containing complex (SCF complex). Six candidate polo interactors, SkpA, Cul1, slmb, Ck1α, Klp61F, and cher were selected for validation and further characterization of the interactions *in vivo.* Inhibition of Ck1α and slmb via RNAi resulted in larval lethality. Live imaging of SkpA RNAi and Cul1 RNAi larvae showed an increase in the cortical localization of polo-GFP during late anaphase/telophase. Together, these results suggest that polo may be degraded in an SCF-dependent manner in *Drosophila*. Further follow up work is needed to gain deeper insight into the relationship between the ubiquitination system and polo.

List of Contents

List of Figures

Abbreviations

AP	affinity purification
APC	anaphase promoting complex
GI	genetic interaction
KD	kinase domain
MS	mass spectroscopy
MT	microtubule
PBD	Polo-box domain
PPI	protein-protein interaction
RNAi	RNA interference
SAC	spindle assembly checkpoint
UAS	upstream activating sequence
VDA	Variable Dose Analysis

Chapter 1: Introduction

Cell division is a vital process essential for a single-celled fertilized egg to develop into a mature organism and for maintaining tissue integrity throughout an organism's lifetime. Moreover, it is a complex process involved in the regulation of DNA damage repair, tissue's response to injury, and diseases such as cancer.

The cell cycle is divided into interphase and M-phase. Interphase encompasses the S, G_1 and G_2 phases, the latter of which represent the gaps in the cell cycle that occur between the two major landmarks, DNA synthesis and mitosis (Morgan, 2007). In the first gap—G_1—the cell is preparing for DNA synthesis. During the S-phase, the cells are synthesising DNA, and therefore have intermediate DNA content between 2N and 4N (Morgan, 2007). The cell prepares for mitosis (M-phase) during the second gap, G_2. Cells that have withdrawn from the cell cycle are found in the G_0 phase (Williams & Stoeber, 2012).The G_0 phase was originally used to indicate a 'resting' phase, classifying cells with potential for division but not actively in the cycle. Now, G_0 can take different forms, such as quiescence and senescence, and occur for a variety of intrinsic and extrinsic reasons (Terzi, Izmirli, & Gogebakan, 2016).

1.1 Polo kinase is a key cell division regulator

The mitotic, or M-phase, of the cell cycle, is responsible for separating the replicated chromosomes into two genetically identical cells and requires a variety of signalling and regulatory proteins (Moura & Conde, 2019). Polo kinase was identified as a key mitotic regulator, with the striking ability to regulate multiple events at distinct subcellular locations and times.

Polo kinase was first identified in the fruit fly model organism, *Drosophila melanogaster,* almost 30 years ago (Sunkel & Glover, 1988). Homozygous *polo* mutants were found to be defective in both meiosis and mitosis. The embryos failed to form a fully developed embryo due to cells arresting at prometaphase and metaphase. The presence of mutant phenotypes of multipolar spindles, aneuploidy,

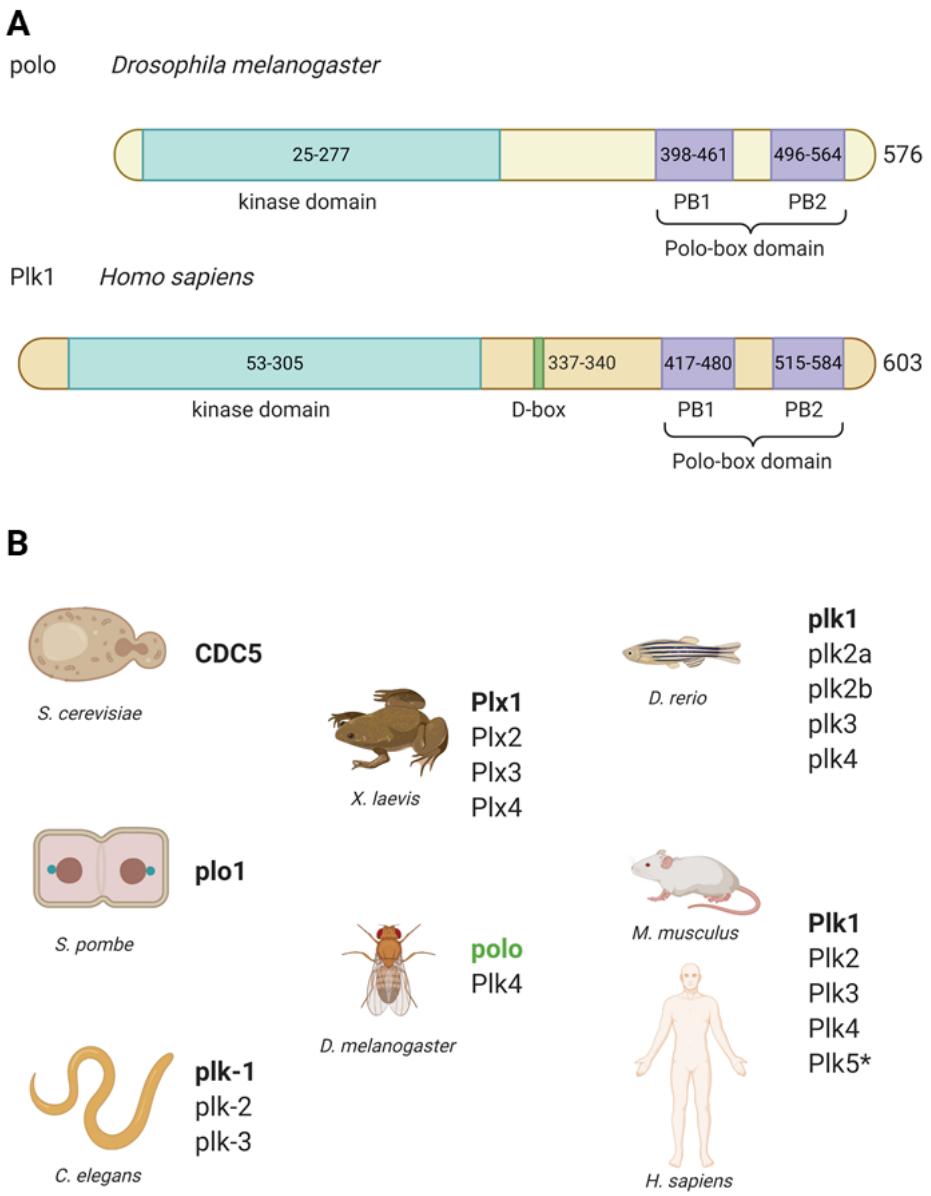

Figure 1. Introduction to the polo kinase.

A) Polo and its human orthologue, Plk1, contain an N-terminal catalytic kinase domain (teal) and a C-terminal polo-box domain (PBD) (purple). The PBD is composed of two similar Polo boxes (PB1 and PB2). The human protein also contains a D-box motif that targets the protein for proteasomal degradation in anaphase. B) Plk family members in different organisms. The founding member of the Polo-like kinase protein family, *Drosophila* polo is in green, with its direct orthologues in other species in bold. Plk5 (marked with an asterisk), is only found in mammals, but the human version is catalytically inactive as it contains a stop codon that produces a truncated protein lacking part of the KD.

A

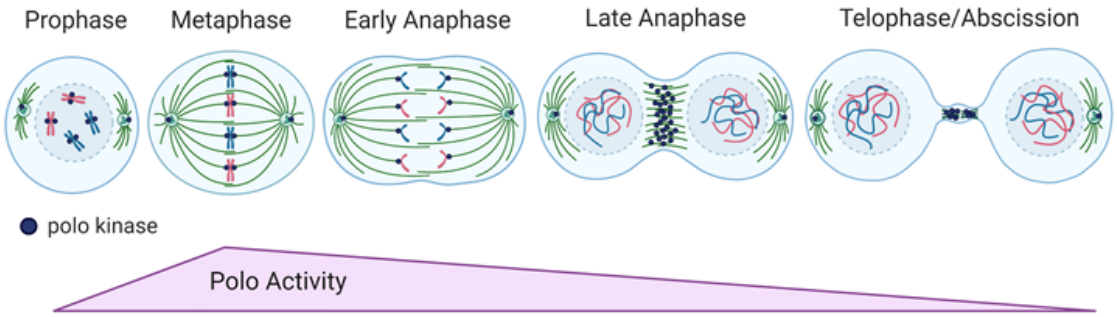

B

Stage of Mitosis	Sub-cellular Localisation	Potential Role at Locale
Prophase	Nucleus Cytoplasm Centrosomes	Mitotic entry and CDK1 activation Bipolar spindle formation APC/C inhibitor degradation Chromosome condensation
Prometaphase	Centrosomes Kinetochores	K-MT attachments MT nucleation Recruitment of PCM components Cohesion dissociation Golgi fragmentation
Metaphase	Centrosomes Kinetochores	APC/C-Cdc20 phosphorylation MT attachments Chromosome alignment at metaphase plate SAC inactivation
Anaphase	Centrosomes Kinetochores Midzone (MTs)	
Telophase/Abscission	Centrosomes Midbody	APC/C-Cdh1 activation Suppression of CEP55 prior to recruitment of ESCRT-complex

Figure 2. Polo kinase sub-cellular localisation and function during mitosis.

A) Polo kinase localizes to several discrete structures during mitosis via the PBD including centrosomes, kinetochores, and the spindle midzone, which resolves into the midbody during telophase. Gradient below (purple) represents relative polo activity changes between prophase and cytokinesis. B) Table outlining polo localization patterns with corresponding functions during M-phase. Adapted from *(van de Weerdt & Medema, 2005; Colicino & Hehnly, 2018)*.

abnormal centrosome structure and microtubule formation, and the localisation of the gene product to multiple mitotic structures suggested that polo was a crucial mitotic regulator needed for the proper establishment of the mitotic spindle (Sunkel & Glover, 1988)(Figure 2).

Its budding yeast, *Saccharomyces cerevisiae* equivalent, CDC5, was independently identified fifteen years earlier in early screens for genes required for cell cycle progression (Hartwell, Mortimer, Culotti, & Culotti, 1973). Both in *Drosophila* and yeast, *polo* is an essential gene for mitosis (Llamazares, et al., 1991; Kitada, et al., 1993). In 1994, the mammalian orthologue, Polo-like kinase 1 (Plk1) was identified (Golsteyn, Mundt, Fry, & Nigg, 1995). Since then, polo was found to be well-conserved between species (Figure 1B; reviewed in Archambault, et al., 2015), but markedly, absent in plants (Karpov, et al., 2010). polo and Plk1 in different species are clear orthologues at the sequence and functional level, and from herein are referred to collectively as 'Polo'.

polo is the founding member of the Polo-like kinase family, composed of five different genes, *Plk1* through *Plk5* in mammals (de Cárcer, Manning, & Malumbres, 2011b). Plk genes are characterized by the canonical N-terminal serine/threonine kinase domain (KD) and a C-terminal Polo-box domain (PBD; Figure 1A). Plks are activated by phosphorylation of the T-loop domain, which also allows them to convert ATP to ADP, transferring the phosphate group to other proteins (Kothe, et al., 2007). The two Polo boxes of Plk proteins fold together to form the functional Polo-box domain (PBD). The C-terminal PBD gives the protein family its identity and plays a pivotal role in the function of these enzymes (Elia, Cantley, & Yaffe, 2003a; Elia, et al., 2003b). PBD regulates the KD, and also confers binding specificity by bringing the KD into proximity of its substrates, mainly through phospho-dependent interactions with its target proteins (reviewed in Park, et al., 2010).

Polo controls a variety of processes during the cell cycle progression. It is necessary for DNA replication, chromosome condensation, and mitotic entry (reviewed in (Combes, Alharbi, Braga, & Elowe, 2017). It is also responsible for centrosome maturation, centromere assembly, Golgi fragmentation, spindle assembly and function, kinetochore function and cytokinesis (reviewed in Archambault, et al., 2015;

Colicino & Hehnly, 2018). Given its many functions in the cell cycle, unsurprisingly Polo has different subcellular localizations during the M-phase (Figure 2). Present in the cytoplasm and centrosomes during interphase, after the cell enters mitosis, Polo concentrates at the spindle poles after nuclear envelope breakdown. After the chromosomes condense, Polo localizes to the kinetochores, assisting in the proper chromosome alignment at the metaphase plate. In late anaphase Polo concentrates at the spindle midzone, which then resolves into the midbody ring, to coordinate cytokinesis and cell abscission (Petronczki, Lénárt, & Peters, 2008). Cells require a functional Polo for the proper progression through mitosis. Inhibition of Polo function makes the cells unable to establish a bipolar spindle, thus prohibiting chromosomes from aligning at the metaphase plate. This activates the Spindle Assembly Checkpoint (SAC), arresting cells at the prometaphase/metaphase stage until they eventually die. This mitotic arrest phenotype is conserved from yeast (Kitada, Johnson, Johnston, & Sugino, 1993) to *Drosophila* (Llamazares, et al., 1991) and higher mammalian organisms (Wachowicz, Fernández-Miranda, Marugán, Escobar, & de Cárcer, 2016).

The evolutionary conservation of Polo highlights the paramount role it plays in cellular division. However, relatively few cell cycle functions have been delegated to other Plks (Archambault & Glover, 2009). The main difference between mammalian Plk1 and Plk2 through 5, is the number of PBDs they contain, their expression pattern in tissues and throughout the cell cycle (Colicino & Hehnly, 2018). Plk4 (also known as Sak, or Plk4/Sak in *Drosophila*) has diverged to contain a single PBD and a cryptic PBD (de Cárcer, Manning, & Malumbres, 2011b). Its activity and localization is restricted to the centrosome where it is required for centriole duplication in *Drosophila* and human cells (Bettencourt-Dias, et al., 2005; Habedanck, Stierhof, Wilkinson, & Nigg, 2005) (humans also additionally require Plk2; Warnke, et al., 2004). Mammalian Plk2, Plk3 and Plk5 are predominantly expressed during interphase. In addition to its role in centriole assembly, Plk2 and its relative, Plk3, have been implicated as mediators of molecular composition and morphology of synapses (Seeburg, Pak, & Sheng, 2005). Plk3 is required for CycE expression and entry into S-phase in part by interaction with the Cdc25 phosphatase

(Zimmerman & Erikson, 2007). Plk2, Plk3 and Plk5 also contribute to the DNA damage response and cell cycle checkpoint (Bahassi, Myer, McKenney, Hennigan, & Stambrook, 2006; Archambault & Glover, 2009; Andrysik, et al., 2010; de Cárcer, Manning, & Malumbres, 2011b). Strikingly, Plk5 has lost its kinase activity in humans, nevertheless it is required during development in mammals (Andrysik, et al., 2010; de Cárcer, et al., 2011a).

1.2 Polo functions pleiotropically during cell division

Polo expression increases from late S phase to mitosis, when the kinase is most active. Polo is a major regulator of mitotic entry. It localizes to the nucleus during G2-phase, where it has many roles in the DNA damage checkpoint (Serrano & D'Amours, 2014). For instance, Polo is required to recruit the initial components of the DNA damage response (DDR), including ataxia-telangiectasia mutated (ATM) and ATM and RAD3-related (ATR) kinases (Hyun, Hwang, & Jang, 2014). Polo is then dephosphorylated in an ATM-Chk1 dependent manner, inactivating the kinase (Lee, Hwang, & Jang, 2010). This downregulates Polo activity until the completion of the DDR, in which Polo is newly activated by Aurora A and Bora (Seki, Coppinger, Jang, Yates, & Fang, 2008), allowing for cell entry into mitosis.

Deregulation of Polo kinase activity induces overriding the DNA damage checkpoint, which can lead to genomic instability and promotes cell transformation and tumourigenesis (Hyun, Hwang, & Jang, 2014; Wakida, et al., 2017). More recently, Polo was found to promote NOTCH1 down-modulation to the G_2-M transition which results in enhanced cell death but at the same time may allow the daughter cells to inherit a defective genome (De Blasio, et al., 2019).

One of the key roles of Polo kinase is the promotion of mitotic entry through activation of CycB/Cdk1, thus inhibiting Wee1 and Myt1 kinases, and activating the Cdc25 phosphatase (reviewed in van de Weerdt & Medema, 2005). Post mitotic entry, Polo regulates centrosome maturation and microtubule nucleation (Archambault, Lepine, & Kachaner, 2015). It is also a vital component of the spindle assembly checkpoint (SAC), during which it directs proper kinetochore-microtubule attachments and

activates the anaphase promoting complex (APC) (Combes, Alharbi, Braga, & Elowe, 2017). In prophase, Polo is involved in the indirect activation of the APC/C by inducing the destruction of Emi1, an APC/C inhibitor (Moshe, Boulaire, Pagano, & Hershko, 2004; Schmidt, et al., 2005).

Degradation of Polo by the APC/C starts in late mitosis and continues throughout G1. Late mitotic functions of Polo are hard to elucidate, as cells defective in Polo trigger the SAC and arrest in metaphase. One workaround would be to use chemical inhibitors that can rapidly affect Polo function in anaphase, after the SAC has been satisfied. Since molecules targeting the Polo KD can also affect other Plk family members, alternative methods of Plk1-specific depletion were needed. Borrowing a yeast strategy for monospecific kinase inhibition involving modifying the catalytic pocket to accept bulky purine analogues (Bishop, et al., 2000), Burkard and colleagues reported that Polo plays a role in cleavage furrow formation and cytokinesis (Burkard, et al., 2007).

1.3 Role of Polo at centrosomes, kinetochores and the midbody

1.3.1 Centrosome maturation and bipolar spindle formation

Polo is involved in centrosome maturation and separation. When it was first identified, the *Drosophila polo* mutants had defective, immature spindle poles (Sunkel & Glover, 1988). In *C. elegans,* Polo recruits pericentriolar matrix (PCM) components SPD-2 and SPD-5 (Woodruff, et al., 2017). In humans, centrosome maturation and recruitment of MT-nucleating components, such as γ-tubulin, and components of the PCM, e.g pericentrin, and CEP215, are dependent on Polo (Lane & Nigg, 1996; Lee & Rhee, 2011; Colicino, et al., 2018). The latter two are essential for recruiting additional PCM components like γ-turc. Inhibiting Polo phosphorylation sites on pericentrin, results in failure to recruit key PCM proteins, e.g. γ-tubulin, CEP192, and γ-turc (Lee & Rhee, 2011).

An early Polo antibody injection study showed that Polo function is essential for centrosome separation, evidenced by monopolar spindles and mitotic arrest (Lane & Nigg, 1996). Centrosome recruitment of Polo was shown to be dispensable for centrosome maturation and bipolar spindle formation, suggesting that Polo does not

need to be bound to centrosomes in order to carry out its centrosomal functions (Hanisch, Wehner, Nigg, & Silljé, 2005). Along with pericentrin, CEP215 and many others, Polo has been implicated in also controlling the orientation of the mitotic spindle (Chen C.-T. , et al., 2014; Hanafusa, et al., 2015; Miyamoto, et al., 2017). Coordination between the mitotic spindle and the subsequent cleavage plane is necessary for ensuring proper developmental outcomes (Moorhouse & Burgess, 2014). Asymmetrical spindle positioning in the dividing cell results in non-disjunction and daughter cells that are unequal in size (McCarthy & Goldstein, 2006). If the spindle is not positioned properly along the division axis it can cease the formation of different cell and tissue types within an embryo, causing downstream defects such as heart septation and microcephaly (Chen C.-T. , et al., 2014; Miyamoto, et al., 2017).

1.3.2 Kinetochore-MT attachments and chromosome alignment and separation

During prometaphase, microtubules of the spindle attach to the kinetochore, a complex of proteins associate with the centromere of a chromosome (Saurin, 2018). In general, increased Polo concentrations are found at the kinetochores in prometaphase. However, it is not exactly clear whether the spatial distribution of Polo within the kinetochore controls its access to substrates and subsequent do wnstream functions in this localisation. Spatial regulation of Polo signalling at the kinetochore remains enigmatic due to multiple Polo interactions and substrates along the kinetochore-centromere axis (Lera, et al., 2016).

In humans, Polo is localized to the kinetochores via initial recruitment by Bub1, BubR1 and NudC (Nishino, et al., 2006; Qi, Tang, & Yu, 2006; Suijkerbuijk, Vleugel, Teixeira, & Kops, 2012). There it phosphorylates BubR1 and CLASP, stabilising kinetochore-microtubule (K-MT) attachments thus promoting chromosome alignment (Suijkerbuijk, Vleugel, Teixeira, & Kops, 2012; Maia, et al., 2012). It also interacts with Kif2b to correct MT attachment errors, maintaining faithful chromosome segregation (Hood, Kettenbach, Gerber, & Compton, 2012). Chromosome dynamics also depend on Polo binding to members of the chromosome passenger complex (Goto, et al., 2006; Colnaghi & Wheatley, 2010). Experiments by Lera and colleagues support the model that Polo operates in pools

within the kinetochore, and at chromatin and the inner centromere in a manner distinct from its role in stabilising MT attachments to the outer kinetochore (Lera, et al., 2016).

1.3.3 Midbody assembly and regulation

After the cell enters anaphase/telophase, Polo transitions away from kinetochores and into the midzone, where it recruits RhoA GTPase and RhoGEF Ect2, allowing for cleavage furrow formation and cytokinetic bridge formation (Burkard, et al., 2007). Polo and numerous abscission proteins are enriched at the midbody (Chen, Hehnly, & Doxsey, 2012). Herein the function of Polo is to ensure faithful abscission. One such way is through phosphorylation of CEP55, preventing its association with the midzone (Bastos & Barr, 2010). Premature CEP55 integration into the midbody due to loss of Plk1 activity causes abscission failure, most likely through the rise of aberrant midbody architecture and failure to recruit ESCRT-III components (Colicino & Hehnly, 2018). The role of Polo at the midbody and cleavage furrow formation remains one of the least understood, despite recent research into the area.

1.4 Polo and cancer

Given Polo's many functions during the cell cycle, it is unsurprising that it is implicated in cancer. As outlined previously, mitotic arrest is the most known loss-of-function phenotype of Polo. However, both up- or downregulation of Plk1 can trigger defects in mitosis that result in aneuploidy and cause tumourigenesis in mammals (de Cárcer & Malumbres, 2014).

There is evidence that Plk1 overexpression is crucial for cancer progression in some tumours (Liu, Sun, & Wang, 2017). Plk1 can modulate tumour proliferation by controlling key oncogenic transcription factors, p53 and Myc (Ando, et al., 2004; Liu, Li, Song, & Liu, 2010; Xiao, et al., 2016; Ren, et al., 2018). Moreover, Polo levels affect oncogenic signalling pathways like the PI3K-MEKK (Li, et al., 2014) or dampen the function of known tumour suppressors such as PTEN or REST (Karlin, et al., 2014; Li, et al., 2014). However, all the experimental data therein has been collected

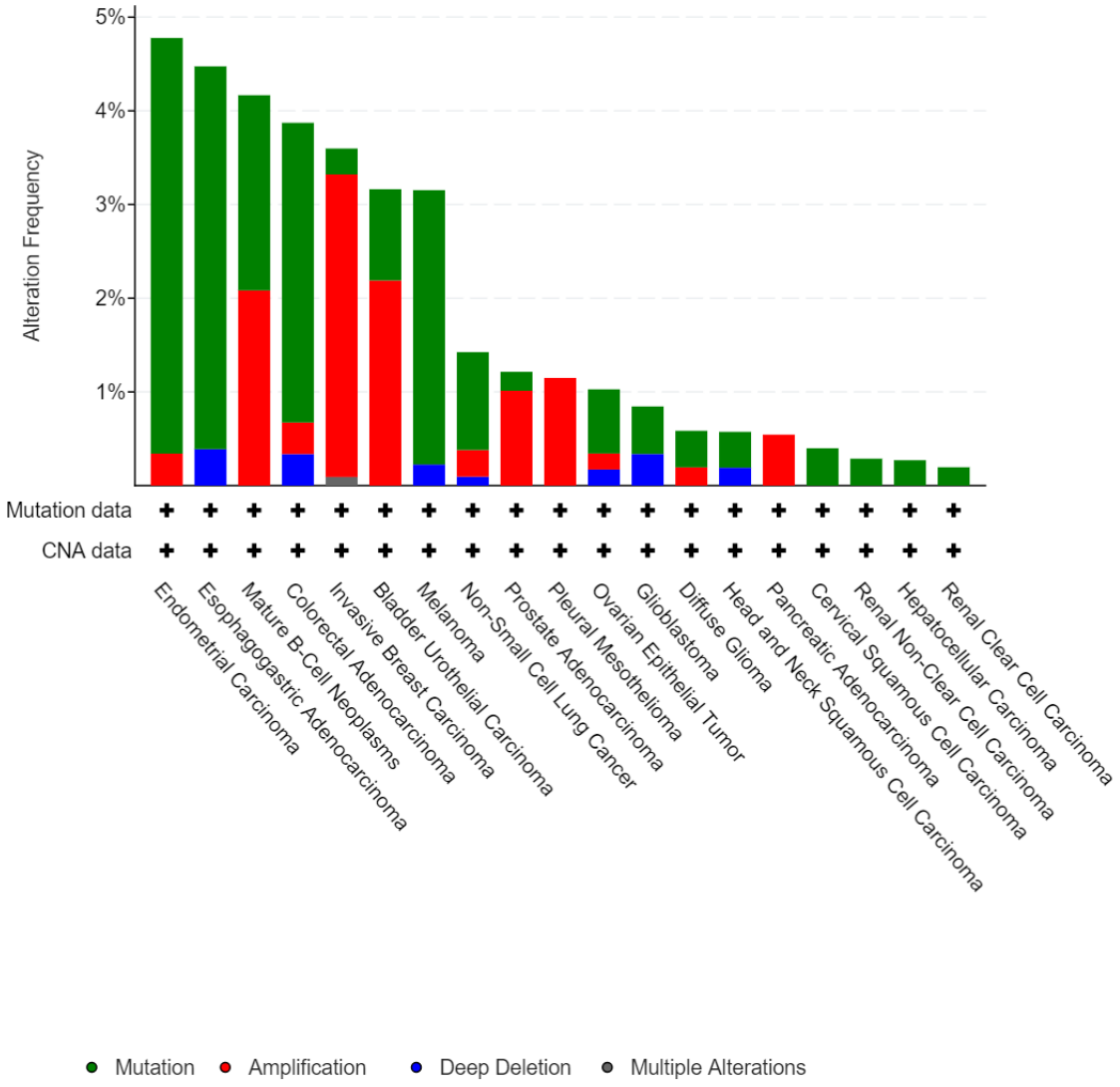

Figure 3. Prevalence of Plk1 alterations in human cancers. Polo function is most affected in uterine, stomach, colorectal, breast, and bladder cancers as well as melanomas. However, only 2% of 10,967 patient tumoural samples show an alteration in Polo (TCGA PanCancer Atlas Studies, cBioPortal for Cancer Genomics).

from cells that are already tumourigenic, indicating that Plk1 can contribute to tumour growth once it is already established, not necessarily that Polo can drive tumour proliferation by itself like a true oncogene (de Cárcer, 2019).

Whilst historically the scientific community has considered Polo as an oncogene, recent research in mouse models also suggests a possible tumour suppressor role in particular cancers, illustrating the duality of this kinase's roles in human cancers (Lu, et al., 2008; Wierer, et al., 2013; de Cárcer, et al., 2018; Raab, et al., 2018). In one of the earliest studies that proposed a tumour suppressor role for Plk1, a transcriptomics analysis in human breast cancer cells revealed that Plk1 is able to directly affect the estrogen receptor (ER)-dependent gene transcription profile (Wierer, et al., 2013). When Plk1 activity was inhibited via the Plk1-specific small molecule inhibitor BI-2536, the downregulated ER-dependent gene sets correlated with tumour-suppressive functions. Another report shows the beneficial effects of Plk1 activity in breast cancer. The histological expression analysis of Plk1 showed that breast tumours with higher levels of Plk1 have a better prognosis compared to the samples with very little to no Plk1 presence (King, et al., 2012). Recent knock-in mouse models have further validated the tumour suppressor role in breast cancer (de Cárcer, et al., 2018). Overexpression of the human Plk1 cDNA in the conditional inducible knock-in mouse revealed that these mice can tolerate high levels of Plk1 without significantly higher rates of tumour appearance when compared to control littermates that do not express Plk1. Surprisingly, when Plk1 expression in mammary glands was combined with mouse strains carrying either the *K-Ras* or *Her2* oncogenes, tumour formation was dramatically reduced in both cases; up to 85% and 50%, respectively (de Cárcer, et al., 2018; de Cárcer, 2019). Raab and colleagues showed the tumour suppression capacity of Plk1 in a colorectal cancer model (Raab, et al., 2018). When colon cancer mouse strains and cell lines with truncated adenomatus polypsis coli gene were treated with the Plk1 inhibitor volasertib (BI-6727) it led to an increased rate of development of colorectal adenomatous polyps compared to the control littermates/cells that had normal Plk1 expression levels.

Plk1 is rarely found mutated or amplified in tumours—only 2% of 10,967 patient tumoural samples show an alteration in Plk1 (TCGA PanCancer Atlas Studies, as

found on the cBioPortal for Cancer Genomics database, http://www.cbioportal.org; Figure 3). A study by Ng et al suggests that the mutations may happen at late stages of the tumoural progression (Ng, Shin, Wang, & Lee, 2017) This low mutation rate is probably due to the fact that Plk1 is absolutely essential to cell division, and therefore cells cannot cope well with its overexpression nor the loss of its function (de Cárcer, 2019).

Despite the low prevalence and complexity of Plk1 mutations in cancer, researchers started to explore the potential of anti-Plk1 therapeutic approaches for cancer treatment. Many studies reveal its remarkable prognostic role for cancer patients (reviewed in Liu, Sun, & Wang, 2017; de Cárcer, 2019). For example, high Plk1 expression levels are linked to poor outcomes for patients with squamous cell carcinomas of the head and neck (Knecht, et al., 1999), elevated levels of Plk1 expression are reliable markers to identify patients at high risk for metastases in melanomas (Kneisel, et al., 2002), and Plk1 depletion via siRNAs in pre-treatment biopsies from rectal cancer patients showed a radiosensitisizing effect, marking Plk1 as a novel predictive marker for radiation response and promising therapeutic agent (Rödel, et al., 2010).

Plk1 became a promising pharmaceutical target due to the fact that Plk1 was overexpressed in tumours and Plk1 inhibition stopped cancer cell proliferation (reviewed in Gutteridge, Ndiaye, Liu, & Ahmad, 2016). Several studies have shown that blocking Plk1 expression via RNA interference (RNAi) or kinase inhibitors can induce apoptosis of tumour cells and inhibit their proliferation (Steegmaier, et al., 2007; Bu, Yang, Li, & Song, 2008; Yuan, et al., 2011; Stehle, Hugle, & Fulda, 2015; Czaplinski, Hugle, Stiehl, & Fulda, 2016). One of the earliest Plk1 inhibitors, BI-2536 inhibits Plk1 enzyme activity at low nanomolar concentrations *in vitro* (Steegmaier, et al., 2007). It causes mitotic arrest and induces apoptosis in HeLa and 32 other human cancer cell lines, representing a diverse set of tissue origins (including the breast, colon, lung, pancreas, and prostate, melanomas, and hematopoietic cancers) and varied patterns of tumour suppressor or oncogene mutations (including RB1, TP53, PTEN, and KRAS status). The half-maximal effective concentration (EC_{50}) values in this cell panel ranged 2–25 nM, whereas a concentration of 100 nM of BI-2536 was typically sufficient for inducing a complete mitotic arrest in HeLa cells.

In mice, cells of human tumour xenografts treated with BI-2536 arrest in prometaphase, accumulate phosphohistone H3, and contain aberrant mitotic spindles, and subsequently entered apoptosis (Steegmaier, et al., 2007). BI-2536 was entered into early stages of clinical trials in patients with advanced solid tumours and was found to have an acceptable safety profile (Mross, et al., 2008; Hofheinz, et al., 2010; Frost, et al., 2012). However, it is no longer used in monotherapy approaches, most likely due to less than ideal response rates (Mross, et al., 2012). Nevertheless, BI-2536 remains the canonical Plk1 inhibitor and is widely used in non-clinical studies to specifically perturb Polo function or arrest cells during mitosis to further elucidate important mitotic functions of proteins of interest.

Interestingly, Plk1 was found to be involved in mechanisms related to resistance to several first-line anticancer drugs (e.g. doxorubicin, paclitaxel, metformin, and gemcitabine) most likely through its role in various signalling pathways (reviewed in Gutteridge, Ndiaye, Liu, & Ahmad, 2016). Consequently, pharmaceutical companies have expanded their portfolios to include Plk1 inhibitors—such as non-ATP competitive small molecule inhibitor rigosertib, and ATP-competitive GSK461364 which have entered clinical trials (Gutteridge, Ndiaye, Liu, & Ahmad, 2016) and volasertib which has reached phase III stages and a “breakthrough designation therapy” status by the FDA for combinatorial therapy for acute myeloid leukaemia and lung cancer (Van den Bossche, et al., 2016; Li, et al., 2020; Döhner, et al., 2014). Many of the small-molecule inhibitors that target the Plk1 KD can also inhibit the activity of other Plk family members, which can be problematic since Plk2 and Plk3 act as tumour suppressors. The newer generation of Plk1 inhibitors that target the PBD, such a Poloxin are being tested preclinically (Gutteridge, Ndiaye, Liu, & Ahmad, 2016). Given the vast knowledge of Plk1 structure/function relationship and regulatory mechanisms, advances can be made in developing drugs that may interfere more specifically with Plk1 functions, expanding its therapeutic potential in cancers.

1.5 Aims and objectives

The relatively small, highly evolutionarily conserved Polo kinase is critical to proper cell division and localises to many discrete cellular structures during mitosis. Since

its initial discovery in *Drosophila,* four other proteins have been added to this family of kinases. In humans Polo KD and PBD domains are capable of reciprocal allosteric inhibition and activation. Protein interactions with the PBD not only dictate substrate recognition and sub-cellular localization of Polo, they also control the activity of the KD. While only a select number of Polo binding substrates have been confirmed, we are still far from having a completed Polo interactome. Numerous studies have demonstrated that the sub-cellular and spatio-temporal distribution of Polo is regulated through its substrates, necessitating a better understanding of its interactors. This thesis aims to fill this gap by **pursuing a functional characterization of 40 identified Polo physical interactor proteins in *Drosophila*.**

Among the many approaches to identifying functional relationships among genes, genetic interaction screening remains one of the most accessible strategies. Genetic interactions (GIs) reveal functional relationships between genes and pathways when there is a significant deviation of the phenotype when two or more genes have been disrupted, from what is expected based on the phenotype resultant from each gene when disrupted alone (Fisher, 1919). A GI can only imply that the two genes involved share a functional relationship. These genes may be involved in the same biological process or pathway, or they may be involved in compensatory pathways (Boucher & Jenna, 2013). Genetic interaction screens, in which pairs of genes are targeted, are a powerful method to gain insights into the structure and function of biological processes and networks (Tong, et al., 2004; Fischer, et al., 2015). Inhibiting Polo function and the expression of its interacting partners and observing the consequent effects on a chosen phenotype would allow me to identify any GIs and therefore shed light on the functional relationship between the two proteins.

To identify potential genetic interactions between Polo and its physical interactors, I aimed to:

1) identify genetic interactions with Polo by performing a highly sensitive assay called Variable Dose Analysis (VDA) in *Drosophila* S2R+ cells (Housden, et al., 2017; Sierzputowska, Baxter, & Housden, 2018)

2) characterise the candidate Polo genetic interactors *in vivo* by disrupting their function via the UAS/Gal4 system

1.6 In vivo gene silencing in *Drosophila*

Drosophila as a model organism contains a vast genetic toolbox to analyze most any process at the researcher's disposal. The yeast Gal4/UAS system has proven to be a highly successful and versatile system for targeted gene expression and has morphed into the gold standard for the analysis of gene function in the fly.

1.6.1 Gal4/UAS transcriptional activation system

The yeast Gal4 protein regulates genes induced by galactose (Guarente, Yocum, & Gifford, 1982) by binding to short, defined DNA sequences upstream of target genes (upstream activating sequence, or UAS). Gal4 can bind cooperatively in the presence of multiple, tandem UAS sites for further enhancement of gene expression (Giniger, Varnum, & Ptashne, 1985; Giniger & Ptashne, 1987). Gal4 is inactive in the absence of galactose, due to the repressor protein Gal80, which inhibits its interaction with the transcriptional machinery (Johnston, Salmeron, & Dincher, 1987; Ma & Ptashne, 1987).

This mechanism for transcriptional activation is conserved throughout eukaryotes, following demonstration that Gal4 expression was capable of stimulating transcription of a reporter gene under UAS control in *Drosophila* (Fischer, Giniger, Maniatis, & Ptashne, 1988) and mammalian cells (Kakidani & Ptashne, 1988). In 1993, Andrea Brand and Norbert Perrimon published their landmark article describing the development of the bipartite Gal4/UAS system for targeted gene expression in *Drosophila* (Brand & Perrimon, 1993). In this approach, the responder, or gene of interest under UAS control, and the Gal4 driver are maintained as separate parental lines. The resultant progeny then expresses the responder in a transcriptional pattern that reflects the pattern of the respective driver. This system can be used to target expression of any responder in a variety of spatial and temporal fashions. Herein, the Gal4/UAS system is used for targeted gene knockdown during early *Drosophila* development.

The RNAi is under the control of a minimal promoter that needs the transcription activator protein Gal4 bound to the enhancer sequence UAS to allow transgene expression. The RNAi is unexpressed without the presence of the Gal4 protein. Gene silencing occurs in the progeny in specific tissues or developmental stages depending on the specific promoter of Gal4 used (see Figure 8A).

Over 7,000 transgenic driver lines that confer specific patterns of Gal4 activity are currently available to *Drosophila* researchers, as well as over 13,000 lines with genes under UAS control, majority of which were generated by the Transgenic RNAi Project at the Harvard Medical School[1]. Since its inception, the Gal4/UAS system has undergone extensive creative modifications such as cellular and sub-cellular marking using fluorescent reporters (reviewed by (Duffy, 2002)) and has been adopted in other model organisms (Halpern, et al., 2008).

[1] https://bdsc.indiana.edu/stocks/gal4/gal4_all.html; https://bdsc.indiana.edu/stocks/rnai/rnai_all.html; http://fgr.hms.harvard.edu/fly-in-vivo-rnai

Chapter 2: *in vitro* results

Identification of Polo genetic interactors via RNAi screening

Protein-protein interactions (PPIs) are essential to almost every process in a cell. Understanding PPIs is crucial to understanding cellular and molecular machinery as many proteins perform their functions within cells in the context of protein complexes. Knowledge of a specific protein's PPI can help elucidate thorough detail about its role within a signaling pathway or characterize the relationship between proteins that form multi-molecular complexes (reviewed by Safari-Alighiarloo, Taghizadeh, Rezaei-Tavirani, Goliaei, & Peyvandi, 2014). Mapping Polo's PPIs can shed more light on how this kinase achieves its spatio-temporal distribution and regulation.

Despite its discovery over 30 years ago, we still lack a complete understanding of Polo kinase and its cellular and molecular roles. Given its pleiotropic functions during the cell cycle, Polo has a vast network of substrates and wide participatory function in a variety of signaling pathways. Although some of Polo's upstream regulators and downstream targets have been reported, the complex relationships of this kinase have not been definitively characterized.

Previously unpublished work in the Wakefield lab set out to identify physical interactors of Polo in *Drosophila* syncytial embryos using a mass spectrometry (MS)-based approach (Figure 4). Syncytial embryos undergo 13 rapid mitotic divisions in the absence of zygotic transcription and contain a large amount of mitotic proteins, making them an ideal model to study Polo function. Using a pipeline based on GFP-TRAP-A affinity purification and mass spectrometry (AP-MS) combined with bioinformatics-based removal of non-specific contaminants, 40 polo-GFP interacting partners were identified (see (Palumbo, et al., 2015) for thorough method description). The list of physical interactors was inputted into the PANTHER GO enrichment analysis tool[2] to identify which (if any) functional classes were found to be particularly enriched based on their biological process gene ontology terms (Ashburner, et al., 2000; Mi, et al., 2019) (Figure 4).

[2] http://pantherdb.org/

Gene symbol	GO—molecular function	GO—biological process
Bruce	Ub-like protein conjugating enzyme activity, Ub-protein transferase activity	protein polyubiquitination, Ub-dependent protein catabolic process, programmed cell death, regulation of cytokinesis, negative regulation of apoptotic process
Cen	protein binding	embryonic cleavage
CG10254	ubiquitin-like protein conjugating enzyme activity, ubiquitin-protein transferase activity	protein polyubiquitination
CG10289	phosphoprotein phosphatase activity, protein phosphatase binding,	protein dephosphorylation, regulation of phosphoprotein phosphatase activity
GCS2α	hydrolase activity, hydrolysing O-glycosyl compounds, carbohydrate binding, alpha-glucosidase activity	carbohydrate metabolic process, N-glycan processing
CG16935	oxidoreductase activity, acting on the CH-CH group of donors, NAD or NADP as acceptor	fatty acid metabolic process
CG17018	mRNA binding, protein-containing complex binding	gene expression, posttranscriptional gene silencing
CG3342	–	–
CG9062	Ub binding	double-strand break repair via homologous recombination, protein deubiquitination
cher	actin binding	cytoplasmic transport, actin assembly, regulation of cytoskeleton organization, actin crosslink formation, syncytial embryo cellularization
Ck1α	protein serine/threonine kinase activity	negative regulation of canonical Wnt signalling pathway, peptidyl-serine phosphorylation
cmet	ATP binding, MT binding, plus-end-directed MT motor activity	mitotic cell cycle, MT-based movement, mitotic metaphase plate congression, regulation of cell cycle
coil	–	Cajal body organization
Cul1	Ub-protein transferase activity, Ub protein ligase binding	protein ubiquitination
dco	protein serine/threonine kinase activity	proteasome-mediated Ub-dependent protein catabolic process, positive regulation of canonical Wnt signalling pathway, membrane invagination, endocytosis, peptidyl-serine phosphorylation
dlt	–	morphogenesis of a polarized epithelium, chromatin organization, imaginal disc morphogenesis, olfactory behaviour, regulation of cell population proliferation
gammatub 37C	GTPase activity, structural constituent of cytoskeleton, GTP binding	mitotic spindle organization, mitotic sister chromatid segregation, MT polymerization, meiotic nuclear division
Grip84	MT binding	spindle assembly, mitotic nuclear division, MT polymerization, cytoplasmic MT organization, meiotic nuclear division
Grip91	MT binding	spindle assembly, mitotic nuclear division, MT polymerization, cytoplasmic MT organization, meiotic nuclear division
Hsp68	ATPase activity, ATP binding, heat shock protein binding, unfolded protein binding	determination of adult lifespan, vesicle-mediated transport, cellular response to unfolded protein, protein refolding, response to starvation, chaperone cofactor-dependent protein refolding
Hsp70b	ATPase activity, ATP binding, heat shock protein binding, unfolded protein binding	response to hypoxia, response to unfolded protein, response to heat, vesicle-mediated transport, protein refolding, chaperone cofactor-dependent protein refolding
Imp	mRNA binding	regulation of gene expression
klp10a	ATPase activity, MT motor activity, MT binding	MT-based movement
Klp61f	ATP-dependent MT motor activity, plus-end-directed	mitotic cell cycle, MT bundle formation, MT-based movement, Golgi organization, mitotic spindle organization, centrosome separation
loki	protein serine/threonine kinase activity, ATP binding, tau-protein kinase activity	DNA damage checkpoint signalling, regulation of DNA repair, protein phosphorylation, apoptotic process, mitotic DNA damage checkpoint signalling
Map205	MT stabilisation	mitotic cell cycle, centrosome cycle
milt	myosin binding	protein targeting, mitochondrion distribution, vesicle transport along MT
msps	catalytic activity, transferase activity, MT binding	centrosome duplication, mitotic spindle organization, establishment or maintenance of cell polarity, mitotic nuclear division, MT polymerization
mtrm	–	female meiosis chromosome segregation, distributive segregation, homologous chromosome segregation, regulation of meiotic cell cycle, regulation of cell cycle
mus101	–	DNA replication initiation, mitotic G2 DNA damage checkpoint signalling, mitotic DNA replication checkpoint signalling
Pli	ubiquitin protein ligase activity	protein polyubiquitination, cell surface receptor signalling pathway
polo	protein serine/threonine kinase activity, protein binding, ATP binding	membrane fission, mitotic nuclear division, regulation of cytokinesis, cytokinesis
SkpA	protein binding	SCF-dependent proteasomal ubiquitin-dependent protein catabolic process
slam	–	cellularization, protein localization, germ cell migration, cleavage furrow formation, membrane organization, syncytial embryo cellularization
sle	–	nucleolus organization
slmb	protein dimerization activity, phosphoprotein binding, molecular adaptor activity, beta-catenin destruction complex binding, Ub ligase-substrate adaptor activity	protein (poly)ubiquitination, proteolysis, regulation of mitotic nuclear division, circadian rhythm, SCF-dependent proteasomal Ub-dependent protein catabolic process
SmD2	RNA binding	spliceosomal snRNP assembly
sxc	catalytic activity, acetylglucosaminyltransferase activity	protein O-linked glycosylation, glycoprotein metabolic process, response to temperature stimulus, regulation of gene expression, wing disc development
tacc	protein binding, MT binding	MT cytoskeleton organization, mitotic cell cycle, negative regulation of microtubule depolymerization, mitotic spindle organization, nuclear migration
toc	MT binding	syncytial blastoderm mitotic cell cycle
WDR79	RNA binding, box C/D RNA binding	Cajal body organization

Figure 4. Polo physical interactors identified via GFP-TRAP/MS.

0-3 hour-old polo-GFP expressing *Drosophila* embryos were affinity purified and analysed via mass spectrometry (MS). After stringent filtering, a set of 40 physical interactors of polo-GFP were identified. The table shows the gene ontology (GO) terms for molecular function and biological process for each interactor. A maximum of 5 biological process GO terms are shown for summary purposes. PANTHER statistical overrepresentation test reveals three functional classes to be particularly enriched: microtubule-associated proteins (green; 25-fold enrichment), proteins involved in ubiquitin-mediated proteolysis (blue; 96-fold enrichment) and cleavage furrow formation (orange; 44-fold enrichment). (Unpublished data, Wakefield lab).

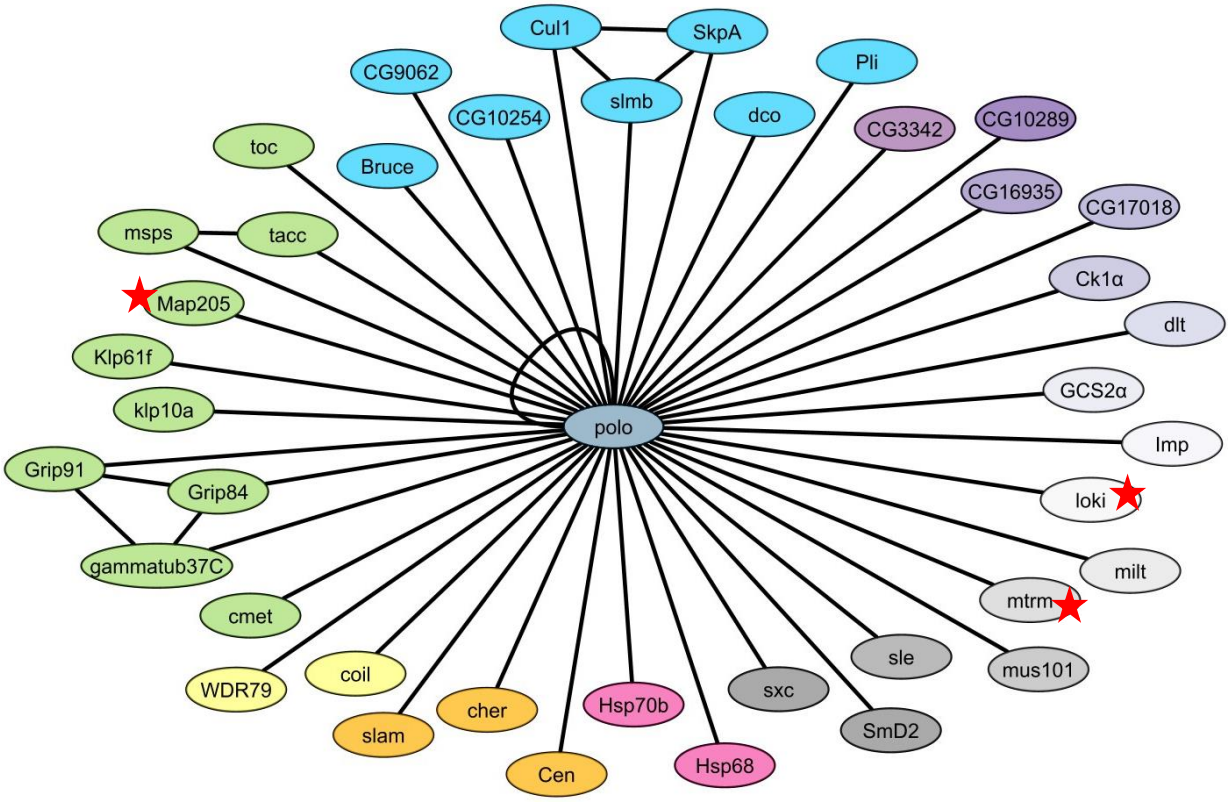

Figure 5. Protein-protein interaction network of identified Polo physical interactors.

PPI network showing the relationships between Polo and its physical interactors. Colour-coding represents genes with similar biological process GO terms: response to unfolded protein (pink), Cajal body organisation (yellow), cleavage furrow formation (orange), MT-associated proteins (green), proteins involved in ubiquitin-mediated proteolysis (blue). Map205, loki and mtrm (red stars) are known polo functional interactors. (Unpublished data, Wakefield lab).

Unsurprisingly, given Polo's functions during mitosis, MT-associated proteins and proteins involved in cleavage furrow formation were enriched (25-fold and 44-fold enrichment, respectively) (Figure 4). Moreover, proteins involved in ubiquitin-mediated proteolysis represented the highest enriched class, with over 96-fold enrichment (Figure 4). Mammalian Polo, like many other mitotic regulators, is targeted for destruction through the ubiquitin-proteasome mediated degradation pathway at the end of mitosis (Ferris, Maloid, & Li, 1998). Although *Drosophila* Polo lacks the D-box motif, many proteins are degraded in a proteasome-dependent mechanism (Ou, Pi, & Chien, 2003) and several phosphorylation sites have been identified in the inter-domain linker region which may play a role in poly-ubiquitination and subsequent degradation of Polo (Zhai, Villén, Beausoleil, Mintseris, & Gygi, 2008). Studies have also shown that (de)ubiquitination of residues in the PBD play a major role in regulating the recruitment of Polo to its many sub-cellular localizations, such as kinetochores (Liu & Zhang, 2017). Three known Polo genetic interactors, matrimony (mtrm) (Xiang, et al., 2007), loki (also known as Chk2) (Xu & Du, 2003), and Map205 (Archambault, D'Avino, Deery, Lilley, & Glover, 2008) were classified among the "top hits", validating the filtering approach at identifying "true" polo-GFP interacting proteins (Figure 5).

The term 'protein interaction' encompasses a variety of events, such as transient and stable complexes, as well as physical interactions. PPI detection methods typically do not reveal information associated with the context in which the interactions are realized, nor their directionality and effect, which is crucial in a signaling context for kinase-substrate interactions (Smits & Vermeulen, 2016). Hence, further work was needed to functionally characterize the identified physical interactors, as the GFP-TRAP-A/MS technique does not reveal the temporal nature, transient versus stable, of the identified protein interaction. This presented the starting point of research work contained herein—elucidating the functional nature of Polo PPIs in the *Drosophila* syncytial embryo.

2.1 Identifying Polo genetic interactors

One common approach to identify the functional relationship between genes is to look at whether they possess a genetic interaction (see Chapter 1). Carrying out a GI screen with polo and its physical interactor genes identified via GFP-TRAP-A/MS would help elucidate their functional relationships.

Several approaches, including RNAi- and CRISPR-based methods, have been developed for high-throughput genetic screening. A novel RNAi high throughput screening method called Variable Dose Analysis (VDA) was developed recently in *Drosophila* S2R+ cells (Housden, et al., 2017; Sierzputowska, Baxter, & Housden, 2018). S2R+ cells are an isolate of the original *Drosophila* S2 line derived from late-stage male embryos that express receptors for wingless signalling (Schneider, 1972; Yanagawa, Lee, & Ishimoto, 1998; Lee, et al., 2014; Stoiber, Celniker, Cherbas, Brown, & Cherbas, 2016). It is a workhorse cell line[3] that has been used extensively in previous genetic screens (Guest, et al., 2011; Kondo & Perrimon, 2011; Dopie, et al., 2015; Bassett, Kong, & Liu, 2015) and in studies involving Polo (D'Avino, et al., 2007; Conde, et al., 2013).

VDA assays are performed by co-transfecting cells with RNAi against the gene of interest that can easily be expressed from a DNA plasmid (shRNA) and a second plasmid expressing a fluorescent reporter protein (i.e. GFP). As the two plasmids are coupled together during transfection, fluorescent protein expression can be used as an indirect readout of shRNA expression and therefore target gene knockdown efficiency (Figure 6A). The knockdown efficiency in each cell can be measured via flow cytometry, and the relationship between the efficiency of target gene disruption and a feature of interest analysed in order to detect phenotypes. This differs from previously described methods, which typically measure the average phenotype over a population of cells and results in approximately a 2.5-fold increase in signal-to-noise ratio compared to standard dsRNA methods (Housden, et al., 2017). In addition, a great advantage of VDA is that it facilitates the study of essential genes because phenotypes can be measured at sub-lethal knockdown efficiency.

[3] Over 590 references associated on Flybase: http://flybase.org/reports/FBtc0000150.html

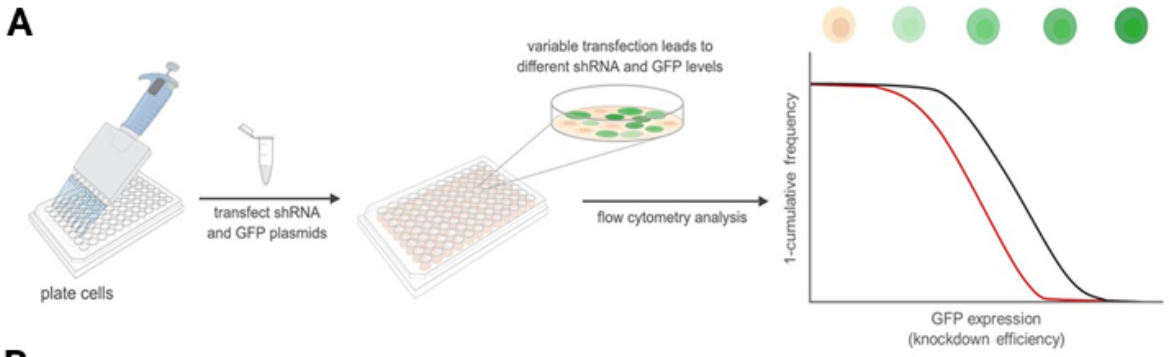
A
plate cells
transfect shRNA
and GFP plasmids
variable transfection leads to
different shRNA and GFP levels
flow cytometry analysis
1-cumulative frequency
GFP expression
(knockdown efficiency)

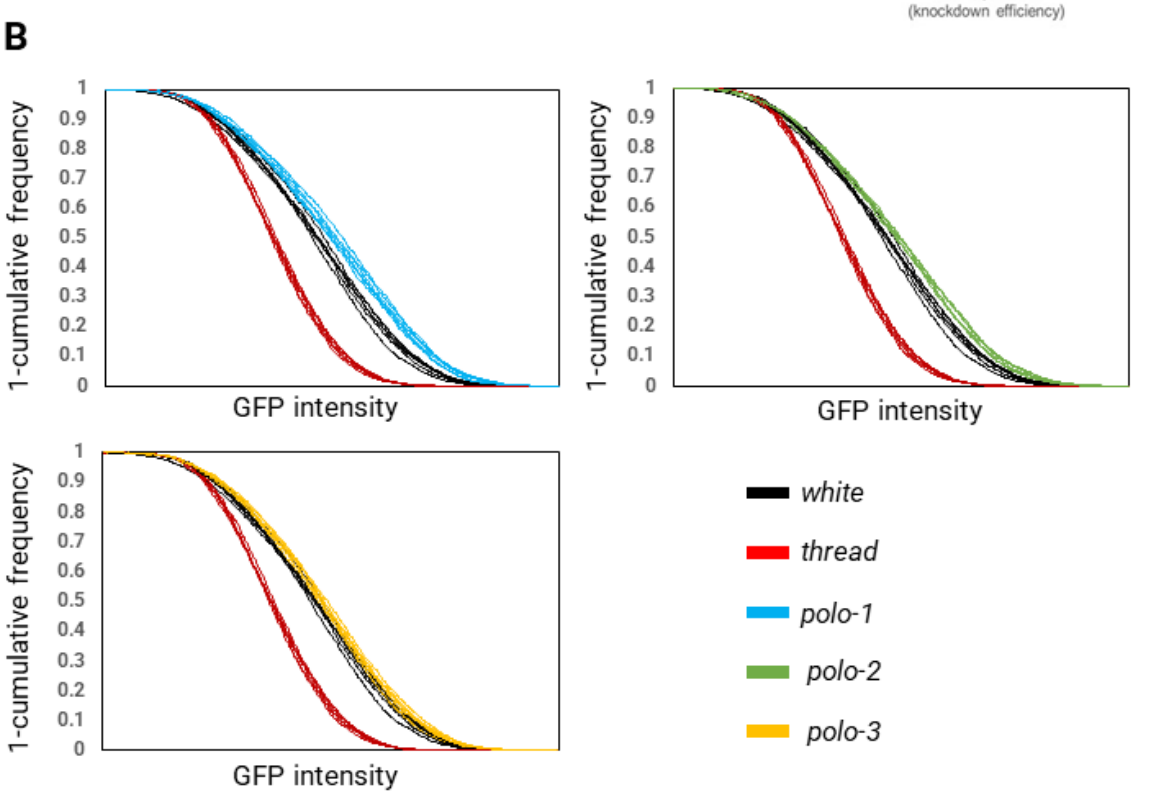
B
1-cumulative frequency
GFP intensity
white
thread
polo-1
polo-2
polo-3

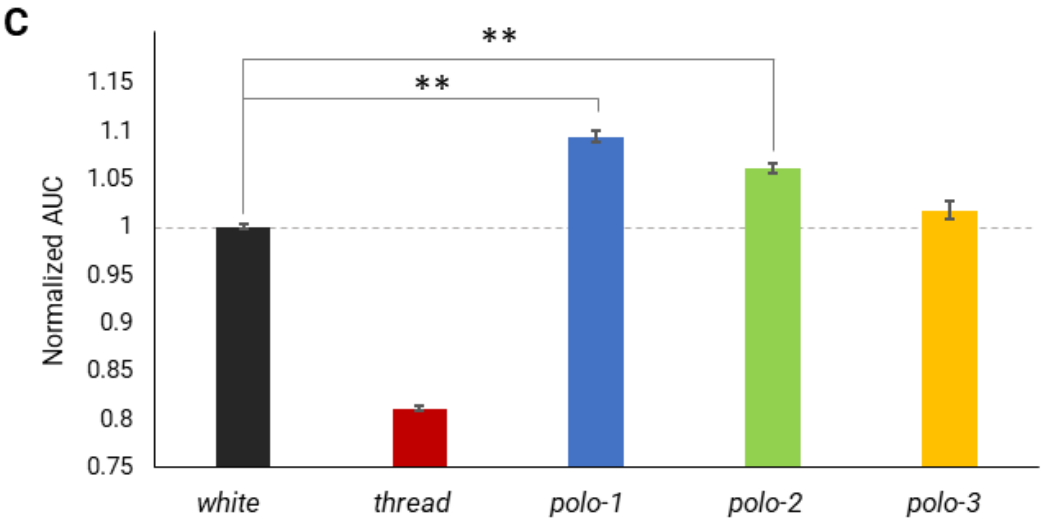
C
Normalized AUC
**
**
white
thread
polo-1
polo-2
polo-3

Figure 6. RNAi screening approach to identify Polo genetic interactors.

A) Schematic depicting the VDA screening workflow. Negative control curve in black, positive control (RNAi with effect on viability) shown in red.

B) Inverted cumulative GFP distribution plots for *polo,* the negative control *white* (black), positive control *thread* (red). The three shRNAs for the *polo* gene are shown separately for maximum clarity (polo-1, blue; polo-2, green; polo-3, yellow). The same effect of curve shifting to the right of *white* can be seen across all three RNAi reagents.

C) Bar graph of area under the curve (AUC) generated in (B). Error bars represent SEM for 3 biological replicates of 6 wells per each target gene (20,000 cells analysed per well) in a single 96-well plate. Area has been normalized to the *white* negative control. A statistically significant shift to the right occurs in two out of the three shRNAs (two-tailed t-test, **p<0.01).

In the context of this research project, a comparison of phenotypes measured using VDA screens against candidate genes in wild type cells and cells with disrupted *polo* would identify *polo* genetic interactors which then could be further analysed for their functional relationships. Given Polo's role in the cell cycle, it was hypothesized that disrupting *polo* would cause an effect on cell viability as cells would no longer be able to divide properly, and any mitotic defects would trigger apoptosis. Moreover, effects on viability are easily visualized and quantized in VDA screening. Therefore, cell viability was selected as the phenotypic readout in the screen.

When we plot the GFP distribution, we can see a clear separation between controls, such as a lethal RNAi or a negative control that has no effect on cell viability (Figure 6A). In the case of the lethal RNAi, the population of cells that took up more GFP (and therefore more of the lethal RNAi reagent) dies more quickly prior to the cytometry readout, causing a curve shift to the left compared to the negative control. Measuring the difference in the areas under the curve gives a numerical read out of the difference in viability.

2.1.1 VDA screen to identify polo genetic interactors

A shRNA library was generated for the candidate interactor genes (3 shRNAs per each gene of interest) including the negative control gene *white*—a well-characterized gene known to have no viability effect in S2R+ cells, and the positive control gene *thread*—an apoptosis inhibitor which robustly induces cell death when inhibited (see Appendix A). Prior to performing the screen in semi high-throughput format, it was important to optimize the assay to establish 3 important aspects of the VDA assay: (1) appropriate levels of *polo* inhibition in order to detect GIs, (2) identifying the *polo* knockdown phenotype, and (3) verifying that GIs can be successfully identified in this particular experimental setup.

As explained earlier, BI-2536 is a well-known small molecule inhibitor specific to Polo (Steegmaier, et al., 2007). Cell viability assays were performed to identify whether Polo inhibition with BI-2536 resulted in reduced cell viability (Figure 7A). Concentration as low as 20 nM was sufficient to cause a 20% decrease in cell viability, and 50 nM concentration caused an 80% decrease in cell viability.

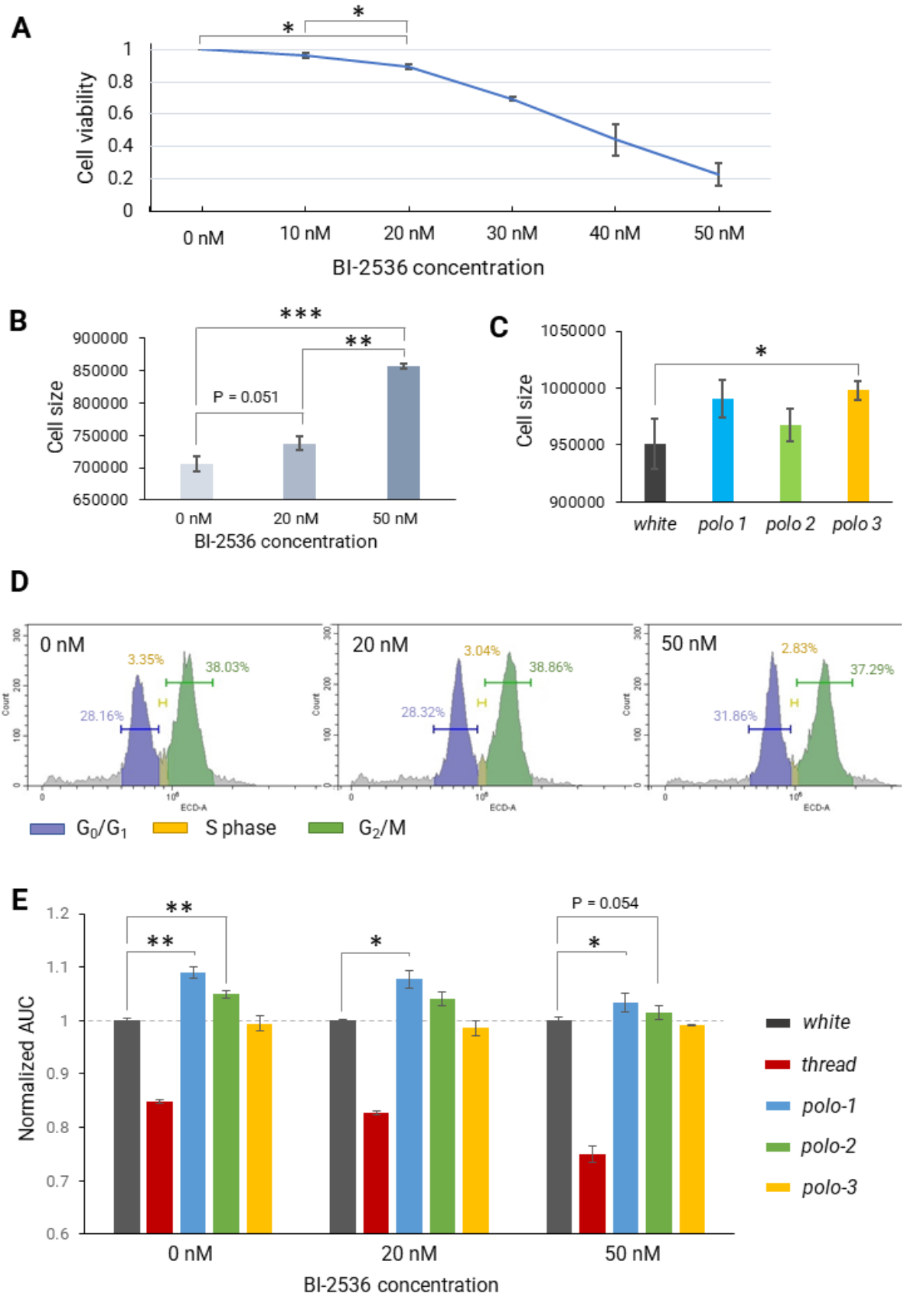
A
Cell viability
1
0.8
0.6
0.4
0.2
0
0 nM
10 nM
20 nM
30 nM
40 nM
50 nM
BI-2536 concentration
B
Cell size
900000
850000
800000
750000
700000
650000
P = 0.051
0 nM
20 nM
50 nM
BI-2536 concentration
C
Cell size
1050000
1000000
950000
900000
white
polo 1
polo 2
polo 3
D
0 nM
3.35%
38.03%
28.16%
20 nM
3.04%
38.86%
28.32%
50 nM
2.83%
37.29%
31.86%
ECD-A
G0/G1
S phase
G2/M
E
Normalized AUC
1.2
1.1
1
0.9
0.8
0.7
0.6
P = 0.054
0 nM
20 nM
50 nM
BI-2536 concentration
white
thread
polo-1
polo-2
polo-3

Figure 7. Polo viability phenotype characterisation.

A) Serial dilutions of the selective Polo inhibitor BI-2536. Luminescence-based cell viability assays were carried out to identify concentrations of BI-2536 that result in about 20% and 80% decrease in cell viability. Even at low BI-2536 concentrations there is a statistically significant decrease in cell viability compared to the 0 nM ethanol-only loading control (*$p<0.05$), and there is a trend in decreased cell viability with increasing BI-2536 concentration ($p<0.001$, not shown on graph). 40 nM and 50 nM BI-2536 produce similar effects on cell viability (no significant difference, $p>0.05$). Error bars represent the SEM of the average luminescence of 3 biological replicates of 10 wells of cells at each concentration.

B) Effect of *polo* inhibition using BI-2536 on cell size. As concentration of BI-2536 increases, the cell size increases. There is a significant difference between the cell size of the ethanol-only loading control (0 nM) and 50 nM BI-2536 (***$p<0.001$). The forward scatter (FSC) reading is used as a proxy for cell size Error bars show SEM of the cell size for 10 wells of cells per each condition (10,000 cells analysed per each well).

C) *polo* inhibition using shRNA slightly affects cell size. Using FSC as a proxy for cell size, an increase in cell size can be observed with each shRNA, however, it only polo-3 shows statistical significance (*$p<0.05$). Error bars represent SEM for 6 wells per gene, 20,000 cells analysed per well.

D) Cell cycle analysis using propidium iodide. Plot of cell count vs fluorescence intensity (ECD channel). *polo* inhibition using BI-2536 in S2R+ cells causes a slight accumulation of cells in G_0/G_1.

E) VDA results for *polo* in the presence of BI-2536. Error bars represent SEM for 3 biological replicates of 6 wells per each target gene (20,000 cells analysed per well) in a single 96-well plate. AUC has been normalized to the *white* negative control. A shift to the right with various levels of statistical significance can be observed for two of the *polo* shRNAs at each BI-2536 concentration (*$p<0.05$, **$p<0.01$).

Next, the resultant polo phenotype in VDA was tested. Three separate shRNA designs against *polo* were co-transfected with GFP using an optimized VDA protocol (Sierzputowska, Baxter, & Housden, 2018). Surprisingly, *polo* knockdown did not have the expected effect on cell viability. Given its crucial role in the cell cycle, it was predicted that silencing *polo* would cause cell death. However, the GFP intensity curve for *polo* shifted to the right instead of towards the positive control *thread* (Figure 6B-E). Previous studies have reported that *polo* inhibition causes mitotic delay or arrest, which in turn would explain the lack of dilution of the GFP signal.

To test whether induced mitotic arrest could explain the observed shift, cell size of wild-type cells and cells with *polo* inhibited chemically via BI-2536 or shRNA was compared. Inhibition of *polo* function with BI-2536 shows that increasing BI-2536 concentration causes an increase in cell size, with 50 nM BI-2536 (Figure 7B) causing a statistically significant increase compared to the 0 nM BI-2536 ethanol-only loading control ($p<0.05$). Inhibiting *polo* via RNAi shows that cell size increases, albeit not significantly in two of the shRNAs ($p<0.05$ for polo-3) (Figure 7C). The more pronounced effect on cell size with chemical disruption of *polo* can be explained by the fact that chemical inhibition is assessing a single level of disruption across all cells in the population. By contrast, the VDA assay measures effects at many different knockdown efficiencies. Therefore, the cell size effect may be diluted by cells with weak knockdown that have no phenotype or cells with very strong knockdown, which may have entered apoptosis.

Next, to test whether the S2R+ cells were in mitotic arrest or delay, the DNA content of the cells was measured to assess the proportion of cells at each stage of the cell cycle. Propidium iodide staining suggests that when *polo* is chemically inhibited, an increased number of cells enter G_0/G_1 with increasing BI-2536 concentration as the proportion of cells in G_0/G_1 increases from 28.16% to 31.86% (Figure 7D). This is consistent with the observed cell size increase—it is known that cells in G_1 increase in size prior to entry into S-phase (Barberis, Klipp, Vanoni, & Alberghina, 2007). Polo has a function in the DNA damage response, so it is possible that when its function is inhibited, S2R+ cells may be entering G_0 as an alternative to undergoing apoptosis, although this hypothesis would require further testing. Reproducing this experiment in cells transfected with polo shRNAs would not be easily feasible as

each individual cell would have a different level of *polo* knockdown, therefore requiring a much greater number of cells to get the appropriate proportion of PI at each point of the curve.

Finally, the ability to observe genetic interactions in the VDA assay was tested. The interactions between the KD and PBD of Polo are well-described in previous works (Elia, et al., 2003b; Kachaner, et al., 2017). Therefore, double disruption of *polo,* using chemical and RNAi methods was predicted to act as a proxy for a genetic interaction through enhancement of the *polo* phenotype. Previous results of Polo inhibition via RNAi were validated, as increase in GFP signal is once again seen with various levels of significance (Figure 7E). After the addition of BI-2536, area under the curve increases compared to the negative control *white.* The increase seems to be less pronounced at higher BI-2536 concentration, and indeed the difference for each shRNA at each concentration is not statistically significant ($p>0.05$). However, despite the statistical insignificance, the trend in a decrease in the AUC for each Polo shRNA is observable and shows enhancement of the *polo* phenotype, perhaps as cells cannot cope with a more complete loss of function of *polo*. An important point to note is that the chemical inhibition with BI-2536 is assessing a single level of disruption. VDA is measuring over a whole range of disruptions so we would not expect the same strength of viability effect as it may be diluted by cells with weak knockdown and therefore we would not see a strong enhancement of the *polo* phenotype.

Following the VDA optimisation, the Polo interactor shRNA library was constructed (Appendix A) and aliquoted into 7 unique assay plates (Figure 8). Each plate contained 6 target genes and 2 control genes, *white* and *thread,* across the 3 different experimental conditions (ethanol loading control, 20 nM BI-2536, 50 nM BI-2536). Limiting the number of shRNAs per plate and instead screening a smaller

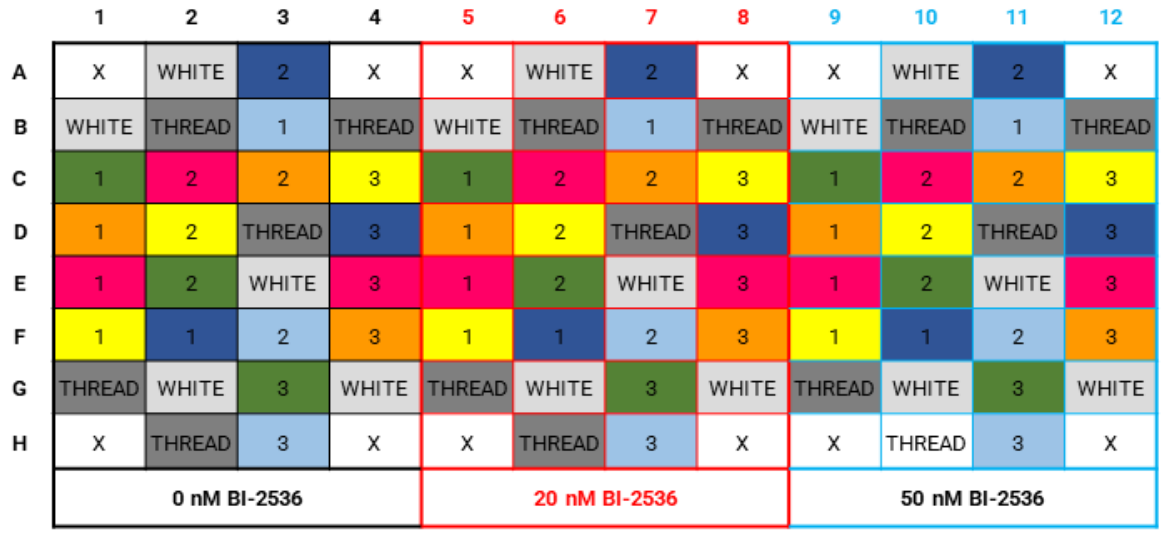

Figure 8. VDA assay plate layout.

All 7 polo interactor library plates have the same layout. Each color represents a different gene, with 3 unique shRNA designs per gene (see Appendix A). There are 5 wells for each control gene, *white* and *thread*. Each gene was distributed in the plate as to minimize any 'edge effects'. All genes are screened under multiple BI-2536 concentrations in the same plate, allowing for control of growth conditions for each *polo* inhibition level. Empty wells are marked with 'X'.

number of reagents under multiple conditions in the same plate would provide a robust readout as cells would be under the same exact set of growth conditions, with and without BI-2536. It was hypothesized that screening at the low BI-2536 concentration (20 nM) would allow identification of Polo enhancers, as their knockdown would enhance the relatively weak polo phenotype. Conversely, knockdown of a Polo suppressor at a 50 nM would suppress the phenotype caused by the high BI-2536 concentration.

The GI VDA screen was carried out in semi high-throughput format in triplicate for each assay plate using the standard VDA pipeline (Sierzputowska, Baxter, & Housden, 2018) (Figure 5A). Areas under the curve for cumulative GFP distribution were plotted and their effect on the *polo* phenotype observed. Figure 9 shows the complete set of results of the Polo interactor VDA screen. Particular attention was paid to the enhancement of the viability phenotype within each shRNA, and the genes that exhibited a marked change in the VDA signal in the presence of BI-2536 were considered as 'hits' (for an example see Map205, Figure 9B). Large scale genetic screens are 'noisy' which can complicate analysis. It is difficult to do sufficient replicates for robust statistical analysis. Therefore, establishing cut-offs is a common approach to find the genes most likely to have an effect, which is usually confirmed with downstream assays. In the context of the Polo interactor VDA screen, high-confidence 'hits' were classified as those genes with strong enhancement of the Polo VDA phenotype in either direction. The effect needed to be observed in at least 2 out of 3 shRNA designs; however, shRNAs which did not show significant difference($0.05 \leq p < 0.1$) were also considered if the enhancement was consistent.

Originally, the two different BI-2536 concentrations were chosen with the aim of identifying Polo enhancers or suppressors. Due to the cell cycle arrest phenotype, Polo enhancement or a suppression could have the same effect in the VDA assay due to the range of gene knockdowns (as described previously). Therefore, at this stage the VDA screen 'hits' aimed to identify potential Polo genetic interactors rather than characterising the nature of the interaction.

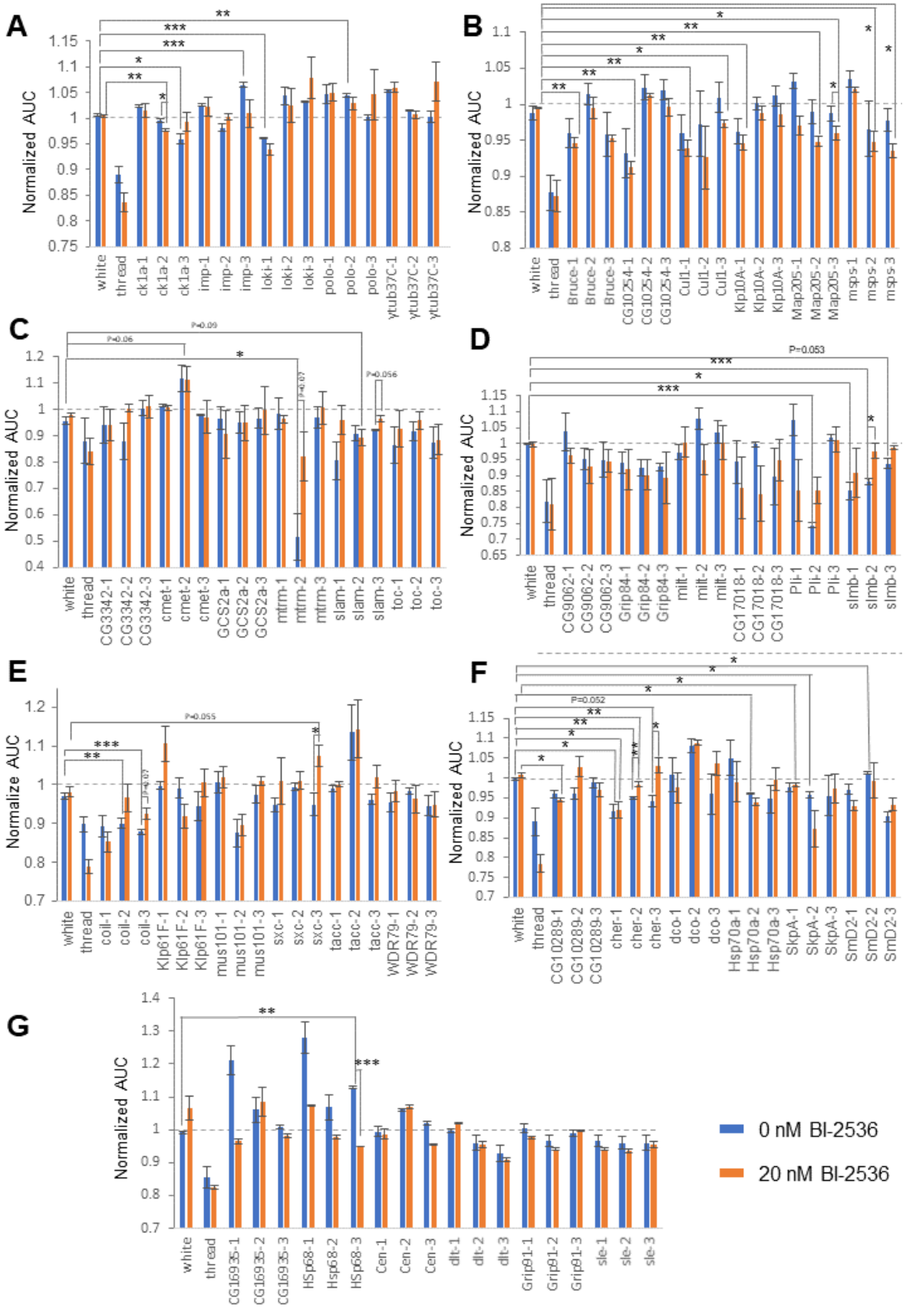
A
Normalized AUC
white
thread
ck1a-1
ck1a-2
ck1a-3
imp-1
imp-2
imp-3
loki-1
loki-2
loki-3
polo-1
polo-2
polo-3
γtub37C-1
γtub37C-2
γtub37C-3
B
Normalized AUC
white
thread
Bruce-1
Bruce-2
Bruce-3
CG10254-1
CG10254-2
CG10254-3
Cul1-1
Cul1-2
Cul1-3
Klp10A-1
Klp10A-2
Klp10A-3
Map205-1
Map205-2
Map205-3
msps-1
msps-2
msps-3
C
Normalized AUC
P=0.09
P=0.06
P=0.07
P=0.056
white
thread
CG3342-1
CG3342-2
CG3342-3
cmet-1
cmet-2
cmet-3
GCS2a-1
GCS2a-2
GCS2a-3
mtrm-1
mtrm-2
mtrm-3
slam-1
slam-2
slam-3
toc-1
toc-2
toc-3
D
Normalized AUC
P=0.053
white
thread
CG9062-1
CG9062-2
CG9062-3
Grip84-1
Grip84-2
Grip84-3
milt-1
milt-2
milt-3
CG17018-1
CG17018-2
CG17018-3
Pli-1
Pli-2
Pli-3
slmb-1
slmb-2
slmb-3
E
Normalize AUC
P=0.055
P=0.07
white
thread
coil-1
coil-2
coil-3
Klp61F-1
Klp61F-2
Klp61F-3
mus101-1
mus101-2
mus101-3
sxc-1
sxc-2
sxc-3
tacc-1
tacc-2
tacc-3
WDR79-1
WDR79-2
WDR79-3
F
Normalized AUC
P=0.052
white
thread
CG10289-1
CG10289-2
CG10289-3
cher-1
cher-2
cher-3
dco-1
dco-2
dco-3
Hsp70a-1
Hsp70a-2
Hsp70a-3
SkpA-1
SkpA-2
SkpA-3
SmD2-1
SmD2-2
SmD2-3
G
Normalized AUC
white
thread
CG16935-1
CG16935-2
CG16935-3
Hsp68-1
Hsp68-2
Hsp68-3
Cen-1
Cen-2
Cen-3
dlt-1
dlt-2
dlt-3
Grip91-1
Grip91-2
Grip91-3
sle-1
sle-2
sle-3
0 nM BI-2536
20 nM BI-2536

Figure 9. VDA screening results.

Each panel shows the AUC for each gene in the library plates (plate 1=A, 2=B, 3=C, 4=D, 5=E, 6=F, 7=G) screened at 0 nM BI-2536 (ethanol-only loading control) in blue,and 20 nM BI-2536 (in orange). Area was normalised to the median AUC of the *white* control gene. SEM shows the average of 20,000 cells analysed from 3 biological replicates of 1 well per target gene and 5 wells per each control gene *(white* and *thread*). Results at 50 nM BI-2536 are not shown due to its effect on cell viability preventing analysing a statistically significant number of cells (on average less than 5,000 live cells per well). Statistical comparison of screen results via a two-tailed t-test is shown using asterisks as follows *p<0.05, **p<0.01, ***p<0.001, unless otherwise specified above the bar.

Gene symbol	Effect out of 3	Gene/Protein Summary	Polo phosphorylation site	Polo phosphobinding site
Hsp68	3	Involved in lifespan determination and response to heat shock and starvation.	+	+
Map205	3	Binds and stabilizes microtubules; binds, inhibits, and stabilizes Polo on MTs during interphase.	+	+
cher	2	F-actin crosslinking protein; functions to organize the F-acting cytoskeleton in multiple contexts including ovarian germline ring canals, migrating somatic cells and neuronal growth cones.	+	+
ck1α	2	Ser/Thr kinase with a preference for acidic substrates; involved in multiple signalling pathways, including Wnt and Hh , that control cell growth and patterning.	/	+
coil	2	Required for Cajal body formation.	+	+
Cul1	2	Exhibits ubiquitin ligase-substrate adaptor activity and ubiquitin protein ligase binding activity. Localizes to SCF ubiquitin ligase complex and nucleus.	+	+
HSP70Ba	2	Involved in response to heat shock and hypoxia.	+	+
Klp61F	2	Allows the crosslinking and sliding apart of adjacent MTs. The 'sliding filament mechanism' is critical for many aspects of mitosis and chromosome segregation.	+	+
msps	2	Binds to the plus end of MTs and regulates MT dynamics and MT organization.	+	+
mtrm	2	Expressed solely during oogenesis; Polo kinase inhibitor required to maintain G_2 arrest in the meiotic cell cycle in females.	+	+
Pli	2	RING-domain-containing ubiquitin E3 ligase that coordinates with E1 and E2 enzymes to degrade target proteins. It functions as a negative regulator of the Toll-mediated innate immunity pathway.	+	+
SkpA	2	A subunit of SCF-containing ubiquitin ligase complexes. It regulates centrosome duplication, chromatin condensation, cell cycle progression, cell polarity, dendrite pruning and endoreduplication.	+	+
slam	2	Involved in cortical polarization and furrow invagination during cellularization, as well in germ cell migration during later embryogenesis.	+	+
slmb	2	Essential, conserved F-box protein, provides substrate specificity to the SCF complex.	+	+

Figure 10. VDA screening identified 14 potential Polo genetic interactors. Table showing the 14 VDA screen 'hits' in alphabetical order based on the enhancement effect for each shRNA design (3 per gene). Gene and protein function summary is taken from the 'Gene snapshot' found on http://flybase.org/. The presence of Polo phosphorylation and phospho-binding sites on each target protein was predicted using the GPS-Polo 1.0 algorithm (http://polo.biocuckoo.org/). Ck1α is the only hit protein that does not have a predicted polo phosphorylation site in any of its isoforms.

Based on the cut-off approach described above, fourteen genes were classified as ‘hits’ based on the observed enhancement of the *polo* phenotype (Figure 10). .

Map205 and *mtrm* are known *polo* inhibitors and were identified among the strongest hits in the screen, exhibiting significantly strong effects in 3 out of 3 shRNAs and 2 out of 3 shRNAs respectively, validating the VDA screening approach used to identify potential polo genetic interactors (Figure 9B and 9C). *mtrm* knockdown showed the most dramatic effect on cell viability, proving to be even more lethal than the positive control *thread*. The strongest curve shift to the right was observed in Hsp68 knockdown ($p<0.001$), and a significant enhancement of the mitotic arrest phenotype was seen with addition of BI-2536 as there was a pronounced effect on cell viability (Figure 9G). Although they were amongst the top hits, the heat shock protein (HSP) genes were not selected for follow-up as it was near impossible to separate whether their silencing causes a phenotypic change due to interaction with Polo or whether the effect on viability is seen as the cells are under environmental stress conditions (which cause upregulation of HSPs).

The resultant list of screen hits was analysed using the PANTHER GO enrichment analysis tool as before. Genes involved in ubiquitination were enriched among the hits (4 out of 15; 88-fold enrichment) (Figure 10). Specifically, SkpA, Cul1, and slmb, the three out of four components of the E3 ligase Skp1-Cullin1-F-box complex (SCF complex), were among them (reviewed by Yumimoto, Yamauchi, & Nakayama, 2020).

Based on results described above, seven genes: *SkpA, Cul1, slmb, slam, Klp61F, cheerio*, and *Ck1α*, were selected for further *in vivo* characterization. Each gene was selected based on the cellular process it was involved in and the strength of its enhancement of the *polo* phenotype (Figure 9 and Figure 10). It was strived to study genes involved in a variety of processes to really dissect the role of Polo interactions during the different stages of the cell cycle.

Chapter 3: *In vivo* results: characterization of RNAi screen hits

Based on the outcome of the VDA screen, seven genes: SkpA, Cul1, slmb, slam, Klp61F, cheerio, and Ck1α, were selected for further *in vivo* characterization. Similar to the studies done *in vitro*, the Polo interactor proteins were disrupted via RNAi *in vivo* and the resultant phenotypes were observed.

3.1Targeted gene knockdown to functionally characterize selected Polo interactors

As mentioned previously, *Drosophila* syncytial embryos undergo 13 rapid mitotic divisions in the absence of zygotic transcription and contain a large amount of mitotic proteins, making them an ideal model to study Polo function. In the context of this research project, flies carrying the construct for transgenic expression of RNAi against the selected Polo interactor needed to be crossed to a fly that would allow for live imaging studies: a transgenic fly with a fluorescently tagged Polo and an appropriate Gal4 driver that would allow for spatio-temporal resolution of any resultant Polo phenotypes in the embryo (see review of Gal4/UAS in Chapter 1; Figure 11A). It was shown previously that maternally loaded Gal4 protein is very efficient at activating zygotic UAS-shRNA constructs and generating phenotypes for genes expressed during mid-embryogenesis (Staller, et al., 2013) .Therefore, a transgenic fly line was generated, harbouring the construct for GFP-tagged Polo and Gal4 protein under a maternal α-tubulin driver (Figure 11B).

Generation of the fly line necessary for study was greatly simplified by a pre-existing transgenic, GFP-tagged polo fly line. The w^+; polo-GFP fly line (gift from C. Sunkel) was previously reported to show canonical Polo localisation and dynamics during syncytial mitotic cycles (Moutinho-Santos, Sampaio, Amorim, Costa, & Sunkel, 2012). Fly lines with target interactor genes under UAS control (referred to as 'RNAi lines' henceforth) were obtained from the Bloomington *Drosophila* Stock Center[4]. Unfortunately, the lack of appropriate *in vivo* reagents prevented further follow up for slam, as there is a single fly line available, albeit with an unstable integration site.

[4] https://bdsc.indiana.edu/

A

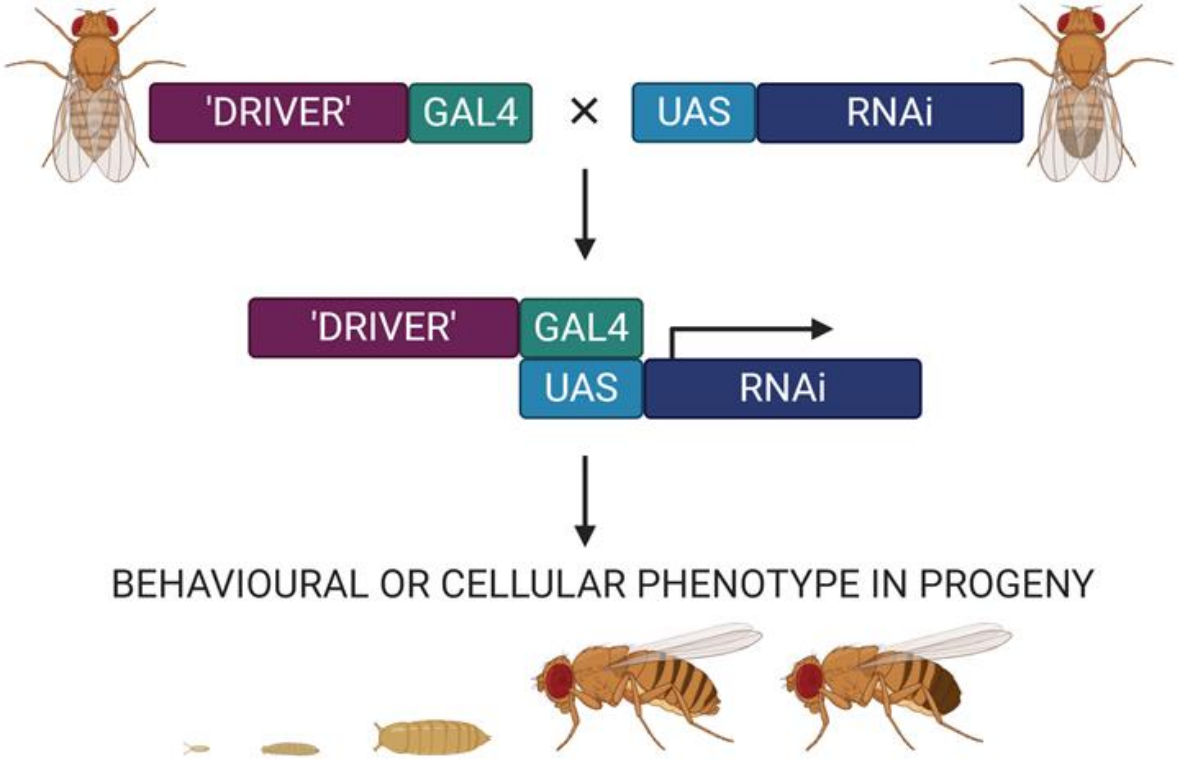
'DRIVER'
GAL4
×
UAS
RNAi
'DRIVER'
GAL4
UAS
RNAi
BEHAVIOURAL OR CELLULAR PHENOTYPE IN PROGENY

B

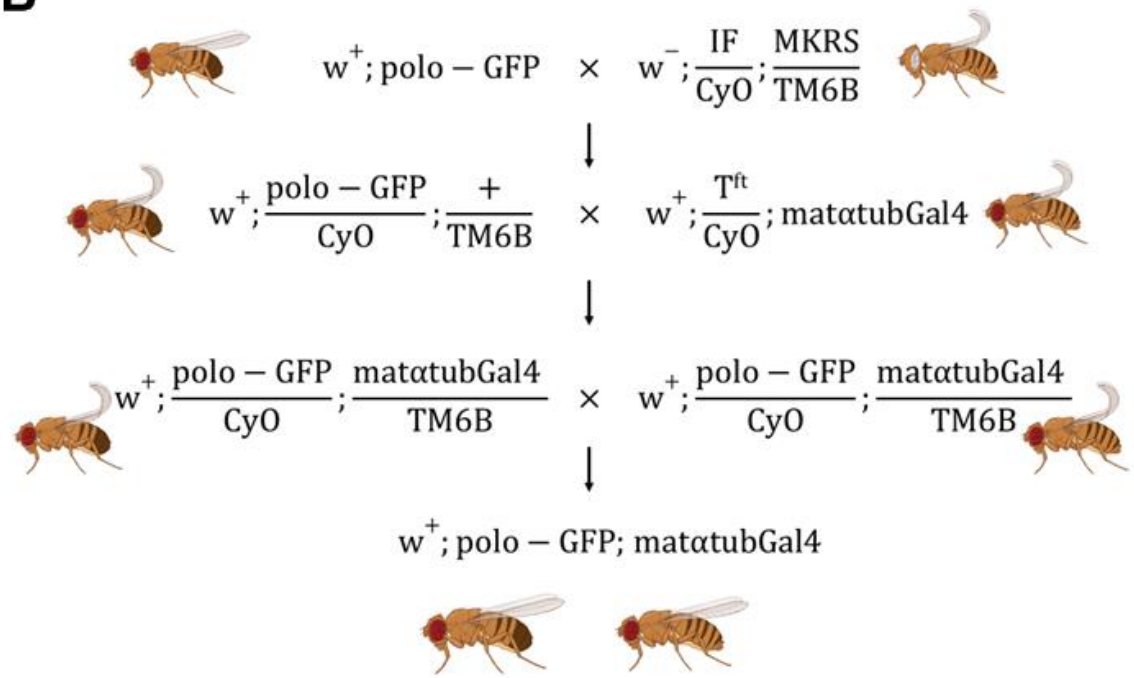
$w^+; polo-GFP \times w^-; \frac{IF}{CyO}; \frac{MKRS}{TM6B}$
$w^+; \frac{polo-GFP}{CyO}; \frac{+}{TM6B} \times w^+; \frac{T^{ft}}{CyO}; matαtubGal4$
$w^+; \frac{polo-GFP}{CyO}; \frac{matαtubGal4}{TM6B} \times w^+; \frac{polo-GFP}{CyO}; \frac{matαtubGal4}{TM6B}$
$w^+; polo-GFP; matαtubGal4$

Figure 11*. Drosophila* gene silencing *in vivo* via Gal4/UAS*.*

A) Gal4/UAS system for gene silencing with RNAi in *Drosophila*. The figure shows the parental flies carrying the construct for transgenic expression of RNAi against a gene of interest and a construct for specific gene expression of the Gal4 protein. When females carrying the Gal4 driver are mated to males carrying the UAS responder, progeny containing both elements of the system are produced. Gene silencing occurs in the progeny in specific tissues dependent on the driver of Gal4 expression used and resultant behavioural or cellular phenotypes can manifest in any developmental stage (embryo, larvae, pupae, adult).

B) Mating scheme used to generate the transgenic w^+; polo-GFP; matαtubGal4 fly line to be used for *in vivo* gene silencing via RNAi. The homozygous w^+; polo-GFP fly line is mated to a stock which carries balancers and dominant visible markers on the 2nd and 3rd chromosomes. Red-eyed (w^+ Polo-GFP), curly-winged (CyO) male progeny with extra humeral hairs (TM6B) are then mated with red-eyed (w^+ maternal alpha-tubulin-GAL4), curly-winged (CyO) virgins with ectopic bristles (T^{ft}). Since CyO is homozygous lethal, the resultant progeny will either carry the T^{ft} marker or the polo-GFP gene. Selecting curly-winged progeny with humeral hairs (but without extra bristles) and mating them with each other will result in flies homozygous for polo-GFP and maternal alpha tubulin-GAL4.

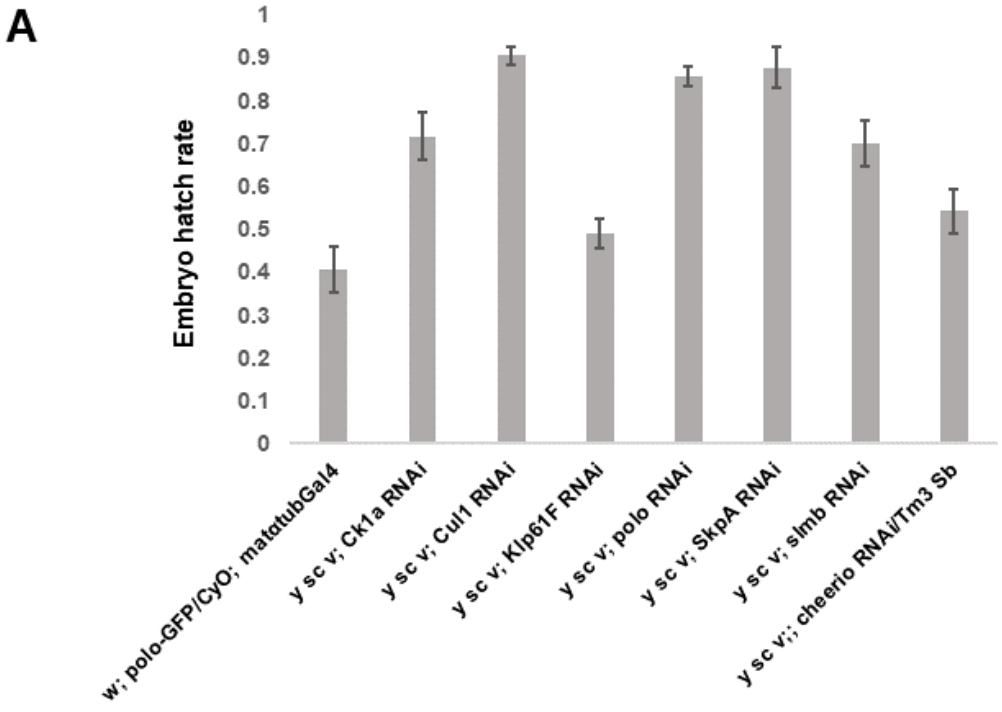
A
Embryo hatch rate
1
0.9
0.8
0.7
0.6
0.5
0.4
0.3
0.2
0.1
0
w; polo-GFP/CyO; matαtubGal4
y sc v; Ck1a RNAi
y sc v; Cul1 RNAi
y sc v; Klp61F RNAi
y sc v; polo RNAi
y sc v; SkpA RNAi
y sc v; slmb RNAi
y sc v;; cheerio RNAi/Tm3 Sb

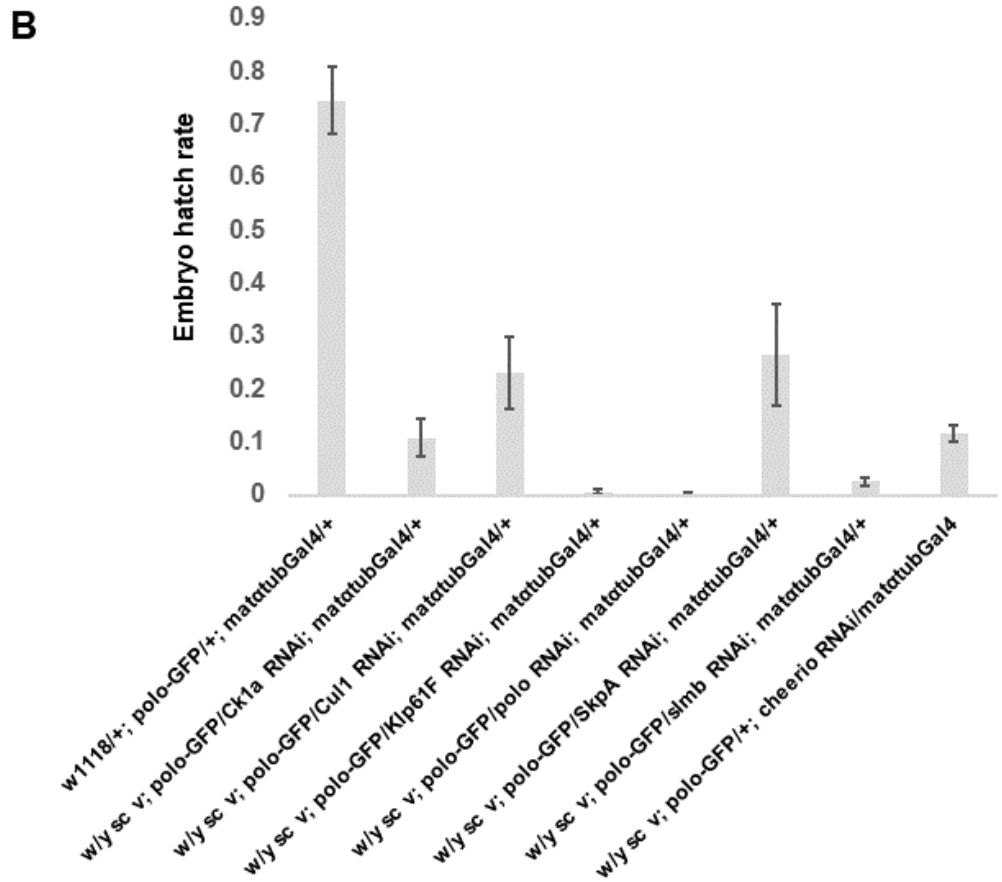
B
Embryo hatch rate
0.9
0.8
0.7
0.6
0.5
0.4
0.3
0.2
0.1
0
w1118/+; polo-GFP/+; matαtubGal4/+
w/y sc v; polo-GFP/Ck1a RNAi; matαtubGal4/+
w/y sc v; polo-GFP/Cul1 RNAi; matαtubGal4/+
w/y sc v; polo-GFP/Klp61F RNAi; matαtubGal4/+
w/y sc v; polo-GFP/polo RNAi; matαtubGal4/+
w/y sc v; polo-GFP/SkpA RNAi; matαtubGal4/+
w/y sc v; polo-GFP/slmb RNAi; matαtubGal4/+
w/y sc v; polo-GFP/+; cheerio RNAi/matαtubGal4

Figure 12. Embryo hatch rates.

A) Embryo hatch rates of fly stocks used for *in vivo* functional Polo interactor characterisation. Scale bars represent SEM of 6 biological replicates of hatch rates of 100 embryos per each genotype. Hatch rate of w/+; polo-GFP/CyO; matαtubGal4/+ was adjusted to out of 75 embryos for maximum possible viable offspring to control for the homozygous-lethal balancer.

B) Embryo hatch rates for resultant progeny of interactor RNAi flies crossed to flies expressing polo-GFP and the maternal α-tubulin GAL4 driver. Scale bars represent SEM of 6 biological replicates of hatch rates of 100 embryos from each cross. Hatch rate of w/y sc v; polo-GFP/+; matαtubGal4/cheerio RNAi was adjusted to out of 75 embryos to account for the homozygous-lethal balancer.

The fitness of the generated w^+; polo-GFP/CyO; matαtubGal4 line (from herein referred to as the 'polo-GFP driver line'), as well as the interactor RNAi lines was assessed via embryo hatch rates. None of the stocks were deemed to be particularly unhealthy, as all had hatch rates above 40%, which is to be expected for *Drosophila* stocks (Figure 12A).

The hatch rates of the resultant progeny of the polo-GFP driver and interactor RNAi cross (henceforth Polo-GFP; RNAi embryos) were also recorded. 74.5% of embryos hatched successfully from a control cross resulted in flies with half the dose of the driver and polo-GFP. Targeted knockdown of Klp61F and polo was embryonic lethal, with a hatch rate of less than 1% (Figure 12B). Knockdown of slmb function also resulted in a severe embryonic viability phenotype (hatch rate of 2.6%). The hatch rate of the embryos from the Ck1α cross was 10.8%. Moreover, silencing this gene resulted in fertility defects in the progeny, as even after an overnight collection, it was impossible to secure 100 embryos needed to set up a full plate for hatching (embryo count ranging from 81 to 11 in 6 biological replicates). Hatch rates from the Ck1α stock line nor from the polo-GFP driver control cross did not suggest viability defects from either individual line (Figure 12A).

3.2 Live imaging of polo-GFP—interactor RNAi cross progeny

Polo-GFP; RNAi embryos - were manually dechorionated and taken for live imaging on the Olympus IX81 Spinning Disc Confocal Microscope. Unsurprisingly, embryos from Klp61F RNAi, polo RNAi and slmb RNAi crosses could not be imaged as knockdown of essential regulators of multiple signalling pathways (*slmb*) and those critical for mitosis (*Klp61F* and *polo*) would have severe impacts on the proper development of the embryo. The embryos from those crosses were incredibly fragile, with most 'popping' during the dechorionation step. Those that did remain intact, did not show a multinucleated syncytium (data not shown). Embryos from the Cul1, SkpA and cheerio cross were also more fragile than normal but were able to be successfully imaged (Figure 12). In the case of cheerio, it is expected that knockdown of a gene involved in organisation of the actin cytoskeleton would have an effect on

A Control: $\frac{w^{1118}}{+}$; $\frac{polo-GFP}{+}$; $\frac{matαtubGal4}{+}$

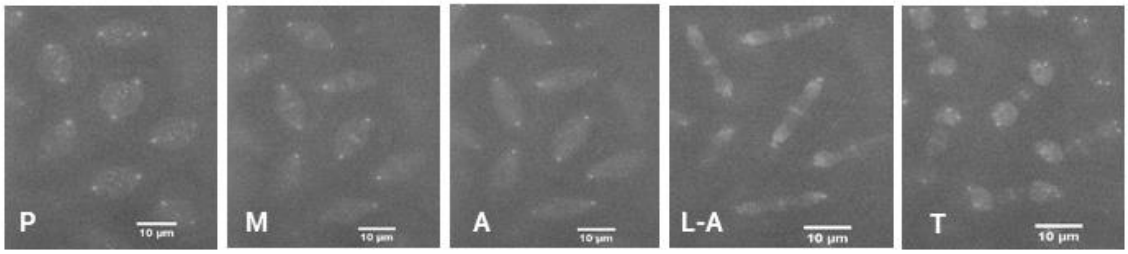

B cheerio RNAi: $\frac{w^{1118}}{+}$; $\frac{polo-GFP}{+}$; $\frac{matαtubGal4}{cheerio\ RNAi}$

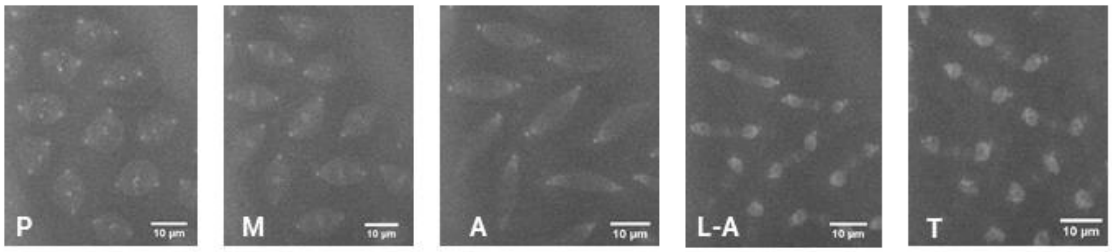

C Cul1 RNAi: $\frac{w^{1118}}{+}$; $\frac{polo-GFP}{Cul1\ RNAi}$; $\frac{matαtubGal4}{+}$

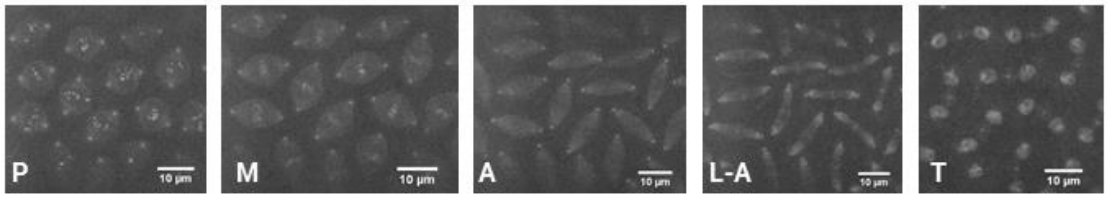

D SkpA RNAi: $\frac{w^{1118}}{+}$; $\frac{polo-GFP}{Cul1\ RNAi}$; $\frac{matαtubGal4}{+}$

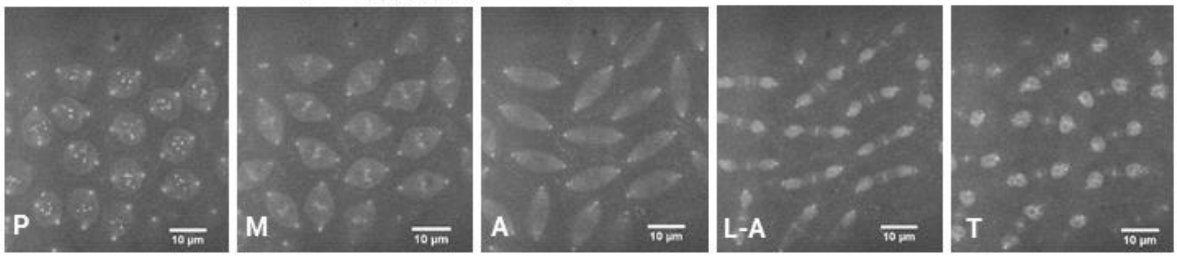

E

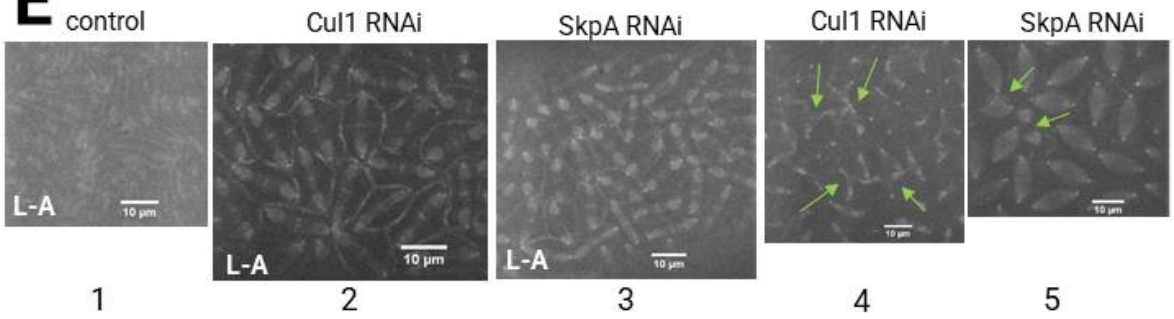

Figure 13. Representative images of polo-GFP localisation during live imaging of interactor RNAi embryos.

Representative stills from movies generated from live imaging of 2-3 hour old Polo-GFP; RNAi embryos on a spinning disk confocal microscope. Stills from each mitotic stage were taken from syncytial cycle 9. P=prophase, M=metaphase, A=anaphase, L-A= late anaphase, T=telophase.

Stills from control (A), cheerio RNAi (B), Cul1 RNAi (C) and SkpA RNAi embryo time lapse image sets. (E) Representative images of observable polo-GFP phenotypes – (1) Late anaphase during cycle 12 in a control embryo. A weak, but discrete cortical localisation of polo-GFP can be seen in anaphase; (2) Late anaphase during cycle 10 in a Cul1 RNAi embryo. An increase in cortical localisation of polo-GFP is observed around the spindle area; (3) Late anaphase during cycle 10 in a SkpA RNAi embryo. An increase in cortical localisation of polo-GFP is observed around the spindle area; (4) spindle abnormalities during cycles 9 through 11 in Cul1 RNAi embryos. Green arrows point to multipolar spindles; (5) spindle abnormalities during cycles 9 through 11 in SkpA RNAi embryos. Green arrows point to a tripolar spindle (top arrow) and two nuclei which have failed to successfully divide (bottom arrow).

embryo integrity. The expected polo-GFP localization (centrosomes, kinetochores, midzone, midbody ring) was observed in all imaged embryos (Figure13A-D). RNAi knockdown of the SCF complex components, SkpA and Cul1, resulted in spindle abnormalities and increased cortical Polo localization, akin to an outline of a cell membrane around the spindle region (Figure 13E). Such corticallocalisation was observed in some wild type embryos during later syncytial mitotic divisions (cycle 12), just prior to cellularisation (Figure 13E), probably reflecting the increase in density of cortical nuclei and/or increased recruitment of Polo-GFP to the cortex in these later cycles. However, discrete cortical localisation of Polo-GFP was not visible in cycles 10-12 in control embryos.

To quantitatively compare the intensity of cortical polo-GFP in wild type SkpA RNAi and Cul1 RNAi embryos, I developed a custom Python script to assess the pixel brightness outside of the spindle region (Figure 14A). Brighter than average pixels were detected using a normalisation strategy using median absolute deviation of the non-spindle region. I found an increase in average pixel intensity in some SkpA and Cul1 RNAi embryos in cycle 10 and 11 (Figure 14D,E), 2 cycles before the same increase can be seen in the control embryos (Figure 14B). The pixel intensity in one cheerio RNAi embryo was higher than normal as the nuclei division progress, however, no polo-GFP cortical phenotypes were observed in the 5 movies recorded (Figure 13B). There is no pixel intensity data available for Cul1 RNAi embryo in cycle 12 as none were imaged during this division cycle.

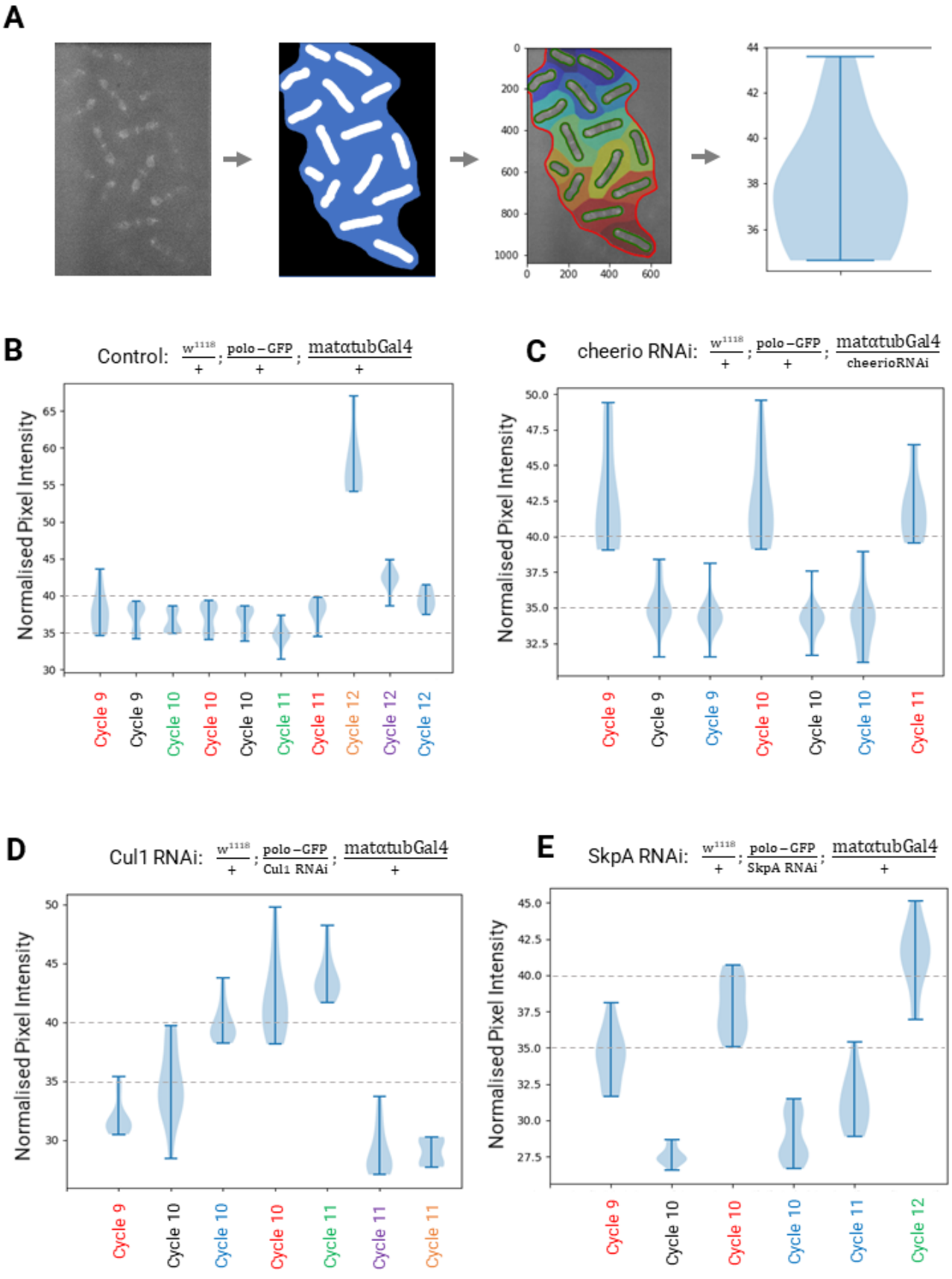
A
B
Control: $\frac{w^{1118}}{+}$; $\frac{polo-GFP}{+}$; $\frac{matαtubGal4}{+}$
Normalised Pixel Intensity
Cycle 9
Cycle 9
Cycle 10
Cycle 10
Cycle 10
Cycle 11
Cycle 11
Cycle 12
Cycle 12
Cycle 12
C
cheerio RNAi: $\frac{w^{1118}}{+}$; $\frac{polo-GFP}{+}$; $\frac{matαtubGal4}{cheerioRNAi}$
Normalised Pixel Intensity
Cycle 9
Cycle 9
Cycle 9
Cycle 10
Cycle 10
Cycle 10
Cycle 11
D
Cul1 RNAi: $\frac{w^{1118}}{+}$; $\frac{polo-GFP}{Cul1\ RNAi}$; $\frac{matαtubGal4}{+}$
Normalised Pixel Intensity
Cycle 9
Cycle 10
Cycle 10
Cycle 10
Cycle 11
Cycle 11
Cycle 11
E
SkpA RNAi: $\frac{w^{1118}}{+}$; $\frac{polo-GFP}{SkpA\ RNAi}$; $\frac{matαtubGal4}{+}$
Normalised Pixel Intensity
Cycle 9
Cycle 10
Cycle 10
Cycle 10
Cycle 11
Cycle 12

Figure 14. Normalised pixel intensity comparison.

A) Pipeline for still image analysis. The 20th frame after anaphase entry is exported as a .png file. A mask for the spindle region (white) and the region outside the embryo (black) is created manually in GIMP. The custom Python script uses the black and white masks to automatically select the areas of interest. The area of interest is transparent—blue background shown herein for visualisation purposes. After selecting the area of interest, the script then calculates the average pixel intensity value of each region. The pixel intensities are then normalised to the average median value of the entire embryo and presented as a violin plot.

B) Normalised pixel intensities for syncytial mitotic cycles 9 thorough 12 for control embryos. Six separate embryos (shown in red, black, green, orange, purple, and blue) were live imaged and analysed using the Python script as outlined in **A**. Each individual embryo is shown using a separate colour, i.e. the colour red signifies that the particular cycle 9 and cycle 10 data were collected from the same embryo. Dotted lines at Normalised Pixel Intensities of 35 and 40, the average range of pixel intensity distribution in the control, were added to aid in comparison across the different genotypes.

C) Normalised pixel intensities for syncytial mitotic cycles 9 thorough 11 for cheerio RNAi embryos. Three separate embryos (shown in red, black, and blue) were live imaged and analysed. Embryo 1 (red) has pixel intensities higher than the control embryos across all cycles imaged. Embryo 2 (black) and embryo 3 (blue) show slightly lower values for normalised pixel intensities compared to the control.

D) Normalised pixel intensities for syncytial mitotic cycles 9 thorough 11 for Cul1 RNAi embryos. Six separate embryos were live imaged and analysed using the Python script. Similarly to above, the data from each individual embryo is shown using different colours. In cycle 10, embryo 1 (red) and embryo 3 (blue) have pixel intensities higher than the control embryos for the same cycle. Embryo 4 (green) shows a higher normalised pixel intensity than the control during cycle 11, whereas embryos 5 and 6 (purple and orange respectively) show lower values.

E) Normalised pixel intensities for syncytial mitotic cycles 9 thorough 12 for SkpA RNAi embryos. Four separate embryos (shown in black, red, blue and green) were live imaged and analysed using the Python script. The analysed embryos do not show a consistent trend across the cycles compared to the control.

Conclusions

In summary, previous work in the Wakefield lab identified 40 proteins that physically interact with Polo in *Drosophila* embryos, but the functional significance of these components remained unknown. In line with the aim of this thesis, I performed a highly sensitive assay called Variable Dose Analysis (VDA) in *Drosophila* S2R+ cells to determine which of the physical interactors also have genetic interactions with Polo. Inhibiting Polo using the selective small-molecule inhibitor BI-2536 and transfecting shRNA against the genes of interest allowed to easily screen cells based on their viability phenotype.

Genetic interaction screens are more complex than single gene screens, as the biological system being investigated modulates its molecular pathways as a result. They are therefore inherently a lot more “noisy”. Screening for interactions with a kinase such as polo is also quite challenging, as due to its pleiotropic functions we may observe different phenotypes at different knockdown levels. One of the advantages of using VDA as a screening method is that it is more sensitive to identifying weak phenotypes. It also allows for the study of interactions with essential genes, due to the observed variable range of knockdown. However, in the context of the Polo interactor VDA screen, with lower number of replicates and the noisy nature of the screen, incomplete statistical significance of results made hit identification challenging. The nature of the interaction (suppressor or enhancer) cannot be identified from the screen as it may be possible that an enhancer could fail to be detected if it creates a balance between cell cycle disruption and cell death—AUC analysis would make this interaction look like a control. It may be worth pursuing a different, more involved form of analysis of the curve distribution shapes as a more complex comparison of curve shape distributions might allow discrimination of enhancers from suppressors, or perhaps even different phenotypes of Polo based on the function disrupted.

The case of γtub37C provides a case in point. The γtub37C gene product is essential in organizing the female meiotic and early embryo mitotic spindle (González, Tavosanis, & Mollinari, 1998) and is involved in the attachment of spindle MTs to kinetochores in female meiosis (Hughes, et al., 2011). Given the

complementary functions of polo and γtub37C, it was hypothesized that they might be genetic interactors. Surprisingly, none of the shRNAs against γtub37C showed a statistically significant effect in the VDA assay (Figure 9A). This could be due to a multitude of factors, such as the issue with enhancer identification described above, the weak strength of the shRNA reagents or due to interaction differences that occur *in vitro* compared to at the organismal level.

Based on the adopted cut-off approach, known Polo genetic interactors, Map205 and mtrm, were identified by the VDA screen, validating its robustness and utility in identifying novel genetic interactors. In total, fourteen genes were selected as 'hits' based on their effect on cell viability in the context of Polo inhibition, with components of the ubiquitination system enriched among them. Interestingly, all member proteins of the Skp, Cullin, F-box containing complex (SCF complex) which catalyses the ubiquitination of proteins for degradation, were identified as hits. This, too, supports the validity of the screen – RNAi of genes whose products form physical and functional complexes would be expected to elicit similar responses in the VDA screen. In addition, four more proteins with roles in cleavage furrow formation (slam), signalling pathways that control cell growth and patterning (Ck1α), chromosome segregation (Klp61F), and cytoskeleton organisation (cher), were selected as top hits and taken further for validation and additional characterization of their interactions with polo-GFP *in vivo* using live imaging and biochemical approaches.

The lack of readily available RNAi fly lines prohibited the study of slam, which would have shed further light on the function of Polo in cleavage furrow formation—the least understood of all its mitotic functions. There is, however, a slam mutant allele that could, in the future, be crossed to the Polo-GFP fly line, to allow the investigation of Polo localisation in the absence of slam to be investigated (Stein, Tarczy Broihier, Moore, & Lehmann, 2002).Inhibition of Ck1α and slmb via RNAi resulted in larval lethality, limiting the insights that could be gained in terms of their relationship to Polo function during *Drosophila* development. Silencing Klp61F expression did not produce any significant results in terms of polo-GFP localisation nor expression levels. However, interestingly, live imaging of Cul1 RNAi embryos showed a consistent and quantifiable increase in the cortical localization of polo-GFP during late anaphase/telophase. An attractive hypothesis to explain these results is that the

SCF complex is responsible for selective degradation of polo at the cortex in normal embryos. Spatio-temporal control of SCF complexes to the cell cortex during the cell cycle in mammalian cells has previously been described (Werner, et al., 2013). In addition, another member of the polo-like kinase family, Plk4, has been reported to be degraded in a SCF-dependent manner (Rogers, Rusan, Roberts, Peifer, & Rogers, 2009; Cunha-Ferreira, et al., 2013). Furthermore, a study has reported that cytoplasmic Polo is ubiquitinated and subsequently degraded by the $SCF^{\beta TrCP}$/proteasome in HeLa cells (βTrCP is the mammalian orthologue of slmb) (Giráldez, et al., 2017). Thus, it is possible that loss of Cul1 and SkpA function in the early embryo could increased levels of polo-GFP in anaphase and telophase, resulting in a significant ectopic accumulation of polo-GFP at the cortex.

Further studies

This study provides an important starting point for further investigating the relationship between Polo and SCF-dependent degradation in *Drosophila*. However, further follow up work is needed to gain deeper insight.

Firstly, it would be prudent to carry out more biochemical studies to confirm whether Polo is degraded in an SCF-dependent manner in *Drosophila*. Embryo populations can be fixed and stained to determine the different stages of mitosis, pooled and subjected to western blotting with an anti-polo antibody. Comparison of total Polo protein levels between control and SkpA or Cul1 RNAi embryos could validate any impairment in its cell-cycle dependent degradation. It would also be interesting to undertake reciprocal GFP-TRAP-A/MS with fly lines expressing GFP-tagged versions of SkpA and Cul1. Such an analysis could validate the physical interaction with Polo, and would perhaps shed light on other proteins involved in the functional relationship.

Cell biological studies could further enhance our understanding. Whilst it is clear that there is some increase in Polo cortical localization in embryos lacking the proteasome components, a larger-scale validation using immunostained embryos would provide useful quantification of the prevalence of this phenotype in the different mitotic cycles within the embryo. Concurrently, the images could be analysed using the Python script and analysis modified to include the median and

averages of all embryos imaged at that particular time point, increasing the robustness of the pixel intensity comparison results. In addition, generating null mutant and fluorescent protein-fusion variants of the Polo interactors would allow for live imaging studies to analyse the sub-cellular localisation and dynamics of Polo and its interactors.

Methods

BI-2536 cell viability assay

1.0 x 10^4 wildtype S2R+ cells were seeded in 100 µl culture media per well of a 96-well plate. Ethanol loading control (matching volume of 50 nM BI-2536) or stock BI-2536 solution was added such that wells of the plate had either 10 nM, 20 nM, 30 nM, 40 nM, or 50 nM final BI-2536 concentration (8 wells per each concentration). The plate was incubated in a humidifying chamber for 5 days at 25°C, after which the cell viability was read out on a plate reader (Tecan) using the standard CellTiter-Glo Luminescent Cell Viability Assay protocol (Promega, G7570). The luminescent signal from each well was normalized to the average luminescence of ethanol-only wells.

Embryo hatch rates

Large egg-laying population cages were set up at 20°C (100mm, one cage/strain). The parental flies were transferred to cages and acclimatized at 20°C for 2 days prior to experiments. Eggs were collected over a 12 hour period on 100 mm Petri dishes filled with apple juice and agar media, coated with fresh yeast paste. Eggs were carefully lifted off the collection plates using a paintbrush and placed onto a fresh 100mm apple juice agar plate in 10 sections of 10 eggs (100 eggs in total per plate). The egg-seeded plates were kept at 20°C for 72 hours, after which a manual count of the number of successfully hatched embryos took place.

Figures

Figures were generated using BioRender[5] under a student license, Cytoscape[6], Microsoft Excel and GIMP[7].

[5] https://biorender.com
[6] https://cytoscape.org/index.html (Shannon, et al., 2003)
[7] GNU Image Manipulation Program; https://www.gimp.org/

Fly husbandry

All flies were reared on standard molasses/flour/yeast/propionic acid/nepagin/agar media-containing vials or bottles, in a 25°C incubator at 70-80% relative humidity with a 12/12h light/dark cycle.

RNAi crosses were carried out at 25°C with 10 female and 5 male flies per vial. A minimum of 10 vials was set up for each cross, with the flies being 'knocked over' every 3 days 3 times for a total of 30 vials per each cross. After being 'knocked over', the vials were placed at 20°C and all subsequent fly work was carried out at this temperature.

Fly stocks

Fly stocks were obtained from the Bloomington Drosophila Stock Center where indicated by a stock number.

w^+;;matαtubGal4
w[*]; P{w[+mC]=matalpha4-GAL-VP16}V37, Stock 7063

w+; polo-GFP
w[*]; P{w[+mW.hs]=GFP-polo}p2, gift from C. Sunkel lab

Cul1 RNAi
y^1 sc* v^1; P{y[+t7.7] v[+t1.8]=TRiP.GL00561}attP2 , Stock 36601

SkpA RNAi
y^1 sc* v^1; P{TRiP}attP2 , stock 32870

slmb RNAi
y^1 sc v^1; P{TRiP}attP2 , stock 33898

cheerio RNAi
y^1 sc v^1; P{TRiP }attP2/TM3,Sb , stock 35755

Ck1α RNAi
y^1 sc v^1; P{TRiP}attP2 , stock 35153

Klp61F RNAi
y^1 sc v^1; P{TRiP}attP40 , stock 35804

polo RNAi
y^1 sc v^1; P{TRiP}attP40 , stock 36093

Live Imaging

On days when live imaging took place, synchronized embryos were collected at 20°C in 60mm Petri dish egg laying cages for an hour. One 1-hour long pre-lay preceded the egg collection in order to encourage females to lay eggs they may have incubated for varying time periods. The embryos were then aged for 2 hours so that 2-3 hour-old embryos could be manually dechorionated for live imaging. Embryos were manually affixed to a glass coverslip using heptane glue and imaged every 5 seconds using the Olympus IX81 Spinning Disc Confocal Microscope at 200ms exposure, 20% 488nm laser power under the UPlanSApo 60x / 1.35 Oil objective. Movies were recorded for qone or two division cycles and no longer than 3 cycles to avoid photobleaching the sample.

Propidium iodide staining

0.3 x 10^6 wildtype S2R+ cells were seeded in 2000 µl culture media per well of a 6-well plate. 1µL of stock BI-2536 solution was added to appropriate wells for a final concentration of 20 nM BI-2536 or 50 nM BI-2536 per well (or 1 µl of EtOH loading control). After a 5 day incubation at 25°C, the cells were harvested and washed in PBS. The cells were then fixed in cold 70% ethanol for 30 min at 4°C. The cells were washed 2x in PBS, spun at 850g and supernatant was discarded. The cells were then treated with 50 µl of Ribonuclease I (100 µg/ml stock). 200 µl of propidium iodide (50 µg/ml stock) was added, and the cells were moved to a 96-well plate for analysis using a flow cytometer (CytoFlex S, Beckman Coulter). FSC and SSC measurements were taken for 10,000 ‘events’ and the gating strategy selected only single cells. The DNA content was measured using the ECD channel and a histogram showing cell count vs dye brightness. The peaks corresponding to 2N (G_0/G_1), 2N-4N (S-phase) and 4N (G_2/M) DNA content were delineated and labelled in the native cytometer software.

Pixel intensity quantification

Movies generated from live imaging were converted into 8-bit .png files in Fiji[8]. For each movie, a frame exactly 20 frames after the onset of anaphase was selected, and a 'spindle mask' for 15 spindles was created in GIMP using brush size '40', maximum hardness. In embryos that didn't have 15 'full spindles', any area of the spindle was masked out for a total of 15 areas of analysis. The area outside the embryo and the selected 15 spindles was also masked out. The images and masks were analyzed using a custom Python script. The median pixel intensity and median-absolute-deviation were calculated. Pixels were marked as 'bright' if they were more than 3 times the median-absolute deviation for the median for that region. Violin plots for each image were generated, showing the intensity values and their distribution.

S2R+ cell maintenance

Cell lines were maintained in an incubator at 25°C, 33% RH in standard S2R+ cell filter-sterilized medium (450 mL Schneider's medium (Gibco#21720024), 50 mL fetal bovine serum (Gibco#A3382001), 5 mL penicillin-streptomycin (Gibco#15070063) (split every 3-4 days to maintain).

shRNA library construction

Three different shRNAs per each target gene were designed using the standard TRiP hairpin design protocol[9] based on the algorithm of Vert et al (Vert, Foveau, Lajaunie, & Vandenbrouck, 2006). The annealed oligos were subsequently cloned into the pValium20 vector (Perkins, et al., 2015) using standard cloning techniques. See Appendix A for detailed hairpin design information.

Statistical analysis

All p-values reported herein are based on independent two-tailed t-tests assuming unequal variance carried out using the built-in t.test formula in Microsoft Excel.

[8] https://imagej.net/Fiji
[9] https://fgr.hms.harvard.edu/cloning-and-sequencing

Variable Dose Analysis

VDA assays were performed by transfecting a mixture of 90 ng shRNA, 20 ng actin-GFP, and 90ng actin-GAL4 plasmids into 1.5 x 10^4 wildtype S2R+ cells seeded in 100 µl culture media per well of a 96-well plate (plated 1 hour prior to transfection), following an optimised FugeneHD transfection reagent protocol (Promega, E2311). Additionally, 1µL of stock BI-2536 solution was added to appropriate wells for a final concentration of 20 nM BI-2536 or 50 nM BI-2536 per well (or 1 µl of EtOH loading control). Following 5 days of culture at 25°C in a humidifying chamber, the plates were analysed using the CytoFlex S flow cytometer (Beckman Coulter). 20,000 events were recorded per sample (well), and GFP intensities and FSC measurements for all GFP-expressing cells were exported for further analysis.

The cytometry data was analysed using custom MATLAB scripts. First, .fcs files were converted into .csv files using a MATLAB script[10]. Then all GFP intensities were normalized to cell size measurements (FSC) and divided into 500 bins based on GFP fluorescence. GFP distributions were normalized between all samples. Finally, the area under the cumulative GFP distribution plots was calculated and normalized to the median value of the negative control samples.

Hits were selected to be genes that showed an effect on the *polo* phenotype. The areas under the curve were annotated by hand in terms of phenotypic effects seen, i.e. enhancement or suppression of *polo* phenotype. Genes with effect in 3 out of 3 shRNA designs were considered to be ‘top hits’, and genes with strong or consistent effect in 2 out of 3 shRNAs were also considered as ‘hits’

[10] available from: uk.mathworks.com/matlabcentral/fileexchange/9608-fca_readfcs

Appendix A. Polo interactor library shRNA hairpin designs.

The shRNA vectors assigned a hairpin ID were a gift from the TRiP at Harvard Medical School. All others were designed and cloned in house at the Living Systems Institute.

shRNA	Top Strand Oligo	Bottom Strand Oligo	TRiP hairpin ID
white	ctagcagtCAGGAGCTTTCGCTCAGCAA Atagttatattcaagcata TTTGCTGAGCGAA AGCTCCTGgcg	aattcgcCAGGAGCTTTCGCTCAGCAAA tatgcttgaatataactaTTTGCTGAGCGAAA GCTCCTGactg	HMS00017
thread	ctagcagtCACCCAAGTCCTCAAATTCAA tagttatattcaagcataTTGAATTTGAGGACT TGGGTGgcg	aattcgcCACCCAAGTCCTCAAATTCAAt atgcttgaatataactaTTGAATTTGAGGACT TGGGTGactg	HMS00752
Bruce-1	ctagcagtTTCGACTACGATGACACTGA Atagttatattcaagcata TTCAGTGTCATCGT AGTCGAAgcg	aattcgcTTCGACTACGATGACACTGAAt atgcttgaatataactaTTCAGTGTCATCGTA GTCGAAactg	
Bruce-2	ctagcagtCAGGTGCAGAATCAACGTAA Atagttatattcaagcata TTTACGTTGATTCT GCACCTGgcg	aattcgcCAGGTGCAGAATCAACGTAAAt atgcttgaatataactaTTTACGTTGATTCTG CACCTGactg	
Bruce-3	ctagcagtTCAGCTCTTAGTGTTCGACTA tagttatattcaagcata TAGTCGAACACTAA GAGCTGAgcg	aattcgcTCAGCTCTTAGTGTTCGACTAt atgcttgaatataactaTAGTCGAACACTAAG AGCTGAactg	
Cen-1	ctagcagtTCGGGACAAGAAGCAGATTA Atagttatattcaagcata TTAATCTGCTTCTT GTCCCGAgcg	aattcgcTCGGGACAAGAAGCAGATTAA tatgcttgaatataactaTTAATCTGCTTCTTG TCCCGAactg	
Cen-2	ctagcagtCAGCGAAATGGAGGTGTTAA Atagttatattcaagcata TTTAACACCTCCAT TTCGCTGgcg	aattcgcCAGCGAAATGGAGGTGTTAAA tatgcttgaatataactaTTTAACACCTCCATT TCGCTGactg	
Cen-3	ctagcagtCAGAGTGTTGAGTTCTCCAA Atagttatattcaagcata TTTGGAGAACTCA ACACTCTGgcg	aattcgcCAGAGTGTTGAGTTCTCCAAAt atgcttgaatataactaTTTGGAGAACTCAAC ACTCTGactg	
CG10254-1	ctagcagtACGGAGATGGATGAAGTTCT Atagttatattcaagcata TAGAACTTCATCCA TCTCCGTgcg	aattcgcACGGAGATGGATGAAGTTCTAt atgcttgaatataactaTAGAACTTCATCCAT CTCCGTactg	
CG10254-2	ctagcagtCACGATCGATTCTACCTCAAA tagttatattcaagcata TTTGAGGTAGAATC GATCGTGgcg	aattcgcCACGATCGATTCTACCTCAAAt atgcttgaatataactaTTTGAGGTAGAATCG ATCGTGactg	
CG10254-3	ctagcagtATGGATGAAGTTCTATGCAAA tagttatattcaagcata TTTGCATAGAACTTC ATCCATgcg	aattcgcATGGATGAAGTTCTATGCAAAt atgcttgaatataactaTTTGCATAGAACTTC ATCCATactg	
CG10289-1	ctagcagtCCGGTCATACCTGATCTAATA tagttatattcaagcata TATTAGATCAGGTAT GACCGGgcg	aattcgcCCGGTCATACCTGATCTAATAt atgcttgaatataactaTATTAGATCAGGTAT GACCGGactg	SH01744.N
CG10289-2	ctagcagtAAGGGCGTTCAGGATAATCT Atagttatattcaagcata TAGATTATCCTGAA CGCCCTTgcg	aattcgcAAGGGCGTTCAGGATAATCTAt atgcttgaatataactaTAGATTATCCTGAAC GCCCTTactg	
CG10289-3	ctagcagtCAGGCTGAGTACGACAATAA Ttagttatattcaagcata TTATTGTCGTACT CAGCCTGgcg	aattcgcCAGGCTGAGTACGACAATAATt atgcttgaatataactaATTATTGTCGTACTC AGCCTGactg	
CG16935-1	ctagcagtCTGCGTGGGCGACAAAGTCA Atagttatattcaagcata TTGACTTTGTCGC CCACGCAGgcg	aattcgcCTGCGTGGGCGACAAAGTCAA tatgcttgaatataactaTTGACTTTGTCGCC CACGCAGactg	
CG16935-2	ctagcagtCCGGGTGACACGGTCATCCA Atagttatattcaagcata TTGGATGACCGTG TCACCCGGgcg	aattcgcCCGGGTGACACGGTCATCCAA tatgcttgaatataactaTTGGATGACCGTGT CACCCGGactg	
CG16935-3	ctagcagtACGGAGGTGTCGCGTCATCT Atagttatattcaagcata TAGATGACGCGAC ACCTCCGTgcg	aattcgcACGGAGGTGTCGCGTCATCTA tatgcttgaatataactaTAGATGACGCGACA CCTCCGTactg	
CG17018-1	ctagcagtAAGTATAATGGTCAAGACAAA tagttatattcaagcata TTTGTCTTGACCATT ATACTTgcg	aattcgcAAGTATAATGGTCAAGACAAAt atgcttgaatataactaTTTGTCTTGACCATT ATACTTactg	SH06400.N
CG17018-2	ctagcagtTGCGACCTTATAGACATTCTA tagttatattcaagcata TAGAATGTCTATAAG GTCGCAgcg	aattcgcTGCGACCTTATAGACATTCTAt atgcttgaatataactaTAGAATGTCTATAAG GTCGCAactg	
CG17018-3	ctagcagtAAGGTGCAGCGTCTTATCAA Atagttatattcaagcata TTTGATAAGACGCT GCACCTTgcg	aattcgcAAGGTGCAGCGTCTTATCAAAt atgcttgaatataactaTTTGATAAGACGCTG CACCTTactg	

CG3342-1	ctagcagtCTGGACAAATATCTAGACGA Atagttatattcaagcata**TTCGTCTAGATATT** TGTCCAGgcg	aattcgcCTGGACAAATATCTAGACGAAt atgcttgaatataactaTTCGTCTAGATATTT GTCCAGactg	
CG3342-2	ctagcagtCGGGTCGGTTATAGCACCTA Atagttatattcaagcata**TTAGGTGCTATAAC** CGACCCGgcg	aattcgcCGGGTCGGTTATAGCACCTAA tatgcttgaatataactaTTAGGTGCTATAAC CGACCCGactg	
CG3342-3	ctagcagtCCGGATGAGAAGGAATTCAT Atagttatattcaagcata**TATGAATTCCTTCT** CATCCGGgcg	aattcgcCCGGATGAGAAGGAATTCATAt atgcttgaatataactaTATGAATTCCTTCTC ATCCGGactg	
CG9062-1	ctagcagtCTGGTTCACTGTTGATCTGAA tagttatattcaagcata**TTCAGATCAACAGT** GAACCAGgcg	aattcgcCTGGTTCACTGTTGATCTGAAt atgcttgaatataactaTTCAGATCAACAGTG AACCAGactg	
CG9062-2	ctagcagtAACGACAAACGTTATATCATA tagttatattcaagcata**TATGATATAACGTTT** GTCGTTgcg	aattcgcAACGACAAACGTTATATCATAt atgcttgaatataactaTATGATATAACGTTT GTCGTTactg	
CG9062-3	ctagcagtCAGTTCCGACGGCACGATCA Atagttatattcaagcata**TTGATCGTGCCGT** CGGAACTGgcg	aattcgcCAGTTCCGACGGCACGATCAA tatgcttgaatataactaTTGATCGTGCCGTC GGAACTGactg	
cher-1	ctagcagtCAGCTGCGATGTGTCGTACA Atagttatattcaagcata**TTGTACGACACAT** CGCAGCTGgcg	aattcgcCAGCTGCGATGTGTCGTACAA tatgcttgaatataactaTTGTACGACACATC GCAGCTGactg	SH02153.N
cher-2	ctagcagtCCAGTGCAAGCTGACATTCA Atagttatattcaagcata**TTGAATGTCAGCTT** GCACTGGgcg	aattcgcCCAGTGCAAGCTGACATTCAAt atgcttgaatataactaTTGAATGTCAGCTTG CACTGGactg	
cher-3	ctagcagtCGAGCTGGTGGTCAAATACA Atagttatattcaagcata**TTGTATTTGACCAC** CAGCTCGgcg	aattcgcCGAGCTGGTGGTCAAATACAA tatgcttgaatataactaTTGTATTTGACCACC AGCTCGactg	
CkIα-1	ctagcagtATACGTGATGATGTACTTCAA tagttatattcaagcata**TTGAAGTACATCATC** ACGTATgcg	aattcgcATACGTGATGATGTACTTCAAt atgcttgaatataactaTTGAAGTACATCATC ACGTATactg	SH10613.N
CkIα-2	ctagcagtACGCGCCATTTCACAATCAA Atagttatattcaagcata**TTTGATTGTGAAAT** GGCGCGTgcg	aattcgcACGCGCCATTTCACAATCAAAt atgcttgaatataactaTTTGATTGTGAAATG GCGCGTactg	
CkIα-3	ctagcagtTACGCGCCATTTCACAATCAA tagttatattcaagcata**TTGATTGTGAAATG** GCGCGTAgcg	aattcgcTACGCGCCATTTCACAATCAAt atgcttgaatataactaTTGATTGTGAAATGG CGCGTAactg	
cmet-1	ctagcagtCAGCAGTTGCGAGACAATAA Atagttatattcaagcata**TTTATTGTCTCGCA** ACTGCTGgcg	aattcgcCAGCAGTTGCGAGACAATAAAt atgcttgaatataactaTTTATTGTCTCGCAA CTGCTGactg	
cmet-2	ctagcagtCAGATACGACTCGATCTGCA Atagttatattcaagcata**TTGCAGATCGAGT** CGTATCTGgcg	aattcgcCAGATACGACTCGATCTGCAAt atgcttgaatataactaTTGCAGATCGAGTC GTATCTGactg	
cmet-3	ctagcagtTCGACTATAGAGAGTCTTCAA tagttatattcaagcata**TTGAAGACTCTCTAT** AGTCGAgcg	aattcgcTCGACTATAGAGAGTCTTCAAt atgcttgaatataactaTTGAAGACTCTCTAT AGTCGAactg	
coil-1	ctagcagtCTGGACCTTCTGTACAATCAA tagttatattcaagcata**TTGATTGTACAGAA** GGTCCAGgcg	aattcgcCTGGACCTTCTGTACAATCAAt atgcttgaatataactaTTGATTGTACAGAAG GTCCAGactg	SH00308.N
coil-2	ctagcagtTACGGCGACTCTGATATTGA Atagttatattcaagcata**TTCAATATCAGAGT** CGCCGTAgcg	aattcgcTACGGCGACTCTGATATTGAAt atgcttgaatataactaTTCAATATCAGAGTC GCCGTAactg	
coil-3	ctagcagtACGGAAGTGCATCTCCGATT Atagttatattcaagcata**TAATCGGAGATGC** ACTTCCGTgcg	aattcgcACGGAAGTGCATCTCCGATTAt atgcttgaatataactaTAATCGGAGATGCAC TTCCGTactg	
Cul1-1	ctagcagtCTGGTTGTATCAGATGTGCA Atagttatattcaagcata**TTGCACATCTGATA** CAACCAGgcg	aattcgcCTGGTTGTATCAGATGTGCAAt atgcttgaatataactaTTGCACATCTGATAC AACCAGactg	
Cul1-2	ctagcagtGCGGTCAGTGCGACAGTTCA Atagttatattcaagcata**TTGAACTGTCGCA** CTGACCGCgcg	aattcgcGCGGTCAGTGCGACAGTTCAA tatgcttgaatataactaTTGAACTGTCGCAC TGACCGCactg	
Cul1-3	ctagcagtCCGCGACGTTATCGAGTGCT Atagttatattcaagcata**TAGCACTCGATAA** CGTCGCGGgcg	aattcgcCCGCGACGTTATCGAGTGCTA tatgcttgaatataactaTAGCACTCGATAAC GTCGCGGactg	
dco-1	ctagcagtCTCGATTGTGGTGCTGTGCA Atagttatattcaagcata**TTGCACAGCACCA** CAATCGAGgcg	aattcgcCTCGATTGTGGTGCTGTGCAAt atgcttgaatataactaTTGCACAGCACCACA ATCGAGactg	
dco-2	ctagcagtTCGAGTCAAAGTTCTACAAG Atagttatattcaagcata**TCTTGTAGAACTTT** GACTCGAgcg	aattcgcTCGAGTCAAAGTTCTACAAGAt atgcttgaatataactaTCTTGTAGAACTTTG ACTCGAactg	

dco-3	ctagcagtAAGAAAGGAGCTCAGACGAA Atagttatattcaagcata TTTCGTCTGAGCT CCTTTCTTgcg	aattcgcAAGAAAGGAGCTCAGACGAAA tatgcttgaatataactaTTTCGTCTGAGCTC CTTTCTTactg	SH10572.N
dlt-1	ctagcagtCCGCAAGTTCCTGTTGCTCA Atagttatattcaagcata TTGAGCAACAGGA ACTTGCGGgcg	aattcgcCCGCAAGTTCCTGTTGCTCAAt atgcttgaatataactaTTGAGCAACAGGAA CTTGCGGactg	SH02999.N
dlt-2	ctagcagtCAGCCTGTTAATGGACCTCA Atagttatattcaagcata TTGAGGTCCATTAA CAGGCTGgcg	aattcgcCAGCCTGTTAATGGACCTCAAt atgcttgaatataactaTTGAGGTCCATTAAC AGGCTGactg	
dlt-3	ctagcagtCAGCAGCTTATGGACAGTAA Atagttatattcaagcata TTTACTGTCCATAA GCTGCTGgcg	aattcgcCAGCAGCTTATGGACAGTAAAt atgcttgaatataactaTTTACTGTCCATAAG CTGCTGactg	
γTub37C-1	ctagcagtCAGCGAGATTATAACCCTTC Atagttatattcaagcata TGAAGGGTTATAAT CTCGCTGgcg	aattcgcCAGCGAGATTATAACCCTTCAt atgcttgaatataactaTGAAGGGTTATAATC TCGCTGactg	
γTub37C-2	ctagcagtTTGGGCCAATGTGGCAATCA Atagttatattcaagcata TTGATTGCCACATT GGCCCAAgcg	aattcgcTTGGGCCAATGTGGCAATCAAt atgcttgaatataactaTTGATTGCCACATTG GCCCAAactg	
γTub37C-3	ctagcagtACCGAAAGATTGCACATCCA Atagttatattcaagcata TTGGATGTGCAAT CTTTCGGTgcg	aattcgcACCGAAAGATTGCACATCCAAt atgcttgaatataactaTTGGATGTGCAATCT TTCGGTactg	
GCS2α-1	ctagcagtAGCGAAATTCGACGAGTACA Atagttatattcaagcata TTGTACTCGTCGA ATTTCGCTgcg	aattcgcAGCGAAATTCGACGAGTACAAt atgcttgaatataactaTTGTACTCGTCGAAT TTCGCTactg	
GCS2α-2	ctagcagtATGATCAAGAATCTTACAGAA tagttatattcaagcata TTCTGTAAGATTCTT GATCATgcg	aattcgcATGATCAAGAATCTTACAGAAt atgcttgaatataactaTTCTGTAAGATTCTT GATCATactg	
GCS2α-3	ctagcagtCACGCCGACAGCTTCATACT Atagttatattcaagcata TAGTATGAAGCTG TCGGCGTGgcg	aattcgcCACGCCGACAGCTTCATACTAt atgcttgaatataactaTAGTATGAAGCTGTC GGCGTGactg	
Grip84-1	ctagcagtAAGGATGAGCGCAACGACTT Atagttatattcaagcata TAAGTCGTTGCGC TCATCCTTgcg	aattcgcAAGGATGAGCGCAACGACTTA tatgcttgaatataactaTAAGTCGTTGCGCT CATCCTTactg	
Grip84-2	ctagcagtTTCGATCTTCAAGCTCTGCAA tagttatattcaagcata TTGCAGAGCTTGAA GATCGAAgcg	aattcgcTTCGATCTTCAAGCTCTGCAAt atgcttgaatataactaTTGCAGAGCTTGAAG ATCGAAactg	
Grip84-3	ctagcagtCGAGCGATACAGCGAATGCA Atagttatattcaagcata TTGCATTCGCTGTA TCGCTCGgcg	aattcgcCGAGCGATACAGCGAATGCAA tatgcttgaatataactaTTGCATTCGCTGTAT CGCTCGactg	
Grip91-1	ctagcagtCTGGGTGGAGCTACAGAAGA Atagttatattcaagcata TTCTTCTGTAGCTC CACCCAGgcg	aattcgcCTGGGTGGAGCTACAGAAGAA tatgcttgaatataactaTTCTTCTGTAGCTCC ACCCAGactg	
Grip91-2	ctagcagtCACGATCGAGTGGTCAAGTT Ttagttatattcaagcata AAACTTGACCACTC GATCGTGgcg	aattcgcCACGATCGAGTGGTCAAGTTTt atgcttgaatataactaAAACTTGACCACTCG ATCGTGactg	
Grip91-3	ctagcagtTCGGCTGGACTTCAACGAGT Atagttatattcaagcata CTCGTTGAAGT CCAGCCGAgcg	aattcgcTCGGCTGGACTTCAACGAGTA tatgcttgaatataactaTACTCGTTGAAGTC CAGCCGAactg	
Hsp68-1	ctagcagtAGCGAGATCAAGGATGTCCT Atagttatattcaagcata AGGACATCCTTG ATCTCGCTgcg	aattcgcAGCGAGATCAAGGATGTCCTA tatgcttgaatataactaTAGGACATCCTTGA TCTCGCTactg	
Hsp68-2	ctagcagtCTGGCCGTTCAAAGTGATCA Atagttatattcaagcata TTGATCACTTTGAA CGGCCAGgcg	aattcgcCTGGCCGTTCAAAGTGATCAAt atgcttgaatataactaTTGATCACTTTGAAC GGCCAGactg	
Hsp68-3	ctagcagtCTGACCAAGGACAACAATGT Atagttatattcaagcata CATTGTTGTCCT TGGTCAGgcg	aattcgcCTGACCAAGGACAACAATGTAt atgcttgaatataactaTACATTGTTGTCCTT GGTCAGactg	
Hsp70Ba-1	ctagcagtTACAAGAAGAGAATACTTTCA tagttatattcaagcata TGAAAGTATTCTCTT CTTGTAgcg	aattcgcTACAAGAAGAGAATACTTTCAt atgcttgaatataactaTGAAAGTATTCTCTT CTTGTAactg	
Hsp70Ba-2	ctagcagtGAGCTACGTATACAACGTAA Atagttatattcaagcata TTTACGTTGTATAC GTAGCTCgcg	aattcgcGAGCTACGTATACAACGTAAAt atgcttgaatataactaTTTACGTTGTATACG TAGCTCactg	SH04445.N
Hsp70Ba-3	ctagcagtAGAGCTACGTATACAACGTA Atagttatattcaagcata TTACGTTGTATACG TAGCTCTgcg	aattcgcAGAGCTACGTATACAACGTAAt atgcttgaatataactaTTACGTTGTATACGT AGCTCTactg	
Imp-1	ctagcagtCAGCTCTATCAACGACATCA Atagttatattcaagcata TTGATGTCGTTGAT AGAGCTGgcg	aattcgcCAGCTCTATCAACGACATCAAt atgcttgaatataactaTTGATGTCGTTGATA GAGCTGactg	SH01803.N

Imp-2	ctagcagtATCGGACTATTCTACAGTGTA tagttatattcaagcataTACACTGTAGAATA GTCCGATgcg	aattcgcATCGGACTATTCTACAGTGTAt atgcttgaatataactaTACACTGTAGAATAG TCCGATactg	SH06428.N
Imp-3	ctagcagtTTCGAGAAGATGCGCGAAGA AtagttatattcaagcataTTCTTCGCGCATCT TCTCGAAgcg	aattcgcTTCGAGAAGATGCGCGAAGAA tatgcttgaatataactaTTCTTCGCGCATCTT CTCGAAactg	
Klp10A-1	ctagcagtCTGGAGGATGGTAAACAGCA AtagttatattcaagcataTTGCTGTTTACCAT CCTCCAGgcg	aattcgcCTGGAGGATGGTAAACAGCAA tatgcttgaatataactaTTGCTGTTTACCATC CTCCAGactg	
Klp10A-2	ctagcagtCTCGACGAAGATCCATGGCA AtagttatattcaagcataTTGCCATGGATCTT CGTCGAGgcg	aattcgcCTCGACGAAGATCCATGGCAA tatgcttgaatataactaTTGCCATGGATCTT CGTCGAGactg	
Klp10A-3	ctagcagtTAGCGTGAATACAAACAGCA AtagttatattcaagcataTTGCTGTTTGTATT CACGCTAgcg	aattcgcTAGCGTGAATACAAACAGCAAt atgcttgaatataactaTTGCTGTTTGTATTC ACGCTAactg	
Klp61F-1	ctagcagtCAGGAGCTGTCCGAAACTGA AtagttatattcaagcataTTCAGTTTCGGAC AGCTCCTGgcg	aattcgcCAGGAGCTGTCCGAAACTGAA tatgcttgaatataactaTTCAGTTTCGGACA GCTCCTGactg	SH00722.N
Klp61F-2	ctagcagtCCGATCTTGCGATCAGTTCA AtagttatattcaagcataTTGAACTGATCGC AAGATCGGgcg	aattcgcCCGATCTTGCGATCAGTTCAAt atgcttgaatataactaTTGAACTGATCGCAA GATCGGactg	
Klp61F-3	ctagcagtCAGCTGCAAATTTGCGAGCA AtagttatattcaagcataTTGCTCGCAAATTT GCAGCTGgcg	aattcgcCAGCTGCAAATTTGCGAGCAAt atgcttgaatataactaTTGCTCGCAAATTTG CAGCTGactg	
loki-1	ctagcagtCAGGATGCGAATCCTAAAGA AtagttatattcaagcataTTCTTTAGGATTCG CATCCTGgcg	aattcgcCAGGATGCGAATCCTAAAGAAt atgcttgaatataactaTTCTTTAGGATTCGC ATCCTGactg	
loki-2	ctagcagtACGTTTGTGAATAACGAGAA AtagttatattcaagcataTTTCTCGTTATTCA CAAACGTgcg	aattcgcACGTTTGTGAATAACGAGAAAt atgcttgaatataactaTTTCTCGTTATTCAC AAACGTactg	
loki-3	ctagcagtCAGCAACAAACTACTTAGCG AtagttatattcaagcataTCGCTAAGTAGTTT GTTGCTGgcg	aattcgcCAGCAACAAACTACTTAGCGAt atgcttgaatataactaTCGCTAAGTAGTTTG TTGCTGactg	SH10629.N
Map205-1	ctagcagtCAGACTTGTGACGATAAGGA AtagttatattcaagcataTTCCTTATCGTCAC AAGTCTGgcg	aattcgcCAGACTTGTGACGATAAGGAAt atgcttgaatataactaTTCCTTATCGTCACA AGTCTGactg	
Map205-2	ctagcagtACGATGGTGACTTCTCGACA AtagttatattcaagcataTTGTCGAGAAGTC ACCATCGTgcg	aattcgcACGATGGTGACTTCTCGACAAt atgcttgaatataactaTTGTCGAGAAGTCAC CATCGTactg	
Map205-3	ctagcagtTAGCAGAAGAGGTTAAGATT AtagttatattcaagcataTAATCTTAACCTCT TCTGCTAgcg	aattcgcTAGCAGAAGAGGTTAAGATTAt atgcttgaatataactaTAATCTTAACCTCTT CTGCTAactg	
milt-1	ctagcagtCTGACGCAAGACAACGACGA AtagttatattcaagcataTTCGTCGTTGTCTT GCGTCAGgcg	aattcgcCTGACGCAAGACAACGACGAA tatgcttgaatataactaTTCGTCGTTGTCTTG CGTCAGactg	
milt-2	ctagcagtCAGCTAAACGATGCTAACTC AtagttatattcaagcataTGAGTTAGCATCG TTTAGCTGgcg	aattcgcCAGCTAAACGATGCTAACTCAt atgcttgaatataactaTGAGTTAGCATCGTT TAGCTGactg	
milt-3	ctagcagtTCCGGACGATGGATTCGTTA AtagttatattcaagcataTTAACGAATCCATC GTCCGGAgcg	aattcgcTCCGGACGATGGATTCGTTAAt atgcttgaatataactaTTAACGAATCCATCG TCCGGAactg	
msps-1	ctagcagtAAGACACTTATTGAAGATGTA tagttatattcaagcataTACATCTTCAATAAG TGTCTTgcg	aattcgcAAGACACTTATTGAAGATGTAt atgcttgaatataactaTACATCTTCAATAAG TGTCTTactg	
msps-2	ctagcagtAAGCCTGTTAGAGGAGTTCA AtagttatattcaagcataTTGAACTCCTCTAA CAGGCTTgcg	aattcgcAAGCCTGTTAGAGGAGTTCAAt atgcttgaatataactaTTGAACTCCTCTAAC AGGCTTactg	
msps-3	ctagcagtCAGGTAGAGTTTGACAAGAA TtagttatattcaagcataATTCTTGTCAAACT CTACCTGgcg	aattcgcCAGGTAGAGTTTGACAAGAATt atgcttgaatataactaATTCTTGTCAAACTC TACCTGactg	
mtrm-1	ctagcagtCACGCCCACGAACAAGACCA AtagttatattcaagcataTTGGTCTTGTTCGT GGGCGTGgcg	aattcgcCACGCCCACGAACAAGACCAA tatgcttgaatataactaTTGGTCTTGTTCGT GGGCGTGactg	
mtrm-2	ctagcagtCCGATGAGGATTGCAACCGT AtagttatattcaagcataTACGGTTGCAATC CTCATCGGgcg	aattcgcCCGATGAGGATTGCAACCGTA tatgcttgaatataactaTACGGTTGCAATCC TCATCGGactg	
mtrm-3	ctagcagtGCGGTTCGCTACCTTCAAGA AtagttatattcaagcataTTCTTGAAGGTAG CGAACCGCgcg	aattcgcGCGGTTCGCTACCTTCAAGAAt atgcttgaatataactaTTCTTGAAGGTAGCG AACCGCactg	

mus101-1	ctagcagtAACGAGGAGTTCTTCAACCA Atagttatattcaagcata TTGGTTGAAGAAC TCCTCGTTgcg	aattcgcAACGAGGAGTTCTTCAACCAAt atgcttgaatataactaTTGGTTGAAGAACTC CTCGTTactg	
mus101-2	ctagcagtAAGCAAATCACCGACTATCTA tagttatattcaagcataTAGATAGTCGGTGA TTTGCTTgcg	aattcgcAAGCAAATCACCGACTATCTAt atgcttgaatataactaTAGATAGTCGGTGAT TTGCTTactg	
mus101-3	ctagcagtAACGGACACCGAGAAGTATA Atagttatattcaagcata TTATACTTCTCGGT GTCCGTTgcg	aattcgcAACGGACACCGAGAAGTATAA tatgcttgaatataactaTTATACTTCTCGGTG TCCGTTactg	
Pli-1	ctagcagtTTCCAGGATAATCTAGATTAA tagttatattcaagcata TTAATCTAGATTATC CTGGAAgcg	aattcgcTTCCAGGATAATCTAGATTAAt atgcttgaatataactaTTAATCTAGATTATC CTGGAAactg	
Pli-2	ctagcagtCTCCAAGTTTGTGCTCCACA Atagttatattcaagcata TTGTGGAGCACAA ACTTGGAGgcg	aattcgcCTCCAAGTTTGTGCTCCACAAt atgcttgaatataactaTTGTGGAGCACAAAC TTGGAGactg	
Pli-3	ctagcagtCACGCTGGTTATACCACGCA Atagttatattcaagcata TTGCGTGGTATAA CCAGCGTGgcg	aattcgcCACGCTGGTTATACCACGCAAt atgcttgaatataactaTTGCGTGGTATAACC AGCGTGactg	
polo-1	ctagcagtCTGGAGAAGATGTTCACATA Atagttatattcaagcata TTATGTGAACATCT TCTCCAGgcg	aattcgcCTGGAGAAGATGTTCACATAAt atgcttgaatataactaTTATGTGAACATCTT CTCCAGactg	SH00482.N
polo-2	ctagcagtTACGAGATCATCGATGTGGA Atagttatattcaagcata TTCCACATCGATG ATCTCGTAgcg	aattcgcTACGAGATCATCGATGTGGAAt atgcttgaatataactaTTCCACATCGATGAT CTCGTAactg	
polo-3	ctagcagtTCCGAACATTGTCAAGTTTCA tagttatattcaagcata TGAAACTTGACAAT GTTCGGAgcg	aattcgcTCCGAACATTGTCAAGTTTCAt atgcttgaatataactaTGAAACTTGACAATG TTCGGAactg	
SkpA-1	ctagcagtACGCAAGACCTTCAACATTAA tagttatattcaagcata TTAATGTTGAAGGTC TTGCGTgcg	aattcgcACGCAAGACCTTCAACATTAAt atgcttgaatataactaTTAATGTTGAAGGTC TTGCGTactg	SH00974.N
SkpA-2	ctagcagtAGCGAACTATCTGGACATTA Atagttatattcaagcata TTAATGTCCAGATA GTTCGCTgcg	aattcgcAGCGAACTATCTGGACATTAAt atgcttgaatataactaTTAATGTCCAGATAG TTCGCTactg	
SkpA-3	ctagcagtCACCTGCAAGACTGTTGCAA Atagttatattcaagcata TTTGCAACAGTCTT GCAGGTGgcg	aattcgcCACCTGCAAGACTGTTGCAAAt atgcttgaatataactaTTTGCAACAGTCTTG CAGGTGactg	
slam-1	ctagcagtCTCGAACGATCCGATGGACA Atagttatattcaagcata TTGTCCATCGGAT CGTTCGAGgcg	aattcgcCTCGAACGATCCGATGGACAA tatgcttgaatataactaTTGTCCATCGGATC GTTCGAGactg	
slam-2	ctagcagtCCGATGGACAACAGTCCGAT Atagttatattcaagcata TATCGGACTGTTG TCCATCGGgcg	aattcgcCCGATGGACAACAGTCCGATA tatgcttgaatataactaTATCGGACTGTTGT CCATCGGactg	
slam-3	ctagcagtCTGGATCGTCAGAGCGATGA Atagttatattcaagcata TTCATCGCTCTGA CGATCCAGgcg	aattcgcCTGGATCGTCAGAGCGATGAA tatgcttgaatataactaTTCATCGCTCTGAC GATCCAGactg	
sle-1	ctagcagtATCGATGTTACCGAGGTTATA tagttatattcaagcata TATAACCTCGGTAA CATCGATgcg	aattcgcATCGATGTTACCGAGGTTATAt atgcttgaatataactaTATAACCTCGGTAAC ATCGATactg	SH00769.N
sle-2	ctagcagtCCGAGGAAAGACCGACAGAA Atagttatattcaagcata TTTCTGTCGGTCTT TCCTCGGgcg	aattcgcCCGAGGAAAGACCGACAGAA AtatgcttgaatataactaTTTCTGTCGGTCTT TCCTCGGactg	
sle-3	ctagcagtAACAACGACACTGATGACTT Atagttatattcaagcata TAAGTCATCAGTGT CGTTGTTgcg	aattcgcAACAACGACACTGATGACTTAt atgcttgaatataactaTAAGTCATCAGTGTC GTTGTTactg	
slmb-1	ctagcagtCTGCGCGAGTTACATCTACA Atagttatattcaagcata TTGTAGATGTAACT CGCGCAGgcg	aattcgcCTGCGCGAGTTACATCTACAAt atgcttgaatataactaTTGTAGATGTAACTC GCGCAGactg	
slmb-2	ctagcagtTCGATACGAAACGAATCGTT Atagttatattcaagcata TAACGATTCGTTTC GTATCGAgcg	aattcgcTCGATACGAAACGAATCGTTAt atgcttgaatataactaTAACGATTCGTTTCG TATCGAactg	
slmb-3	ctagcagtTTGGATGCAGTACCTCTTCAA tagttatattcaagcata TTGAAGAGGTACTG CATCCAAgcg	aattcgcTTGGATGCAGTACCTCTTCAAt atgcttgaatataactaTTGAAGAGGTACTGC ATCCAAactg	
SmD2-1	ctagcagtTCGGTTCATATCGAAGATGTT tagttatattcaagcata ACATCTTCGATATG AACCGAgcg	aattcgcTCGGTTCATATCGAAGATGTTt atgcttgaatataactaACATCTTCGATATG AACCGAactg	SH06417.N
SmD2-2	ctagcagtCACGCAGTCCGTGAAGAACA Atagttatattcaagcata TTGTTCTTCACGGA CTGCGTGgcg	aattcgcCACGCAGTCCGTGAAGAACAA tatgcttgaatataactaTTGTTCTTCACGGA CTGCGTGactg	

SmD2-3	ctagcagtCAACACCCAGGTGCTCATCA AtagttatattcaagcataTTGATGAGCACCT GGGTGTTGgcg	aattcgcCAACACCCAGGTGCTCATCAAt atgcttgaatataactaTTGATGAGCACCTG GGTGTTGactg	
sxc-1	ctagcagtCACGAGAGCAATTCAAATTAA tagttatattcaagcataTTAATTTGAATTGCT CTCGTGgcg	aattcgcCACGAGAGCAATTCAAATTAAt atgcttgaatataactaTTAATTTGAATTGCT CTCGTGactg	SH03246.N
sxc-2	ctagcagtCTGCACTAAGACTATGTTCAA tagttatattcaagcataTTGAACATAGTCTTA GTGCAGgcg	aattcgcCTGCACTAAGACTATGTTCAAt atgcttgaatataactaTTGAACATAGTCTTA GTGCAGactg	
sxc-3	ctagcagtAAGGAAGCTATTAGAATTCAA tagttatattcaagcataTTGAATTCTAATAGC TTCCTTgcg	aattcgcAAGGAAGCTATTAGAATTCAAt atgcttgaatataactaTTGAATTCTAATAGC TTCCTTactg	
tacc-1	ctagcagtCTGATCAAGCGTATTACAGA AtagttatattcaagcataTTCTGTAATACGCT TGATCAGgcg	aattcgcCTGATCAAGCGTATTACAGAAt atgcttgaatataactaTTCTGTAATACGCTT GATCAGactg	SH09157.N
tacc-2	ctagcagtTACGGAGGATAAGACGCACA AtagttatattcaagcataTTGTGCGTCTTATC CTCCGTAgcg	aattcgcTACGGAGGATAAGACGCACAA tatgcttgaatataactaTTGTGCGTCTTATCC TCCGTAactg	
tacc-3	ctagcagtACAGCGCTACGACAAGATGA AtagttatattcaagcataTTCATCTTGTCGTA GCGCTGTgcg	aattcgcACAGCGCTACGACAAGATGAA tatgcttgaatataactaTTCATCTTGTCGTAG CGCTGTactg	
toc-1	ctagcagtGCGACAGACATTGACAAGCA AtagttatattcaagcataTTGCTTGTCAATGT CTGTCGCgcg	aattcgcGCGACAGACATTGACAAGCAA tatgcttgaatataactaTTGCTTGTCAATGTC TGTCGCactg	
toc-2	ctagcagtCAGCTGGACGCTAGAGATCG AtagttatattcaagcataTCGATCTCTAGCG TCCAGCTGgcg	aattcgcCAGCTGGACGCTAGAGATCGA tatgcttgaatataactaTCGATCTCTAGCGT CCAGCTGactg	
toc-2	ctagcagtAAGGAAGAAACCACAAGACG AtagttatattcaagcataTCGTCTTGTGGTTT CTTCCTTgcg	aattcgcAAGGAAGAAACCACAAGACGA tatgcttgaatataactaTCGTCTTGTGGTTTC TTCCTTactg	
WDR79-1	ctagcagtTTGCGACGATTACCCTGTCA AtagttatattcaagcataTTGACAGGGTAAT CGTCGCAAgcg	aattcgcTTGCGACGATTACCCTGTCAAt atgcttgaatataactaTTGACAGGGTAATCG TCGCAAactg	
WDR79-2	ctagcagtCAGTTCCACTTTACAGACCAA tagttatattcaagcataTTGGTCTGTAAAGT GGAACTGgcg	aattcgcCAGTTCCACTTTACAGACCAAt atgcttgaatataactaTTGGTCTGTAAAGTG GAACTGactg	
WDR79-3	ctagcagtTACGATGCCGTAGACGAAGT AtagttatattcaagcataTACTTCGTCTACG GCATCGTAgcg	aattcgcTACGATGCCGTAGACGAAGTA tatgcttgaatataactaTACTTCGTCTACGG CATCGTAactg	

Bibliography

Ando, K., Ozaki, T., Yamamoto, H., Furuya, K., Hosoda, M., Hayashi, S., . . . Nakagawara, A. (2004). Polo-like kinase 1 (Plk1) inhibits p53 function by physical interaction and phosphorylation. *The Journal of Biological Chemistry, 279*(24), 25549-61. doi:10.1074/jbc.M314182200

Andrysik, Z., Bernstein, W., Deng, L., Myer, D., Li, Y.-Q., Tischfield, J., . . . Bahassi, E. (2010). The novel mouse Polo-like kinase 5 responds to DNA damage and localizes in the nucleolus. *Nucleic Acids Research, 38*(9), 2931-2943. doi:10.1093/nar/gkq011

Archambault, V., & Glover, D. (2009). Polo-like kinases: conservation and divergence in their functions and regulation. *Nature Reviews. Molecular Cell Biology, 10*(4), 265-75. doi:10.1038/nrm2653

Archambault, V., D'Avino, P., Deery, M., Lilley, K., & Glover, D. (2008). Sequestration of Polo kinase to microtubules by phosphopriming-independent binding to Map205 is relieved by phosphorylation at a CDK site in mitosis. *Genes & Development, 22*(19), 2707-20. doi:10.1101/gad.486808

Archambault, V., Lepine, G., & Kachaner, D. (2015). Understanding the Polo Kinase machine. *Oncogene, 34*, 4799-4807. doi:10.1038/onc.2014.451

Ashburner, M., Ball, C., Blake, J., Botstein, D., Butler, H., Cherry, J., . . . SHerlock, G. (2000). Gene ontology: tool for the unification of biology. The Gene Ontology Consortium. *Nature Genetics, 25*(1), 25-9. doi:10.1038/75556

Bahassi, E., Myer, D., McKenney, R., Hennigan, R., & Stambrook, P. (2006). Priming phosphorylation of Chk2 by polo-like kinase 3 (Plk3) mediates its full activation by ATM and a downstream checkpoint in response to DNA damage. *Mutation Research/Fundamental and Molecular Mechanisms of Mutagenesis, 596*(1-2), 166-176. doi:10.1016/j.mrfmmm.2005.12.002

Barberis, M., Klipp, E., Vanoni, M., & Alberghina, L. (2007). Cell Size at S Phase Initiation: An Emergent Property of the G1/S Network. *PLoS Computational Biology, 3*(4), e64. doi:10.1371/journal.pcbi.0030064

Bassett, A., Kong, L., & Liu, J. (2015). A Genome-Wide CRISPR Library for High-Throughput Genetic Screening in Drosophila Cells. *Journal of Genetics and Genomics, 42*(6), 301-9. doi:10.1016/j.jgg.2015.03.011

Bastos, R., & Barr, F. (2010). Plk1 negatively regulates Cep55 recruitment to the midbody to ensure orderly abscission. *Journal of Cell Biology, 191*(4), 751-60. doi:10.1083/jcb.201008108

Bettencourt-Dias, M., Rodrigues-Martins, A., Carpenter, L., Riparbelli, M., Lehmann, L., Gatt, M., . . . Glover, D. (2005). SAK/PLK4 is required for

centriole duplication and flagella development. *Current Biology, 15*(24), 2199-207. doi:10.1016/j.cub.2005.11.042

Bishop, A., Ubersax, J., Petsch, D., Matheos, D., Gray, N., Blethrow, J., . . . Shokat, K. (2000). A chemical switch for inhibitor-sensitive alleles of any protein kinase. *Nature, 407*(6802), 395-401. doi:10.1038/35030148

Boucher, B., & Jenna, S. (2013). Genetic interaction networks: better understand to better predict. *Frontiers in Genetics, 4*, 1-16. doi:10.3389/fgene.2013.00290

Brand, A., & Perrimon, N. (1993). Targeted gene expression as a means of altering cell fates and generating dominant phenotypes. *Development, 118*(2), 401-15.

Bu, Y., Yang, Z., Li, Q., & Song, F. (2008). Silencing of polo-like kinase (Plk) 1 via siRNA causes inhibition of growth and induction of apoptosis in human esophageal cancer cells. *Oncology, 74*(3-4), 198-206. doi:10.1159/000151367

Burkard, M., Randall, C., Larochelle, S., Zhang, C., Shokat, K., Fisher, R., & Jallepalli, P. (2007). Chemical genetics reveals the requirement for Polo-like kinase 1 activity in positioning RhoA and triggering cytokinesis in human cells. *Proceedings of the National Academy of Sciences of the Unites States of America, 104*(11), 4383-88. doi:10.1073/pnas.0701140104

Chen, C., Hehnly, H., & Doxsey, S. (2012). Orchestrating vesicle transport, ESCRTs and kinase surveillance during abscission. *Nature Reviews Molecular Cell Biology, 13*, 483-88. doi:10.1038/nrm3395

Chen, C.-T., Hehnly, H., Yu, Q., Farkas, D., Zheng, G., Redick, S., . . . Doxsey, S. (2014). A unique set of centrosome proteins requires pericentrin for spindle-pole localization and spindle orientation. *Current Biology, 24*(19), 2327-34. doi:10.1016/j.cub.2014.08.029

Colicino, E., & Hehnly, H. (2018). Regulating a key mitotic regulator, polo-like kinase 1 (PLK1). *Cytoskeleton, 71*(11), 481-494. doi:10.1002/cm.21504

Colicino, E., Garrastegui, A., Freshour, J., Santra, P., Post, D., Kotula, L., & Hehnly, H. (2018). Gravin regulates centrosome function through PLK1. *Molecular Biology of the Cell, 29*(5), 532-541. doi:10.1091/mbc.E17-08-0524

Colnaghi, R., & Wheatley, S. (2010). Liaisons between survivin and Plk1 during cell division and cell death. *The Journal of Biological Chemistry, 285*(29), 22592-604. doi:10.1074/jbc.M109.065003

Combes, G., Alharbi, I., Braga, L., & Elowe, S. (2017). Playing polo during mitosis: PLK1 takes the lead. *Oncogene, 36*(34), 4819-27. doi:10.1038/onc.2017.113

Conde, C., Osswald, M., Barbosa, J., Moutinho-Santos, T., Pinheiro, D., Guimarães, S., . . . Sunkel, C. (2013). Drosophila Polo regulates the spindle assembly checkpoint through Mps1-dependent BubR1 phosphorylation. *The EMBO Journal, 32*(12), 1761-77. doi:10.1038/emboj.2013.109

Cunha-Ferreira, I., Bento, I., Pimenta-Marques, A., Chandra Jana, S., Lince-Faria, M., Duarte, P., ..., B.-D. M. (2013). Regulation of autophosphorylation controls PLK4 self-destruction and centriole number. *Current Biology, 23*(22), 2245-54. doi:10.1016/j.cub.2013.09.037

Czaplinski, S., Hugle, M., Stiehl, V., & Fulda, S. (2016). Polo-like kinase 1 inhibition sensitizes neuroblastoma cells for vinca alkaloid-induced apoptosis. *Oncotarget, 7*(8), 8700-11. doi:10.18632/oncotarget.3901

D'Avino, P., Archambault, V., Przewloka, M., Zhang, W., Lilley, K., Laue, E., & DM, G. (2007). Recruitment of Polo kinase to the spindle midzone during cytokinesis requires the Feo/Klp3A complex. *PLoS One, 2*(6), e572. doi:10.1371/journal.pone.0000572

De Blasio, C., Zonfrilli, A., Franchitto, M., Mariano, G., Cialfi, S., Verma, N., . . . Talora, C. (2019). PLK1 targets NOTCH1 during DNA damage and mitotic progression. *Journal of Biological Chemistry, 294*(47), 17941-50. doi:10.1074/jbc.RA119.009881

de Cárcer, G. (2019). The Mitotic Cancer Target Polo-Like Kinase 1: Oncogene or Tumor Suppressor? *Genes, 10*(3), 208. doi:10.3390/genes10030208

de Cárcer, G., & Malumbres, M. (2014). A centrosomal route for cancer genome instability. *Nature Cell Biology, 16*(6), 504-6. doi:10.1038/ncb2978

de Cárcer, G., Escobar, B., Higuero, A., García, L., Ansón, A., Pérez, G., . . . Malumbres, M. (2011a). Plk5, a polo box domain-only protein with specific roles in neuron differentiation and glioblastoma suppression. *Molecular and Cellular Biology, 31*(6), 1225-39. doi:10.1128/MCB.00607-10

de Cárcer, G., Manning, G., & Malumbres, M. (2011b). From Plk1 to Plk5: functional evolution of polo-like kinases. *Cell Cycle, 10*(14), 2255-62. doi:10.4161/cc.10.14.16494

de Cárcer, G., Venkateswaran, S., Salgueiro, L., El Bakkali, A., Somogyi, K., Rowald, K., . . . Sotillo, R. (2018). Plk1 overexpression induces chromosomal instability and suppresses tumor development. *Nature Communications, 9*(1), 3012. doi:10.1038/s41467-018-05429-5

Döhner, H., Lübbert, M., Fiedler, W., Fouillard, L., Haaland, A., Brandwein, J., . . . Maertens, J. (2014). Randomized, phase 2 trial of low-dose cytarabine with or without volasertib in AML patients not suitable for induction therapy. *Blood, 124*(9), 1426-1433. doi:0.1182/blood-2014-03-560557

Dopie, J., Rajakylä, E., Joensuu, M., Huet, G., Ferrantelli, E., Xie, T., . . . Vartiainen, M. (2015). Genome-wide RNAi screen for nuclear actin reveals a network of cofilin regulators. *Journal of Cell Science, 128*(13), 2388-400. doi:10.1242/jcs.169441

Duffy, J. (2002). GAL4 System in Drosophila: A Fly Geneticist's Swiss Army Knife. *Genesis, 34*(1-2), 1-15. doi:10.1002/gene.10150

Elia, A., Cantley, L., & Yaffe, M. (2003a). Proteomic screen finds pSer/pThr-binding domain localizing Plk1 to mitotic substrates. *Science, 299*(5610), 1228-31. doi:10.1126/science.1079079

Elia, A., Rellos, P., Haire, L., Chao, J., Ivins, F., Hoepker, K., . . . Yaffe, M. (2003b). The molecular basis for phosphodependent substrate targeting and regulation of Plks by the Polo-box domain. *Cell, 115*(1), 83-95. doi:0.1016/s0092-8674(03)00725-6

Ferris, D., Maloid, S., & Li, C.-C. H. (1998). Ubiquitination and Proteasome Mediated Degradation of Polo-like Kinase. *Biochemical and Biophysical Research Communications, 252*(2), 340-344. doi:10.1006/bbrc.1998.9648

Fischer, B., Sandmann, T., Horn, T., Billmann, M., Chaudhary, V., Huber, W., & Boutros, M. (2015). A map of directional genetic interactions in a metazoan cell. *Elife, 4*, e05464. doi:10.7554/eLife.05464

Fischer, J., Giniger, E., Maniatis, T., & Ptashne, M. (1988). GAL4 activates transcription in Drosophila. *Nature, 332*(6167), 853-6. doi:10.1038/332853a0

Fisher, R. (1919). The correlation between relatives on the supposition of mendelian inheritance. *Earth and Environmental Science Transactions of the Royal Society of Edinburgh, 52*, 399-433. doi:10.1017/S0080456800012163

Frost, A., Mross, K., Steinbild, S., Hedbom, S., Unger, C., Kaiser, R., . . . Munzert, G. (2012). Phase I study of the Plk1 inhibitor BI 2536 administered intravenously on three consecutive days in advanced solid tumours. *Current Oncology, 19*(1), e28-35. doi:10.3747/co.19.866

Giniger, E., & Ptashne, M. (1987). Transcription in yeast activated by a putative amphipathic alpha helix linked to a DNA binding unit. *Nature, 330*(6149), 670-2. doi:10.1038/330670a0

Giniger, E., Varnum, S., & Ptashne, M. (1985). Specific DNA binding of GAL4, a positive regulatory protein of yeast. *Cell, 40*(4), 767-74. doi:10.1016/0092-8674(85)90336-8

Giráldez, S., Galindo-Moreno, M., Limón-Mortés, M., Rivas, C., Herrero-Ruiz, J., Mora-Santos, M., . . . Romero, F. (2017). G1/S phase progression is

regulated by PLK1 degradation through the CDK1/βTrCP axis. *FASEB Journal, 31*(7), 29125-2936. doi:10.1096/fj.201601108R

Golsteyn, R., Mundt, K., Fry, A., & Nigg, E. (1995). Cell cycle regulation of the activity and subcellular localization of Plk1, a human protein kinase implicated in mitotic spindle function. *The Journal of Cell Biology, 129*(6), 1617-28. doi:10.1083/jcb.129.6.1617

González, C., Tavosanis, G., & Mollinari, C. (1998). Centrosomes and microtubule organisation during Drosophila development. *Journal of Cell Science, 111*(Pt 18), 2697-706.

Goto, H., Kiyono, T., Tomono, Y., Kawajiri, A., Urano, T., Furukawa, K., . . . Inagaki, M. (2006). Complex formation of Plk1 and INCENP required for metaphase-anaphase transition. *Nature Cell Biology, 8*(2), 180-7. doi:10.1038/ncb1350

Guarente, L., Yocum, R., & Gifford, P. (1982). A GAL10-CYC1 hybrid yeast promoter identifies the GAL4 regulatory region as an upstream site. *Proceedings of the National Academy of Science of the USA, 79*(23), 7410-4. doi:10.1073/pnas.79.23.7410

Guest, S., Yu, J., Liu, D., Hines, J., Kashat, M., & Finley, R. (2011). A protein network-guided screen for cell cycle regulators in Drosophila. *BMC Systems Biology, 5*, 65. doi:10.1186/1752-0509-5-65

Gutteridge, R., Ndiaye, M., Liu, X., & Ahmad, N. (2016). Plk1 inhibitors in cancer therapy: From laboratory to clinics. *Molecular Cancer Therapeutics, 15*(7), 1427-35. doi:10.1158/1535-7163.MCT-15-0897

Habedanck, R., Stierhof, Y.-D., Wilkinson, C., & Nigg, E. (2005). The Polo kinase Plk4 functions in centriole duplication. *Nature Cell Biology, 7*(1), 1140-46. doi:10.1038/ncb1320

Halpern, M., Rhee, J., Goll, M., Akitake, C., Parsons, M., & Leach, S. (2008). Gal4/UAS Transgenic Tools and Their Application to Zebrafish. *Zebrafish, 5*(2), 97-110. doi:10.1089/zeb.2008.0530

Hanafusa, H., Kedashiro, S., Tezuka, M., Funatsu, M., Usami, S., Toyoshima, F., & Matsumoto, K. (2015). PLK1-dependent activation of LRRK1 regulates spindle orientation by phosphorylating CDK5RAP2. *Nature Cell Biology, 17*(8), 1024-35. doi:10.1038/ncb3204

Hanisch, A., Wehner, A., Nigg, E., & Silljé, H. (2005). Different Plk1 Functions Show Distinct Dependencies on Polo-Box Domain-mediated Targeting. *Molecular Biology of the Cell, 17*(1), 448-59. doi:10.1091/mbc.e05-08-0801

Hartwell, L., Mortimer, R., Culotti, J., & Culotti, M. (1973). Genetic Control of the Cell Division Cycle in Yeast: V. Genetic Analysis of cdc Mutants. *Genetics, 74*(2), 267-86.

Hofheinz, R., Al-Batran, S., Hochhaus, A., Jager, E., Reichardt, V., Fritsch, H., . . . Munzert, G. (2010). An open-label, phase I study of the polo-like kinase-1 inhibitor, BI 2536, in patients with advanced solid tumors. *Clinical Cancer Research, 16*(18), 4666-4674. doi:10.1158/1078-0432.CCR-10-0318

Hood, E., Kettenbach, A., Gerber, S., & Compton, D. (2012). Plk1 regulates the kinesin-13 protein Kif2b to promote faithful chromosome segregation. *Molecular Biology of the Cell, 23*(12), 2264-74. doi:10.1091/mbc.E11-12-1013

Housden, B., Li, Z., Kelley, C., Wang, Y., Hu, Y., Valvezan, A., . . . Perrimon, N. (2017). Improved detection of synthetic lethal interactions in Drosophila cells using variable dose analysis (VDA). *Proceedings of the National Academy of Sciences of the USA, 114*(50), E10755-62. doi:10.1073/pnas.1713362114

Hughes, S., Beeler, J., Seat, A., Slaughter, B., Unruh, J., Bauerly, E., . . . Hawley, R. (2011). Gamma-Tubulin Is Required for Bipolar Spindle Assembly and for Proper Kinetochore Microtubule Attachments during Prometaphase I in Drosophila Oocytes. *PLoS Genetics, 7*(8), e1002209. doi:10.1371/journal.pgen.1002209

Hyun, S.-Y., Hwang, H.-I., & Jang, Y.-J. (2014). Polo-like kinase-1 in DNA damage response. *BMB reports, 47*(5), 249-55. doi:10.5483/bmbrep.2014.47.5.061

Johnston, S., Salmeron, J., & Dincher, S. (1987). Interaction of positive and negative regulatory proteins in the galactose regulon of yeast. *Cell, 50*(1), 143-6. doi:10.1016/0092-8674(87)90671-4

Kachaner, D., Garrido, D., Mehsen, H., Normandin, K., Lavoie, H., & Archambault, V. (2017). Coupling of Polo kinase activation to nuclear localization by a bifunctional NLS is required during mitotic entry. *Nature Communications, 8*(1), 1701. doi:10.1038/s41467-017-01876-8

Kakidani, H., & Ptashne, M. (1988). GAL4 activates gene expression in mammalian cells. *Cell, 52*(2), 161-7. doi:10.1016/0092-8674(88)90504-1

Karlin, K., Mondal, G., Hartman, J., Tyagi, S., Kurley, S., Bland, C., . . . Westbrook, T. F. (2014). The oncogenic STP axis promotes triple-negative breast cancer via degradation of the REST tumor suppressor. *Cell Reports, 9*(4), 1318-32. doi:10.1016/j.celrep.2014.10.011

Karpov, P., Nadezhdina, E., Yemets, A., Matusov, V., Nyporko, A., Shashina, N., & Blume, Y. (2010). Bioinformatic search of plant microtubule-and cell cycle related serine-threonine protein kinases. *BMC Genomics, 11*(Suppl 1), S14. doi:10.1186/1471-2164-11-S1-S14

King, S., Purdie, C., Bray, S., Quinlan, P., Jordan, L., Thompson, A., & Meek, D. (2012). Immunohistochemical detection of Polo-like kinase-1 (PLK1) in

primary breast cancer is associated with TP53 mutation and poor clinical outcome. *Breast Cancer Research, 14*(2), R40. doi:10.1186/bcr3136

Kitada, K., Johnson, A., Johnston, L., & Sugino, A. (1993). A multicopy suppressor gene of the Saccharomyces cerevisiae G1 cell cycle mutant gene dbf4 encodes a protein kinase and is identified as CDC5. *Molecular And Cellular Biology, 13*(7), 4445-57. doi:10.1128/mcb.13.7.4445

Knecht, R., Elez, R., Oechler, M., Solbach, C., Von Ilberg, C., & Strebhardt, K. (1999). Prognostic significance of polo-like kinase (PLK) expression in squamous cell carcinomas of the head and neck. *Cancer Research, 59*(12), 2794-2797.

Kneisel, L., Strebhardt, K., Bernd, A., Wolter, M., Binder, A., & Kaufmann, R. (2002). Expression of polo-like kinase (PLK1) in thin melanomas: A novel marker of metastatic disease. *Journal of Cutaneous Pathology, 29*(6), 354-358.

Kondo, S., & Perrimon, N. (2011). A Genome-Wide RNAi Screen Identifies Core Components of the G2-M DNA Damage Checkpoint. *Science Signaling, 4*(154), rs1. doi:10.1126/scisignal.2001350

Kothe, M., Kohls, D., Low, S., Coli, R., Cheng, A., Jacques, S., . . . Ding, Y.-H. (2007). Structure of the catalytic domain of human polo-like kinase 1. *Biochemistry, 46*(20), 5960-71. doi:10.1021/bi602474j

Lane, H., & Nigg, E. (1996). Antibody microinjection reveals an essential role for human polo-like kinase 1 (Plk1) in the functional maturation of mitotic centrosomes. *The Journal of Cell Biology, 135*(6 Pt 2), 1701-13. doi:10.1083/jcb.135.6.1701

Lee, H., McManus, C., Cho, D., Eaton, M., Renda, F., Somma, M., . . . MacAlpine, D. (2014). DNA copy number evolution in Drosophila cell lines. *Genome Biology, 15*(8), R70. doi:10.1186/gb-2014-15-8-r70

Lee, H.-J., Hwang, H.-I., & Jang, Y.-J. (2010). Mitotic DNA damage response: Polo-like kinase-1 is dephosphorylated through ATM-Chk1 pathway. *Cell Cycle, 9*(12), 2389-98. doi:10.4161/cc.9.12.11904

Lee, K., & Rhee, K. (2011). PLK1 phosphorylation of pericentrin initiates centrosome maturation at the onset of mitosis. *Journal of Cell Biology, 195*(7), 1093-101. doi:10.1083/jcb.201106093

Lera, R., Potts, G., Suzuki, A., Johnson, J., Salmon, E., Coon, J., & Burkard, M. (2016). Decoding Polo-like kinase 1 signaling along the kinetochore-centromere axis. *Nature Chemical Biology, 12*(6), 411-18. doi:10.1038/nchembio.2060

Li, L., Xue, W., Shen, Z., Liu, J., Hu, M., Cheng, Z., . . . Zhao, J. (2020). A Cereblon Modulator CC-885 Induces CRBN- and p97-Dependent PLK1

Degradation and Synergizes with Volasertib to Suppress Lung Cancer. *Molecular Therapy Oncolytics, 18*(1), 215-25. doi:0.1016/j.omto.2020.06.013

Li, Z., Li, J., Bi, P., Lu, Y., Burcham, G., Elzey, B., . . . Liu, X. (2014). Plk1 phosphorylation of PTEN causes a tumor-promoting metabolic state. *Molecular and Cellular Biology, 34*(19), 3642-61. doi:10.1128/MCB.00814-14

Liu, J., & Zhang, C. (2017). The equilibrium of ubiquitination and deubiquitination at PLK1 regulates sister chromatid separation. *Cellular and Molecular Life Sciences, 74*, 2127-34. doi:10.1007/s00018-017-2457-5

Liu, X., Li, H., Song, B., & Liu, X. (2010). Polo-like kinase 1 phosphorylation of G2 and S-phase-expressed 1 protein is essential for p53 inactivation during G2 checkpoint recovery. *EMBO reports, 11*(8), 626-32. doi:10.1038/embor.2010.90

Liu, Z., Sun, Q., & Wang, X. (2017). PLK1, A Potential Target for Cancer Therapy. *Translational Oncology, 10*(1), 22-32. doi:10.1016/j.tranon.2016.10.003

Llamazares, S., Moreira, A., Tavares, A., Girdham, C., Spruce, B., Gonzalez, C., . . . CE, S. (1991). polo encodes a protein kinase homolog required for mitosis in Drosophila. *Genes & Development, 5*(12A), 2153-65. doi:10.1101/gad.5.12a.2153

Lu, L., Wood, J., Minter-Dykhouse, K., Ye, L., Saunders, T., Yu, X., & Chen, J. (2008). Polo-like kinase 1 is essential for early embryonic development and tumor suppression. *Molecular and Cellular Biology, 28*(22), 6870-6. doi:10.1128/MCB.00392-08

Ma, J., & Ptashne, M. (1987). The carboxy-terminal 30 amino acids of GAL4 are recognized by GAL80. *Cell, 50*(1), 137-42. doi:10.1016/0092-8674(87)90670-2

Maia, A., Garcia, Z., Kabeche, L., Barisic, M., Maffini, S., Macedo-Ribeiro, S., . . . Maiato, H. (2012). Cdk1 and Plk1 mediate a CLASP2 phospho-switch that stabilizes kinetochore-microtubule attachments. *Journal of Cell Biology, 199*(2), 285-301. doi:10.1083/jcb.201203091

McCarthy, E., & Goldstein, B. (2006). Asymmetric spindle positioning. *Current Opinions in Cell Biology, 18*(1), 79-85. doi:10.1016/j.ceb.2005.12.006

Mi, H., Muruganujan, A., Huang, X., Ebert, D., Mills, C., Guo, X., & Thomas, P. (2019). Protocol Update for Large-scale genome and gene function analysis with PANTHER Classification System (v.14.0). *Nature Protocols, 14*(3), 703-721. doi:10.1038/s41596-019-0128-8

Miyamoto, T., Akutsu, S., Fukumitsu, A., Morino, H., Masatsuna, Y., Hosoba, K., . . . Matsuura, S. (2017). PLK1-mediated phosphorylation of WDR62/MCPH2

ensures proper mitotic spindle orientation. *Human Molecular Genetics, 26*(22), 4429-40. doi:10.1093/hmg/ddx330

Moorhouse, K., & Burgess, D. (2014). How to be at the right place at the right time: The importance of spindle positioning in embryos. *Molecular Reproduction and Development, 81*(10), 884-895. doi:10.1002/mrd.22418

Morgan, D. (2007). *The Cell Cycle: Principles of Control.* OUP/New Science.

Moshe, Y., Boulaire, J., Pagano, M., & Hershko, A. (2004). Role of Polo-like kinase in the degradation of early mitotic inhibitor 1, a regulator of the anaphase promoting complex/cyclosome. *Proceedings of the National Academy of Sciences of the United States of America, 101*(21), 7937-42. doi:10.1073/pnas.0402442101

Moura, M., & Conde, C. (2019). Phosphatases in Mitosis: Roles and Regulation. *Biomolecules, 9*(2), 1-55. doi:10.3390/biom9020055

Moutinho-Santos, T., Sampaio, P., Amorim, I., Costa, M., & Sunkel, C. (2012). In vivo localisation of the mitotic POLO kinase shows a highly dynamic association with the mitotic apparatus during early embryogenesis in Drosophila. *Biology of the Cell, 91*(8), 585-96. doi:10.1111/j.1768-322X.1999.tb01104.x

Mross, K., Dittrich, C., Aulitzky, W., Strumberg, D., Schutte, J., Schmid, R., . . . Scheulen, M. (2012). A randomised phase II trial of the Polo-like kinase inhibitor BI 2536 in chemo-naïve patients with unresectable exocrine adenocarcinoma of the pancreas – a study within the Central European Society Anticancer Drug Research (CESAR) collaborative network. *British Journal of Cancer, 107*, 280-286. doi:10.1038/bjc.2012.257

Mross, K., Frost, A., Steinbild, S., Hedbom, S., Rentschler, J., Kaiser, R., . . . Munzert, G. (2008). Phase I dose escalation and pharmacokinetic study of BI 2536, a novel Polo-like kinase 1 inhibitor, in patients with advanced solid tumors. *Journal of Clinical Oncology, 26*(34), 5511-5517. doi:10.1200/JCO.2008.16.1547

Ng, W., Shin, J.-S., Wang, B., & Lee, C. (2017). Exploration of mutation and DNA methylation of polo-like kinase 1 (PLK1) in colorectal cancer. *Open Journal of Pathology, 7*(13). doi:10.4236/ojpathology.2017.73005

Nishino, M., Kurasawa, Y., Evans, R., Lin, S.-H., Brinkley, B., & Yu-Lee, L.-Y. (2006). NudC is required for Plk1 targeting to the kinetochore and chromosome congression. *Current Biology, 16*(14), 1414-21. doi:10.1016/j.cub.2006.05.052

Ou, C.-Y., Pi, H., & Chien, C.-T. (2003). Control of protein degradation by E3 ubiquitin ligases in Drosophila eye development. *Trends in Genetics, 19*(7), 382-89. doi:10.1016/S0168-9525(03)00146-X

Palumbo, V., Pellacani, C., Heesom, K., Rogala, K., Deane, C., Mottier-Pavie, V., . . . Wakefield, J. (2015). Misato Controls Mitotic Microtubule Generation by Stabilizing the Tubulin Chaperone Protein-1 Complex. *Current Biology, 25*(13), 1777-83. doi:10.1016/j.cub.2015.05.033

Park, J.-E., Soung, N.-K., Johmura, Y., Kang, Y., Liao, C., Lee, K., . . . Nicklaus, M. L. (2010). Polo-box domain: a versatile mediator of polo-like kinase function. *Cellular and Molecular Life Sciences, 67*(12), 1957-70. doi:10.1007/s00018-010-0279-9

Perkins, L., Holderbaum, L., Tao, R., Hu, Y., Sopko, R., McCall, K., . . . Perrimon, N. (2015). The Transgenic RNAi Project at Harvard Medical School: Resources and Validation. *201*(3), 843-52. doi:10.1534/genetics.115.180208

Petronczki, M., Lénárt, P., & Peters, J.-M. (2008). Polo on the Rise-from Mitotic Entry to Cytokinesis with Plk1. *Developmental Cell, 14*(5), 646-59. doi:10.1016/j.devcel.2008.04.014

Qi, W., Tang, Z., & Yu, H. (2006). Phosphorylation- and polo-box-dependent binding of Plk1 to Bub1 is required for the kinetochore localization of Plk1. *Molecular Biology of the Cell, 17*(8), 3705-16. doi:10.1091/mbc.e06-03-0240

Raab, M., Sanhaji, M., Matthess, Y., Hörlin, A., Lorenz, I., Dötsch, C., . . . Strebhardt, K. (2018). PLK1 has tumor-suppressive potential in APC-truncated colon cancer cells. *Nature Communications, 9*(1), 1106. doi:10.1038/s41467-018-03494-4

Ren, Y., Bi, C., Zhao, X., Lwin, T., Wang, C., Yuan, J., . . . Tao, J. (2018). PLK1 stabilizes a MYC-dependent kinase network in aggressive B cell lymphomas. *The Journal of Clinical Investigation, 128*(12), 5517-5530. doi:10.1172/JCI122533

Rödel, F., Keppner, S., Capalbo, G., Bashary, R., Kaufmann, M., Rödel, C., . . . Spänkuch, B. (2010). Polo-like kinase 1 as predictive marker and therapeutic target for radiotherapy in rectal cancer. *The American Journal of Pathology, 177*(2), 918-929. doi:10.2353/ajpath.2010.100040918

Rogers, G., Rusan, N., Roberts, D., Peifer, M., & Rogers, S. (2009). The SCF Slimb ubiquitin ligase regulates Plk4/Sak levels to block centriole reduplication. *Journal of Cell Biology, 184*(2), 225-39. doi:10.1083/jcb.200808049

Safari-Alighiarloo, N., Taghizadeh, M., Rezaei-Tavirani, M., Goliaei, B., & Peyvandi, A. (2014). Protein-protein interaction networks (PPI) and complex diseases. *Gastroenterol and Hepatology from Bed to Bench, 7*(1), 17-31.

Saurin, A. (2018). Kinase and Phosphatase Cross-Talk at the Kinetochore. *Frontiers in Cell and Developmental Biology, 6*, 62. doi:10.3389/fcell.2018.00062

Schafer, K. (1998). The cell cycle: a review. *Veterinary Pathology, 35*(6), 461-78. doi:10.1177/030098589803500601

Schmidt, A., Duncan, P., Rauh, N., Sauer, G., Fry, A., Nigg, E., & Mayer, T. (2005). Xenopus polo-like kinase Plx1 regulates XErp1, a novel inhibitor of APC/C activity. *Genes and Development*, 502-13. doi:10.1101/gad.320705

Schneider, I. (1972). Cell lines derived from late embryonic stages of Drosophila melanogaster. *Journal of Embryology and Experimental Morphology, 27*(2), 353-65.

Seeburg, D., Pak, D., & Sheng, M. (2005). Polo-like kinases in the nervous system. *Oncogene, 24*(2), 292-8. doi:10.1038/sj.onc.1208277

Seki, A., Coppinger, J., Jang, C., Yates, J., & Fang, G. (2008). Bora and the kinase Aurora a cooperatively activate the kinase Plk1 and control mitotic entry. *Science, 320*(5883), 1655-8. doi:10.1126/science.1157425

Serrano, D., & D'Amours, D. (2014). When genome integrity and cell cycle decisions collide: roles of polo kinases in cellular adaptation to DNA damage. *Systems and Synthetic Biology, 8*(3), 195-203. doi:10.1007/s11693-014-9151-9

Shannon, P., Markiel, A., Ozier, O., Baliga, N., Wang, J., Ramage, D., . . . Ideker, T. (2003). Cytoscape: a software environment for integrated models of biomolecular interaction networks. *Genome Research, 13*(11), 2498-504. doi:10.1101/gr.1239303

Sierzputowska, K., Baxter, C., & Housden, B. (2018). Variable Dose Analysis: A Novel High-throughput RNAi Screening Method for Drosophila Cells. *Bio-protocol, 8*(24), e3112. doi:10.21769/BioProtoc.3112

Smits, A., & Vermeulen, M. (2016). Characterizing Protein–Protein Interactions Using Mass Spectrometry: Challenges and Opportunities. *Trends in Biotechnology, 34*(10), 825-834. doi:10.1016/j.tibtech.2016.02.014

Staller, M., Yan, D., Randklev, S., Bragdon, M., Wunderlich, Z., Tao, R., . . . Perrimon, N. (2013). Depleting Gene Activities in Early Drosophila Embryos with the “Maternal-Gal4–shRNA” System. *Genetics, 193*(1), 51-61. doi:10.1534/genetics.112.144915

Steegmaier, M., Hoffmann, M., Baum, A., Lénárt, P., Petronczki, M., Krssák, M., . . . Rettig, W. (2007). BI 2536, a potent and selective inhibitor of polo-like kinase 1, inhibits tumor growth in vivo. *Current Biology, 17*(4), 16-22. doi:10.1016/j.cub.2006.12.037

Stehle, A., Hugle, M., & Fulda, S. (2015). Eribulin synergizes with Polo-like kinase 1 inhibitors to induce apoptosis in rhabdomyosarcoma. *Cancer Letters, 365*(1), 57-46. doi:10.1016/j.canlet.2015.04.011

Stein, J., Tarczy Broihier, H., Moore, L., & Lehmann, R. (2002). Slow as Molasses is required for polarized membrane growth and germ cell migration in Drosophila. *Development, 129*(16), 3925-34. doi:10.1242/dev.129.16.3925

Stoiber, M., Celniker, S., Cherbas, L., Brown, B., & Cherbas, P. (2016). Diverse Hormone Response Networks in 41 Independent Drosophila Cell Lines. *G3 Genes|Genomes|Genetics, 6*(3), 683-94. doi:10.1534/g3.115.023366

Suijkerbuijk, S., Vleugel, M., Teixeira, A., & Kops, G. (2012). Integration of kinase and phosphatase activities by BUBR1 ensures formation of stable kinetochore-microtubule attachments. *Developmental Cell, 23*(4), 745-55. doi:10.1016/j.devcel.2012.09.005

Sunkel, C., & Glover, D. (1988). Polo, a mitotic mutant of Drosophila displaying abnormal spindle poles. *Journal of cell science, 89*(1), 25-38.

Terzi, M., Izmirli, M., & Gogebakan, B. (2016). The cell fate: senescence or quiescence. *Molecular Biology Reports, 43*(11), 1213-1220. doi:10.1007/s11033-016-4065-0

Tong, A., Lesage, G., Bader, G., Ding, H., Xu, H., Xin, X., . . . Li, Z. (2004). Global mapping of the yeast genetic interaction network. *Science, 303*(5659), 808-13. doi:10.1126/science.1091317

van de Weerdt, B., & Medema, R. (2005). Polo-Like Kinases. A Team in Control of the Division. *Cell Cycle, 5*(8), 853-64. doi:10.4161/cc.5.8.2692

Van den Bossche, J., Lardon, F., Deschoolmeester, V., De Pauw, I., Vermorken, J., Specenier, P., . . . Wouters, A. (2016). Spotlight on Volasertib: Preclinical and Clinical Evaluation of a Promising Plk1 Inhibitor. *Medicinal Research Reviews, 36*(4), 749-86. doi:10.1002/med.21392

Vert, J.-P., Foveau, N., Lajaunie, C., & Vandenbrouck, Y. (2006). An accurate and interpretable model for siRNA efficacy prediction. *Bioinformatics, 7*, 520. doi:10.1186/1471-2105-7-520

Wachowicz, P., Fernández-Miranda, G., Marugán, C., Escobar, B., & de Cárcer, G. (2016). Genetic depletion of Polo-like kinase 1 leads to embryonic lethality due to mitotic aberrancies. *Bioessays, 38*(Suppl 1), S96-106. doi:10.1002/bies.201670908

Wakida, T., Ikura, M., Kuriya, K., Ito, S., Shiroiwa, Y., Habu, T., . . . Furuya, K. (2017). The CDK-PLK1 axis targets the DNA damage checkpoint sensor protein RAD9 to promote cell proliferation and tolerance to genotoxic stress. *eLife, 6*, e29953. doi:10.7554/eLife.29953

Warnke, S., Kemmler, S., Hames, R., Tsai, H.-L., Hoffmann-Rohrer, U., Fry, A., & Hoffmann, I. (2004). Polo-like Kinase-2 Is Required for Centriole Duplication in Mammalian Cells. *Current Biology, 14*(13), 1200-07. doi:10.1016/j.cub.2004.06.059

Werner, A., Disanza, A., Reifenberger, N., Habeck, G., Becker, J., Calabrese, M., . . . Melchior, F. (2013). SCFFbxw5 mediates transient degradation of actin remodeller Eps8 to allow proper mitotic progression. *Nature Cell Biology, 15*(2), 179-88. doi:10.1038/ncb2661

Wierer, M., Verde, G., Pisano, P., Molina, H., Font-Mateu, J., Di Croce, L., & Beato, M. (2013). PLK1 signaling in breast cancer cells cooperates with estrogen receptor-dependent gene transcription. *Cell Reports, 3*(6), 2021-32. doi:10.1016/j.celrep.2013.05.024

Williams, G., & Stoeber, K. (2012). The cell cycle and cancer. *The Journal of Pathology, 226*(2), 352-64. doi:10.1002/path.3022

Woodruff, J., Ferreira Gomes, B., Widlund, P., Mahamid, J., Honigmann, A., & Hyman, A. (2017). The Centrosome Is a Selective Condensate that Nucleates Microtubules by Concentrating Tubulin. *Cell, 169*(6), 1066-77.e10. doi:10.1016/j.cell.2017.05.028

Xiang, Y., Takeo, S., Florens, L., Hughes, S., Huo, L.-J., Gilliland, W., . . . Hawley, R. (2007). The inhibition of polo kinase by matrimony maintains G2 arrest in the meiotic cell cycle. *PLoS Biology, 5*(12), e323. doi:10.1371/journal.pbio.0050323

Xiao, D., Yue, M., Su, H., Ren, P., Jiang, J., Li, F., . . . Qing, G. (2016). Polo-like Kinase-1 Regulates Myc Stabilization and Activates a Feedforward Circuit Promoting Tumor Cell Survival. *Molecular Cell, 64*(3), 493-506. doi:10.1016/j.molcel.2016.09.016

Xu, J., & Du, W. (2003). Drosophila chk2 plays an important role in a mitotic checkpoint in syncytial embryos. *FEBS letters, 545*(2-3), 209-12. doi:10.1016/s0014-5793(03)00536-2

Yanagawa, S., Lee, J., & Ishimoto, A. (1998). Identification and characterization of a novel line of Drosophila Schneider S2 cells that respond to wingless signaling. *The Journal of Biological Chemistry, 273*(48), 32353-9. doi:10.1074/jbc.273.48.32353

Yuan, J., Sanhaji, M., Krämer, A., Reindl, W., Hofmann, M., Kreis, N.-N., . . . Strebhardt, K. (2011). Polo-box domain inhibitor poloxin activates the spindle assembly checkpoint and inhibits tumor growth in vivo. *The American Journal of Pathology, 179*(4), 2091-9. doi:10.1016/j.ajpath.2011.06.031

Yumimoto, K., Yamauchi, Y., & Nakayama, K. (2020). F-Box proteins and cancer. *Cancers, 12*(5), 1249. doi:10.3390/cancers12051249

Zhai, B., Villén, J., Beausoleil, S., Mintseris, J., & Gygi, S. (2008). Phosphoproteome analysis of Drosophila melanogaster embryos. *Journal of Proteome Research, 7*(4), 1675-82. doi:10.1021/pr700696a

Zimmerman, W., & Erikson, R. (2007). Polo-like kinase 3 is required for entry into S phase. *Proceedings of the National Academy of Sciences of the United States of America, 104*(6), 1847-52. doi:10.1073/pnas.0610856104